## General Disclaimer

### One or more of the Following Statements may affect this Document

- This document has been reproduced from the best copy furnished by the organizational source. It is being released in the interest of making available as much information as possible.

- This document may contain data, which exceeds the sheet parameters. It was furnished in this condition by the organizational source and is the best copy available.

- This document may contain tone-on-tone or color graphs, charts and/or pictures, which have been reproduced in black and white.

- This document is paginated as submitted by the original source.

- Portions of this document are not fully legible due to the historical nature of some of the material. However, it is the best reproduction available from the original submission.

NATIONAL AERONAUTICS AND SPACE ADMINISTRATION

# EARTH RESOURCES SURVEY PROGRAM

## TECHNICAL LETTER NASA-88

# An Engineering Feasibility Study of an Orbiting Scanning Radiometer

By

J. Braithwaite, A. W. Krause, and W. L. Brown

Willow Run Laboratories of the Institute of Science and Technology,
University of Michigan, Ann Arbor, Michigan

May 1967

Prepared by the Geological Survey for the
National Aeronautics and Space Administration (NASA)
under Contract No. ~~14-08-0001-10108~~
R-09-020-011

MANNED SPACECRAFT CENTER
HOUSTON, TEXAS

UNITED STATES
DEPARTMENT OF THE INTERIOR
GEOLOGICAL SURVEY
WASHINGTON, D.C. 20242

Technical Letter
NASA-88
May 1967

Dr. Peter C. Badgley
Program Chief,
Earth Resources Survey
Code SAR - NASA Headquarters
Washington, D.C. 20546

Dear Peter:

Transmitted herewith is one copy of:

TECHNICAL LETTER NASA-88

AN ENGINEERING FEASIBILITY STUDY OF AN

ORBITING SCANNING RADIOMETER*

by

J. Braithwaite**
A. W. Krause**
W. L. Brown**

Sincerely yours,

William A. Fischer
Research Coordinator
Earth Orbiter Program

*Work performed under NASA Contract ~~No. 14-08-0001-10108~~ R-09-120-011

**Willow Run Laboratories of the Institute of Science and Technology,
University of Michigan, Ann Arbor, Michigan

UNITED STATES

DEPARTMENT OF THE INTERIOR

GEOLOGICAL SURVEY

# TECHNICAL LETTER NASA-88

# AN ENGINEERING FEASIBILITY STUDY OF AN ORBITING SCANNING RADIOMETER*

by

J. Braithwaite**
A. W. Krause**
W. L. Brown**

May 1967

The work reported herein was conducted by the Willow Run Laboratories of the Institute of Science and Technology, University of Michigan on behalf of the U.S. Geological Survey, Branch of Theoretical Geophysics, under Contract 14-08-0001-10108

*Work performed under NASA Contract No. 14-08-0001-10108

**Willow Run Laboratories of the Institute of Science and Technology, University of Michigan, Ann Arbor, Michigan

## FOREWORD

The work described in this report was conducted by the Infrared and Optical Sensor Laboratory (M. R. Holter, Head) of Willow Run Laboratories, a unit of The University of Michigan's Institute of Science and Technology. D. S. Lowe was the Principal Investigator. In addition to the Principal Investigator and the authors listed on the title page, substantial contributions were made to the program and to the writing of this report by the following: J. Cook, V. Larrowe, E. Work, and L. Larsen. J. Cook was also the author of a separate but related technical report entitled A Survey of Lunar Geology.

The work reported here is consonant with and fulfills part of the objectives of a comparative multispectral remote-sensing program of the Infrared and Optical Sensor Laboratory. The goal of the program is to develop methods of improving and extending current remote-sensing capabilities by studying the spectral characteristics of surface features of objects being sought. Improvements are being sought in the kinds and quantities of data obtainable and in the quality, speed, and economy of the image-interpretation process. The present study is very closely related to and dependent upon other studies completed by Willow Run Laboratories under contract to the U. S. Geological Survey (~~Contract No. 14-80-0001-10053~~ R-09-020-011) and under contract to the National Aeronautics and Space Administration Contract No. NAS8-2100. Previous related reports issued by the Infrared and Optical Sensor Laboratory are listed on the following pages.

## RELATED REPORTS

COMPARATIVE MULTISPECTRAL SENSING (U), M. R. Holter and F. C. Polcyn, Report No. 2900-484-R, Willow Run Laboratories of the Institute of Science and Technology, The University of Michigan, Ann Arbor, June 1965, AD 362 283 (CONFIDENTIAL).

DIURNAL AND SEASONAL VARIATIONS IN RADIATION OF OBJECTS AND BACKGROUNDS, 4.5-5.5-$\mu$ SPECTRAL REGION (U), L. D. Miller and R. Horvath, Report No. 6400-32-T, Willow Run Laboratories of the Institute of Science and Technology, The University of Michigan, Ann Arbor, June 1965, AD 362 620 (CONFIDENTIAL).

THE INVESTIGATION OF A METHOD FOR REMOTE DETECTION AND ANALYSIS OF LIFE ON A PLANET, M. R. Holter, D. S. Lowe, and R. J. Shay, Report No. 6590-1-P, Institute of Science and Technology, The University of Michigan, Ann Arbor, November 1964.

SPECTRUM MATCHING (U), R. E. Hamilton, Report No. 6400-18-T, Willow Run Laboratories of the Institute of Science and Technology, The University of Michigan, Ann Arbor, June 1965, AD 363 001 (CONFIDENTIAL).

TARGET SIGNATURE STUDY, INTERIM REPORT, VOLUME I: SURVEY (U), R. R. Legault and T. Limperis, Report No. 5698-22-T(I), Institute of Science and Technology, The University of Michigan, Ann Arbor, October 1964, AD 354 106 (CONFIDENTIAL).

TARGET SIGNATURE STUDY, INTERIM REPORT, VOLUME II: RECOMMENDATIONS (U), R. R. Legault and T. Limperis, Report No. 5698-22-T(II), Institute of Science and Technology, The University of Michigan, Ann Arbor, October 1964 (CONFIDENTIAL).

TARGET SIGNATURE STUDY, INTERIM REPORT, VOLUME III: POLARIZATION (U), R. R. Legault and T. Limperis, Report No. 5698-22-T(III), Institute of Science and Technology, The University of Michigan, Ann Arbor, October 1964, AD 354 025 (CONFIDENTIAL).

TARGET SIGNATURE STUDY, INTERIM REPORT, VOLUME IV: BIBLIOGRAPHY (ACOUSTIC, ULTRAVIOLET, VISIBLE, INFRARED, AND RADAR) (U), T. Limperis and R. S. Gould, Report No. 5698-22-T(IV), Institute of Science and Technology, The University of Michigan, Ann Arbor, October 1964, AD 354 232 (SECRET).

TARGET SIGNATURE STUDY, INTERIM REPORT, VOLUME V: CATALOG OF SPECTRAL REFERENCE DATA, R. R. Legault, R. S. Gould, and T. Limperis, Report No. 5698-22-T(V), Institute of Science and Technology, The University of Michigan, Ann Arbor, October 1964,

A COMPREHENSIVE TARGET-SIGNATURE MEASUREMENT PROGRAM, FIRST INTERIM TECHNICAL REPORT, VOLUME I: TECHNICAL DISCUSSION (U), Report No. 7251-3-P(I), Willow Run Laboratories of the Institute of Science and Technology, The University of Michigan, Ann Arbor, December 1965 (CONFIDENTIAL).

A COMPREHENSIVE TARGET-SIGNATURE MEASUREMENT PROGRAM, SECOND INTERIM TECHNICAL REPORT, VOLUME I: DATA PROCESSING, STORAGE, AND ANALYSIS (U), Report No. 7251-9-P(I), Willow Run Laboratories of the Institute of Science and Technology, The University of Michigan, Ann Arbor, June 1966 (CONFIDENTIAL).

A COMPREHENSIVE TARGET-SIGNATURE MEASUREMENT PROGRAM, SECOND INTERIM TECHNICAL REPORT, VOLUME II: MEASUREMENT IMPLEMENTATION (U), Report No. 7251-9-P(II), Willow Run Laboratories of the Institute of Science and Technology, The University of Michigan, Ann Arbor, June 1966 (CONFIDENTIAL).

A COMPREHENSIVE TARGET-SIGNATURE MEASUREMENT PROGRAM, THIRD INTERIM TECHNICAL REPORT (U), Report No. 7251-15-P, Willow Run Laboratories of the Institute of Science and Technology, The University of Michigan, Ann Arbor, February 1966 (CONFIDENTIAL).

A COMPREHENSIVE TARGET-SIGNATURE MEASUREMENT PROGRAM, FINAL REPORT (U), T. Limperis, Report No. 7251-21-F, Willow Run Laboratories of the Institute of Science and Technology, The University of Michigan, Ann Arbor, December 1966, AD 378 112 (CONFIDENTIAL).

DISPERSIVE MULTISPECTRAL SCANNING: A FEASIBILITY STUDY, FINAL REPORT, J. Braithwaite, Report No. 7610-5-F, Willow Run Laboratories of the Institute of Science and Technology, The University of Michigan, Ann Arbor, September 1966.

AN INVESTIGATIVE STUDY OF A SPECTRUM-MATCHING IMAGING SYSTEM, FINAL REPORT, D. S. Lowe, J. Braithwaite, and V. L. Larrowe, Report No. 8201-1-F, Willow Run Laboratories of the Institute of Science and Technology, The University of Michigan, Ann Arbor, October 1966.

TARGET SIGNATURES ANALYSIS CENTER: DATA COMPILATION, D. G. Earing and J. A. Smith, Report No. 7850-2-B, Willow Run Laboratories of the Institute of Science and Technology, The University of Michigan, Ann Arbor, July 1966, AD 489 968.

INVESTIGATION OF SPECTRUM-MATCHING SENSING IN AGRICULTURE, SEMIANNUAL REPORT (U), F. C. Polcyn, Report 6590-7-P, Willow Run Laboratories of the Institute of Science and Technology, The University of Michigan, Ann Arbor, in publication, Vol. I; UNCLASSIFIED; Vol. II, CONFIDENTIAL.

OPTICAL SENSING OF THE MOISTURE CONTENT IN FINE FOREST FUELS, C. E. Olson, Jr., Report 8036-1-F, Willow Run Laboratories of the Institute of Science and Technology, The University of Michigan, Ann Arbor, in publication.

**ABSTRACT**

Specifications for two general-purpose optical mechanical scanners suitable for use in orbiting vehicles are recommended. The systems are a medium resolution scanning radiometer and a multispectral scanner-spectrograph. The specifications are such that they can be utilized for a wide variety of scientific applications. Preliminary design studies for the instruments are reported. Two instruments which are more specialized—a very high resolution scanner and a lunar cold-side scanner—are briefly discussed. (There appears to be a need for experiments which are beyond the scope of the two general-purpose instruments; these experiments should probably have lower priority.) Technical problem areas connected with the designs are identified and discussed. In most of these areas it would be inappropriate to recommend definitive solutions prior to the selection of orbital flight parameters and vehicles.

## CONTENTS

## FIGURES

# AN ENGINEERING FEASIBILITY STUDY OF AN ORBITING SCANNING RADIOMETER

## Final Report
## January 1966 Through November 1966

## 1 INTRODUCTION

The contract for this study issued by the U. S. Geological Survey to The University of Michigan's Willow Run Laboratories came into effect on 10 January 1966. The statement of work required the contractor to ". . . make an engineering feasibility study of a lunar orbiting scanning radiometer leading to the definition of feasible infrared experiments and the required instrumentation including configuration and specifications." A later, revised work statement required the contractor to

> . . . redirect efforts and study toward identifying and recommending solutions to engineering problems including but not limited to the following, with particular emphasis on earth orbiting systems:
> 1. Detector cooling techniques
> 2. Data recording techniques
> 3. Calibration techniques

Although the work statement had been amended, investigators were still required to report the work done under the original statement and include it in a final report together with the work done under the new statement. Sections 2 and 3 of the present report contain discussions of work done under the original statement, but modified according to the new emphasis on earth orbits. Section 4 deals with technical problem areas under the new work statement. The appendixes are mathematical analyses which bear upon work done under the original statement.

Requirements for experiments with both earth and lunar orbiters are presented in section 2. In the early "lunar" phase of this study, a fairly extensive review of the literature was undertaken in an attempt to find a rational basis for the definition of lunar orbital experiments. The results of the review have been made into a separate report [1]. We recommend in section 2 that a high resolution thermal scanner should be developed for initial use in both earth and lunar experiments. It would have an angular resolution of a little less than 1 milliradian and would have a simple design. Some multispectral capability would be added by using additional short wavelength detectors. This instrument is described in section 3.1. A multispectral in-

strument which would have second priority is the scanner-spectrograph combination described in section 3.2. These two instruments would provide data of general use to earth resource and lunar scientists of many disciplines. However, it appears that there are important requirements not covered by either of them, and brief preliminary discussions of two instruments which meet these requirements are given in section 3.3 and 3.4. They are a modest angular resolution, very high sensitivity scanner for thermal mapping of the cold face of the moon and a very high angular resolution scanner to meet the needs for a spatial resolution finer than that provided by the medium resolution scanner. It should be considered, however, that the requirements for these two instruments and their optimum specifications may well change in the light of further research, particularly the results of experiments with the first and second priority instruments.

In section 4, technical problem areas are identified and specific problems are discussed. It is apparent that most of these problems are common to earth and lunar orbital experiments. It is also apparent that, though solutions are available, the optimum solution is never clear because (1) the state of the art is changing rapidly, and a difficult decision between a tried and reliable technique and a novel one may have to be reversed on the basis of experiments carried out in the near future (particularly for cryogenic techniques); (2) we do not know the extent to which the optimum solution would be affected by the unknown capabilities and limitations of the spacecraft, particularly in regard to data recording. An example of the latter difficulty would occur with a multichannel, or very high resolution scanner, which used more than its own weight of recording tapes; the problem of orbiting and retrieving this weight, if allowed, could significantly affect other aspects of the spacecraft and flight. Because of these uncertainties, section 4 is not definitive in recommending solutions and in this respect departs from the revised work statement quoted above.

As to developing optimum instrumentation specifications, it is clear that there are very complicated interrelations among system sophistication, reliability, probable value to each prospective user group, and cost. Initial systems, therefore, should be relatively simple and reliable general purpose systems, and it should be recognized that their resolution may be insufficient in meeting some specific user requirements.

Three mathematical analyses carried out during the performance of the contract are presented as three appendixes. The first is an attempt to analyze the practicability of using a K mirror to counteract the image rotation occurring in certain types of scanners. The results are discouraging and, as explained, the use of a K mirror in this way is not recommended. However, the analysis is presented for completeness. In appendix II, methods developed in a previous study [2] are extended in various ways. In particular, scanner performance can now be obtained directly in terms of target temperature or emittance differences. The third appen-

dix contains an analysis of the effects of using a rectangular rather than a square entrance slit in a scanner-spectrograph system. Though a square slit is recommended for the scanner-spectrograph system discussed in section 3.2, rectangular slits might prove desirable in future modifications of that system.

# 2
# EXPERIMENTAL REQUIREMENTS

## 2.1. EQUIPMENT DEFINITION

In selecting specifications for a remote sensing instrument, it will almost inevitably be necessary to compromise between what is technically feasible and what a specific user requires. When there are many users to be considered, the compromise becomes more complex. The choices discussed here are based on a discussion of the relevant instrumental requirements of many disciplines concerned with remote sensing of the earth's surface from orbit [3] and a survey of the current status of lunar geology [1]. The latter, unfortunately, does nothing to solve the disagreement among scientists about the nature of the moon's surface, except, perhaps, to indicate the paucity of experimental data on which many of the theories are based. The high resolution photographs from the Rangers and Surveyors have demolished some theories but appear to have done little to resolve the basic disagreements. The Apollo experiments will add a wealth of new data; in particular, they will make possible mineralogical analysis of small pieces of lunar surface material. On the other hand, by exploring the surface directly, we will be able to investigate only a tiny fraction of the lunar surface in the foreseeable future. It is therefore clearly desirable to extend the range of surface exploration by using remote sensing or geophysical techniques. The attenuating and distorting effects of the earth's atmosphere, as well as the great distance, limit the value of earth-based observation. Thus it is clear that lunar orbital experiments will play a major part both in expanding the results of surface exploration through comparison and investigating extended features which cannot easily be studied from lunar bases.

Since World War I, and increasingly since World War II, aerial photography has been the prime remote sensing technique for a wide variety of political, economic, and scientific inquiries. For both terrestrial and lunar orbital experiments, it is clear that photographic techniques will play a large and perhaps predominant part. However, it is also clear that photographic imagery should be supplemented by other techniques. For example, in terrestrial observations, noncoherent radar imaging has been shown to be capable of measuring sea-state and ice and snow areas, even when cloud cover makes such measurements impossible by photographic

other shorter wavelength techniques; and by using infrared techniques, it is possible to make radiance measurements from which surface temperatures and other properties can be inferred.

The simplest infrared instrument is the radiometer, and the simplest infrared orbital experiment would consist of a fixed radiometer monotoring the radiance profile of the orbiter's ground track. Greater sophistication could be added to the experiment by using a spectroradiometer rather than a wideband radiometer. The radiometer could be gimbaled to investigate angular effects and specific targets not on the ground track. A further refinement would be to use scanning radiometers capable of mapping the radiance over a wide strip centered on the ground track. Although such scanners are likely to be less sensitive than corresponding radiometers, they do offer some advantages: since the output could be processed to form an image, the results would be more directly comparable to those of other imaging sensors than would be the results of nonimaging radiometers; and the advantages (particularly for survey applications) of interrogating an area rather than a line are obvious. Gimbaled and nongimbaled radiometers and spectroradiometers have been recommended for both earth and moon orbiters; however, the present study is restricted to infrared scanners.

Consider a thermal scanner from the point of view of scanner technology. In section 3.1, it is shown that a scanner of straightforward design using a single-element detector and a single-faced scan mirror can be constructed. It would have an angular resolution of slightly better than 1 milliradian and a Noise Equivalent Temperature Difference (NE$\Delta$T) better than 1/2$^{o}$K for terrestrial operation or for most of the hot face of the moon. While many prospective experimenters would prefer a finer angular resolution, the corresponding ground resolution (1000 ft from a 200-mi earth orbit or 250 ft from a 50-mi lunar orbit) is adequate for many purposes. It is clear that finer angular resolution would necessitate a much more complex scanner. Also, the increased data rate would probably enforce restriction of surface area coverage in order to keep data bulk within reason. Thus, for initial survey experiments, the device described in section 3.1 appear ideal on the basis of current technology. Wavelength coverage could be extended by adding other detectors (filtered if necessary) either as alternates for the thermal band detector or arranged to scan a following or adjacent path. It is also possible to use a thermal band detector with a larger area; this would produce a sensor with poorer spatial resolution but higher sensitivity and would be useful for studies of the cold side of the moon. However, since estimates of cold side temperatures have recently been lowered, it is unlikely that the sensitivity would be adequate for accurate thermal mapping. Specialized second generation scanners should therefore be considered both for fine resolution and sufficient sensitivity for cold side thermal mapping. Some initial consideration is given to these devices in section 3.3.

The practicability of combining a scanner and a spectrograph has been established in reference 2, where it is recommended that separate scanner-spectrographs be designed for predominantly short and predominantly long wavelength applications, since the optimum angular resolution for the former is five or six times greater. However, the possibility of a compromise instrument covering the range from 0.35 to 14.5 $\mu$ is also indicated. In reference 4, a design for an instrument covering the 0.35- to 13.5-$\mu$ range is developed. Although this design would be inadequate for some proposed experiments, there is little doubt that the instrument would be ideal for preliminary survey purposes. The design is discussed in section 3.2, where we point out that it lends itself to modification for special applications by allowing straightforward changes in the slit size and dispersing element.

The ground resolution capabilities which have been proposed for the medium resolution scanner (typically 1000 to 4000 ft for earth orbits) will be adequate for many applications, but others will require a much finer instantaneous field of view (FOV). For example, in assessing crop acreage, a resolution on the order of an acre (~200 ft) appears reasonable. In detecting forest fires or determining individual tree size, it will be necessary to observe areas as small as 20 ft. While this may be unrealistic from a 200 nmi terrestrial orbit, 200 ft not only appears reasonable but almost essential for a wide range of highly promising applications. As a result, a low resolution scanner (3 milliradians) and a high resolution scanner (1/6 milliradians, ~200 ft) limited to a $2.3^{\circ} \times 2.3^{\circ}$ total FOV have been proposed in reference 3.

## 2.2. PROPOSED TERRESTRIAL APPLICATIONS

The major areas of terrestrial orbital experimentation include geography, geology, agriculture, forestry, hydrology, wildlife management, oceanography, air pollution, and archaeology. A great many experiments of more or less potential benefit have been recommended, each requiring specific measurement parameters and instrument capabilities [3, 5]. However, there are enough instances of overlap among these disciplines to indicate that remote sensors can generate data applicable simultaneously to many of them. Much of the data will be spatial, dealing, for example, with the extent of crop planting, the area of a flood's effect, political and sociological boundaries, or the generation of accurate topographic base maps. In many instances, synoptic coverage will be required, such as for a world vegetation inventory for a study of biomass or forestry resources, and it may be desirable to sacrifice high resolution in order to obtain timely coverage at a tolerable data rate. In other applications, such as small scale mapping, studying an individual lake or river basin, or surveying crops, a resolution element on the order of an acre or less (~200 ft) will be required. This would not be sufficient for detecting individual animals for agricultural or wildlife studies, but it would be possible to accomplish

such major goals as identifying crops, assessing acreage allotments, and predicting crop yield, maturity, and health. In forestry, no world-wide inventory has ever been obtained; a synoptic coverage at this resolution could yield valuable information on the location, distribution, density, potential yields, and diseases of, and damage to, the world's forests. A world vegetation map including such important parameters as surface-soil temperatures, evapotranspiration rates, and $CO_2$ content of surface air would be useful for energy balance studies. In water resource studies, measurement of the extent and distribution of snow and ice, of flooded areas, of the extent and depth of soil freeze, permafrost, and lake and river ice, and of the topology of streams and watersheds should be practicable with this resolution. It should be possible to delineate surface temperatures and ocean currents. In geology, the detection and delineation of fractures, folds, lineaments, domes, basins, faults, and ore deposits may be practicable under appropriate conditions. The study of the ozone content in the atmosphere above large cities may provide a means of evaluating air pollution. In archaeology, large-scale markings may be used to identify important sites.

Studies of soil composition, vegetation species, and the health and potential yield of agricultural crops will require multispectral sensing in as many wavelength bands as practical. A wide variety of experimental designs have tentatively designated a minimum of five bands in the 0.3- to 16 $\mu$ region [4].

## 2.3. PROPOSED LUNAR APPLICATIONS

For remote sensing of the lunar surface from a lunar orbit, the preliminary goals are somewhat more fundamental, concerned with such problems as surface structure and composition, temperature measurements, and possible volcanic activity, all of which may contribute to our understanding of the origin and history of the earth-moon system. Much of the confusion and conflict with respect to the interpretation of lunar data arises from the fact that all evidence for the physical nature of the moon has been obtained indirectly through inferences drawn from reflected and emitted radiation. In general, average characteristics of large areas of lunar terrain have been compared to those of laboratory-size samples of terrestrial materials.

The answer to the question of the moon's origin is fundamental to a better understanding of the terrestrial planets. A great many theories have been advanced, all of which depend upon knowledge of lunar composition, mass, internal temperature, and possible volcanic activity. Significant information concerning, for example, the formation of the maria may be obtained from high resolution photographic or infrared surveys of the Imbrium Basin, including the Jura, Teneriffe and Spitzberger Mountains, the Apennines, the Alps, the Rümker Hills, and Sinus Iriduim. Specifically, Mt. Hugens, the highest mountain of the Apennines, has a steep slope

facing the Basin which may provide a record of subsurface layering; an investigation of this area may indicate the composition and nature of the mountain, the composition of maria material, and surficial keys to subsurface structures such as faults, fractures, and thermal anomalies.

If there is any appreciable volcanic activity present on the moon today, infrared imaging techniques could detect its surface manifestations better than any other known remote sensing method. Even discounting present-day endogenous thermal activity in surficially detectable amounts, the exsistence of surface or subsurface faulting may still be discernible because of differing values of thermal conductivity or specific heat. Such features may be expected to appear as linear anomalies on the infrared image. There are numerous lunar surface details which seem to indicate volcanic activity; many subtleties of morphology, discoverable only through high resolution inspection, might be used to distinguish between volcanic and impact events. General surface details which should be inspected include the many rilles (especially crater rilles), chains of craters, various crater alignments, central and rim mountains displaying summit pits, polygonal craters, onray craters, interray structure, summit pit domes, and fault and fracture patterns.

Terrestrial maars often tend to be aligned in rows. Usually there is no geolcgic surface feature connecting the various craters, but subsurface detail becomes apparent in infrared imagery. In terrestrial basaltic areas, basaltic domes with summit pits are common. Thus, the composition of lunar areas with similar domes may be an important key to their origin and history. Compositional effects may also explain differences in lunar albedo and color as well as the many thermal anomalies detected. It is reasonable to assume that there is considerable inhomogeneity, but that resolution limitations and consequent averaging effects would preclude accurate evaluation through earth-based observations. High resolution photographic, infrared, multispectral, and microwave techniques will be required to assess the myriad local variations which probably contribute to observed behavior.

# 3
# PRELIMINARY DESIGN

## 3.1. MEDIUM RESOLUTION SCANNING RADIOMETER

3.1.1. GENERAL DESCRIPTION. This instrument is a dual-resolution scanning radiometer capable of operating at resolutions of 0.7 and 3.2 milliradians in order to give useful temperature sensitivities over the extreme range of lunar surface temperatures. For earth orbital operations, the low resolution mode, designed for use on the dark side of the moon, may either

be omitted or used simultaneously with the higher resolution mode to give an increased temperature sensitivity. The detector used for the higher resolution mode on the illuminated side of the moon will be filtered to eliminate reflected solar radiation below 5 $\mu$ and the detector used for the low resolution mode may either be filtered or unfiltered. Both detectors will be mercury-doped germanium, mounted beside each other in the same cryostat. Mercury-doped detectors are selected because their spectral response matches the spectrum of the thermal emission from the earth and from the hot side of the moon. The use of Ge:Cu or Ge:Zn detectors which operate out to 25 and 40 $\mu$, respectively, would, however, be advantageous for orbital operation over the colder parts of the moon, because these detectors make a much better match to the emission spectra of sources at cold-side temperatures. Unfortunately, these detectors must be cooled to the temperature of liquid helium rather than liquid neon or hydrogen. This compounds greatly the problems associated with the cryogenic system; therefore, these longer wavelength detectors are not considered for the medium resolution radiometer design. Although the radiometer is intended primarily to operate out to approximately 13.5 $\mu$ in the broad spectral band of emitted radiation, a limited multispectral capability may be acquired by including additional detectors, either filtered or unfiltered. However, for the design considered here, these detectors must be compatible with the cryogenic system required for the Ge:Hg detectors, which must be operated below approximately 35$^{o}$K. Alternatively, fiber optics may be used to slice the image at the first focal plane and relay part of it to the additional detectors without obstructing the primary optical path.

Figure 1 is a sectional view of the optical layout chosen for the radiometer. In operation, the incoming radiation is deviated 90$^{o}$ by the large flat scanning mirror M1 and is then focussed by a folded telescope consisting of a positive primary mirror M2 and a negative secondary mirror M3. The radiation is then folded and reimaged on the detector by the mirrors M4 and M5. Scanning is achieved by rotating the drum containing the scanning mirror and telescope with an electric motor. The motor drive includes an optical shaft-angle encoder which continually monitors the drum position and provides the scan-angle information required to synchronize the visual display of the radiometer signal. Since only one fourth of each revolution of the scanner is used for thermal mapping, there is ample "dead time" during which instrument calibration may be accomplished. The detailed considerations involved in providing accurate calibration signals are discussed in section 5.6; the basic components required are a calibrated source of radiation and some means of optically substituting this source into the field of view of the detector. The calibrated source consists of several blackbody sources (only one of which is shown) operating at different temperatures to cover the range of radiation levels encountered in operation. These sources are alternately viewed by the small scan-

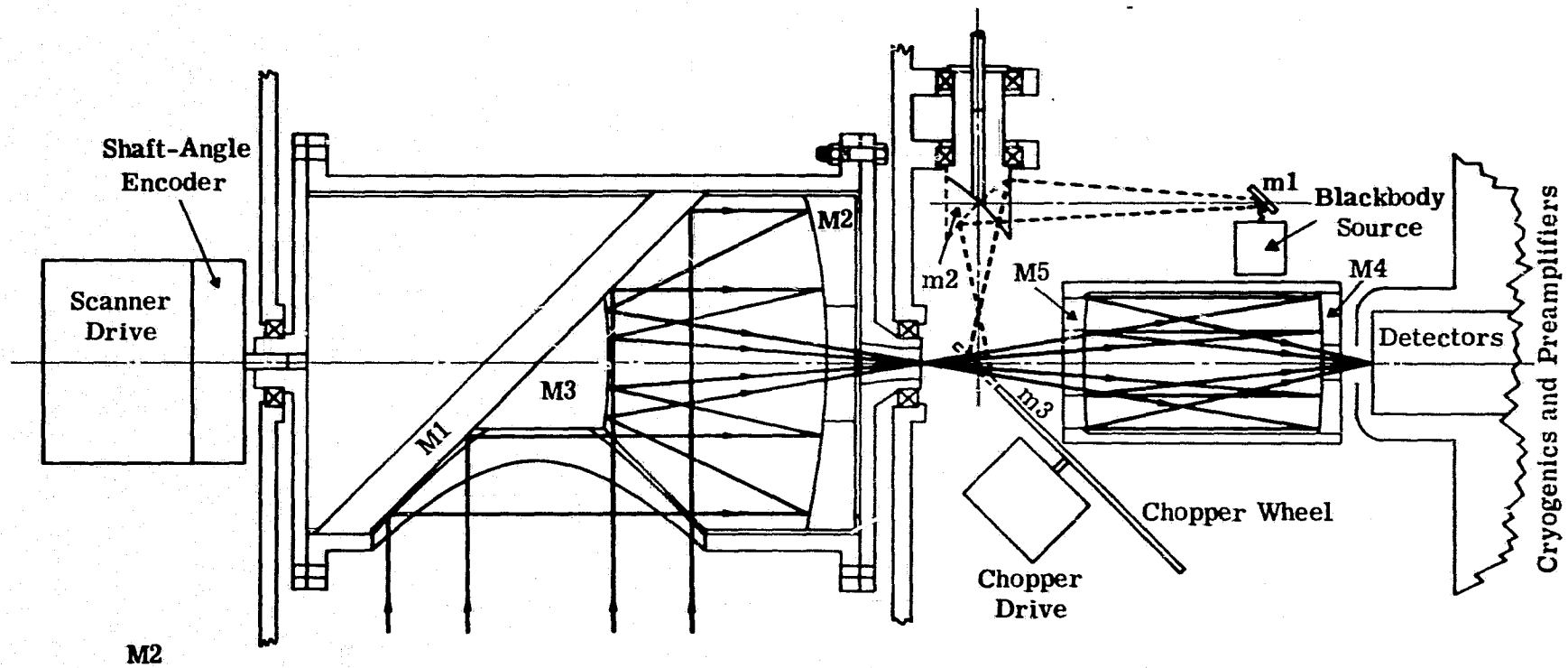


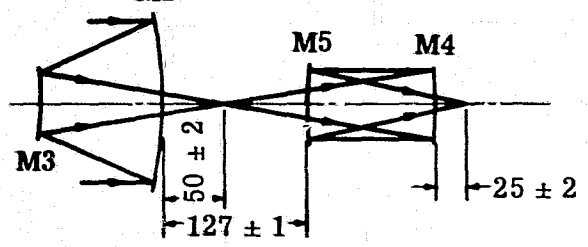


Dimensions and Tolerances

| Mirror | Type | Focal Length | Diameter |
|---|---|---|---|
| M1 | Plane | - | 170 |
| M2 | Paraboloid | 165 | 165 |
| M3 | Hyperboloid | 57-157 | 65 |
| M4 | Paraboloid | 195 | 70 |
| M5 | Paraboloid | 143 | 65 |
| m1 | Plane | - | - |
| m2 | Ellipsoid | 50-150 | 32 |
| m3 | Plane | - | - |

All Dimensions in Millimeters

FIGURE 1. OPTICAL LAYOUT OF THE RADIOMETER

ner containing mirror m1 and m2 and inserted into the field of view of the detector by the reflecting surface of the chopper m3, which simultaneously blocks the external radiation from the scanner.

### 3.1.2. DESIGN CONSIDERATIONS

3.1.2.1. Optics. The first consideration in determining the physical layout of the optics (once the aperture and the effective focal length have been specified) is the means by which scanning is to be accomplished. In order to achieve an angular field of view of $90^{o}$ with the required resolution, it will be necessary to accomplish scanning in the object plane, thereby limiting the otherwise wide choice of scanning techniques. In practice, wide-angle object plane scanning has been successfully accomplished using single or multifaced plane mirrors rotating about an axis which is either parallel or perpendicular to the optical axis. Although a multifaced plane mirror has several advantages where high-speed scanning is required, it also has serious disadvantages where good resolution and high sensitivity are required. In particular, this mirror may introduce spurious signals because of variations in reflective characteristics across its surface, since different portions of it are used as the scan angle changes. In order to avoid these difficulties, a single-faced scanning mirror rotating about the optical axis was chosen.

The normal configuration for this type of scanner includes a drum which supports the scanning mirror rotating inside two large bearings, with the telescope optics outside of the drum. For rotational speeds in the vicinity of 2,000 rpm (used in the present application), bearings with the required diameter would present no problem in a normal airborne environment. However, space-qualified bearings fall short of the size requirements, so that the use of an alternate configuration is necessary. For this reason, the telescope is included with the scanning mirror in a revolving drum, thus reducing appreciably the size of the bearings.

An f/1.0 primary mirror was chosen for the telescope in order to keep the length of the drum as short as possible; the remaining optics were chosen for compactness as well as ease of insertion of the components required for calibration. Although each nonplane element would normally be an aspheric, it may be practical to substitute spherical mirrors for one or more of these aspherics without compromising the optical performance. The effective aperture (15 cm diameter) for the scanner is established by mirror M5, while the effective focal length of 33.3 cm is determined by a combination of the four mirrors M2 to M5. The telescope has an effective central obscuration of 7.5 cm which is established by the size of the hole in mirror M5. This central obscuration reduces the amount of signal power to the detector by 25%, and

although this loss could be reduced by modifying the design, the modifications considered increased the size of the system. Therefore, a compromise was required, and we feel that the present system represents a reasonable balance between the conflicting requirements. For the optical layout shown in figure 1, vignetting will not occur within six milliradians of the optical axis, thereby allowing for slight errors in alignment and the insertion of additional detectors in the focal plane.

3.1.2.2. Calibration. In order to provide accurate calibration for the radiometer throughout the wide range of surface temperatures (from <100° to approximately 400°K) which will be observed during an orbit of the moon, calibrated radiation sources which cover this range will be required. Since the radiometer will view areas where the surface temperatures may vary by as much as 50°K along a single scan line, a single blackbody source whose temperature is slowly varied during the orbit will not be adequate, and one whose temperature is cycled at a relatively high rate would be impractical for several reasons. Therefore, it was decided that a number of sources operating at different temperatures should be used. The design chosen provides a reasonably compact system and permits the completion of calibration using several reference sources after each scan in a relatively short time. Although mirror M1 could be eliminated from the calibrating system, it is included to provide, so far as possible, the same mirror losses which occur in the scanner. The effects of deterioration of mirrors in the space environment will tend to be annulled, provided that all the mirrors deteriorate in the same way.

As an alternative, two thermoelectrically controlled blackbodies might be used. The temperature of these would be controlled electronically so that the calibration signals they produce would bracket the video signals being received. A fairly fast control system would be required because of the rapidity with which the temperature of the surface being overflown can change during either earth or lunar orbits. It is doubtful whether this technique would be satisfactory for the cold side of the moon where it will probably be necessary to use special equipment (see sec. 3.3).

3.1.2.3. Geometrical Parameters: v/h and Resolution. The scanner rotation rate r is linked with the v/h by the following equation:

$$r = (v/h)/\beta$$

where $\beta$ is the angular resolution. The required electrical bandwidth $\Delta f$ is related to v/h as follows:

$$\Delta f = \frac{\pi r}{\beta} = \frac{\pi (v/h)}{\beta^2}$$

It is important that r be kept as close as possible to the above value in order to maintain contiguity of scan lines. The v/h will vary with orbital paramcters and, for an elliptical orbit, will vary continuously during each orbital period. Figure 2 shows the v/h as a function of orbital altitude for both lunar and terrestrial orbits. Based upon minimum satellite altitudes of 200 mi (earth orbit) and 50 mi (lunar orbit), the maximum v/h ratios will be 0.024 and 0.021, respectively. These quantities will fix the rotation rate and bandwidth requirements.

Earth Orbit: $V_E = 1.112 \times 10^6 (3959 + H)^{-1/2}$

Lunar Orbit: $V_L = 1.235 \times 10^5 (1060 + H)^{-1/2}$

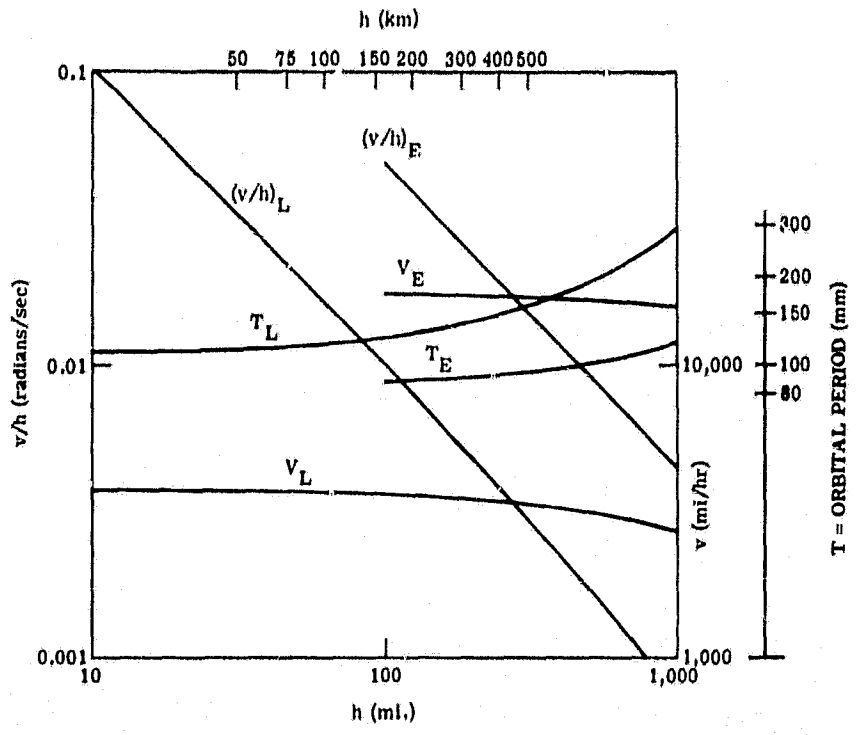


FIGURE 2. ORBITAL PARAMETERS

The resolution, $\beta$, is limited by a constellation of variables. These include the detector diameter,

$$d = \beta FD$$

where F = the f number of the beam at the detector

D = the diameter of the collector minor

the signal-to-noise ratio,

$$SNR \propto \frac{\beta^2 D}{F}$$

and the detector time-constant T

$$T \leq \frac{1}{2\pi \Delta f} = \frac{\beta^2}{2\pi^2 (v/h)}$$

Since it is desirable to maximize the SNR, D should be a maximum and F a minimum (and it is usually desirable that $\beta$ be small, although this degrades the sensitivity). However, F must be large enough to keep d reasonable. The limitations on D are such that a reasonable maximum is 15 cm. Detector diameters must not be less than 0.025 cm for purposes of fabrication. Assuming that D is maximized and d minimized, $\beta$ may be plotted against F, as in figure 3. Likewise, with D and d fixed, $\beta^2 D/F$ may be plotted against F (figure 4).

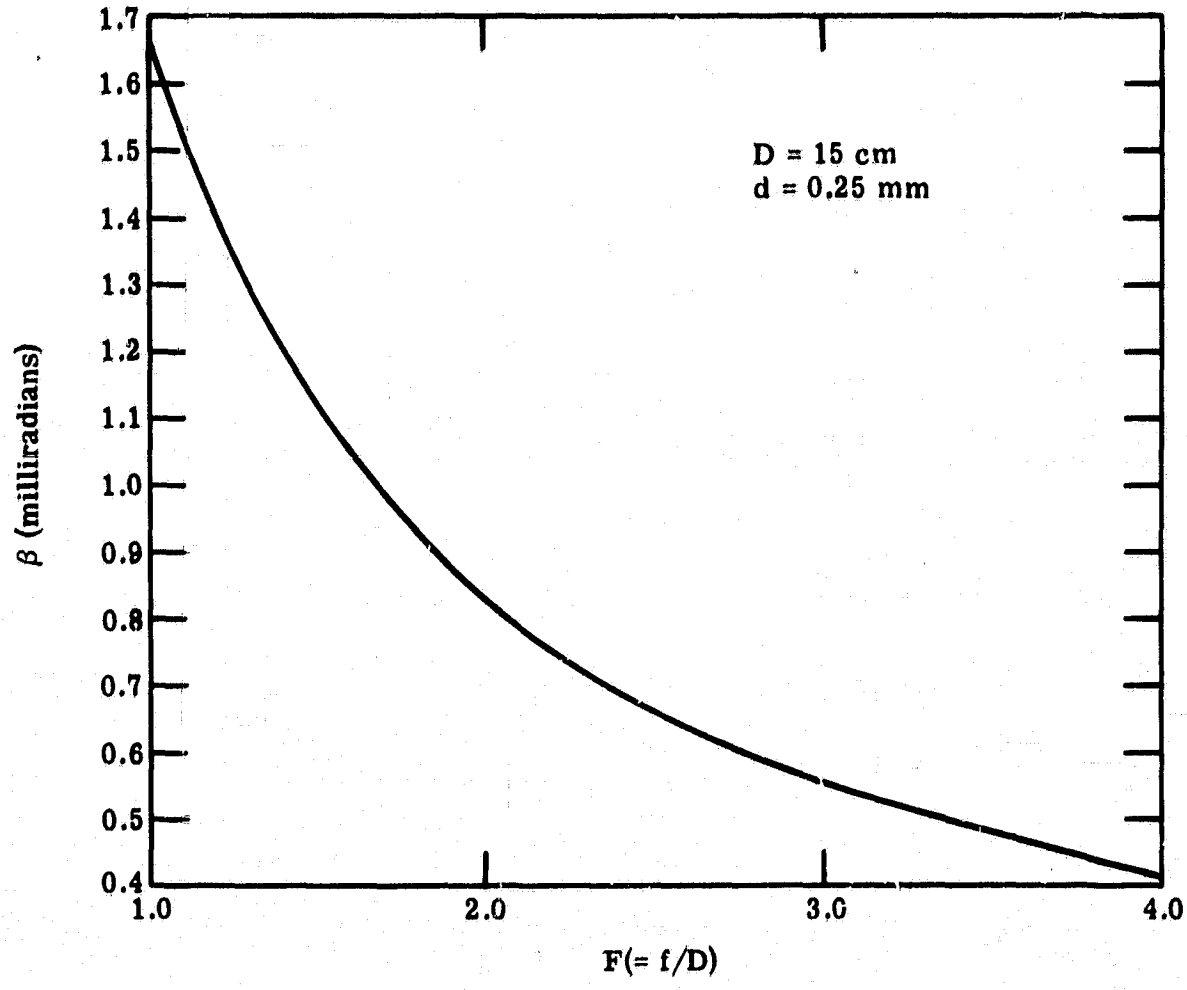


FIGURE 3. RESOLUTION $\beta$ VERSUS f NUMBER

Performance curves for scanning radiometers are developed in appendix II. It is shown also in this appendix that the limited dynamic range of the recording system imposes constraints in addition to those imposed by the inherent sensitivity. It is shown in appendix II that if the

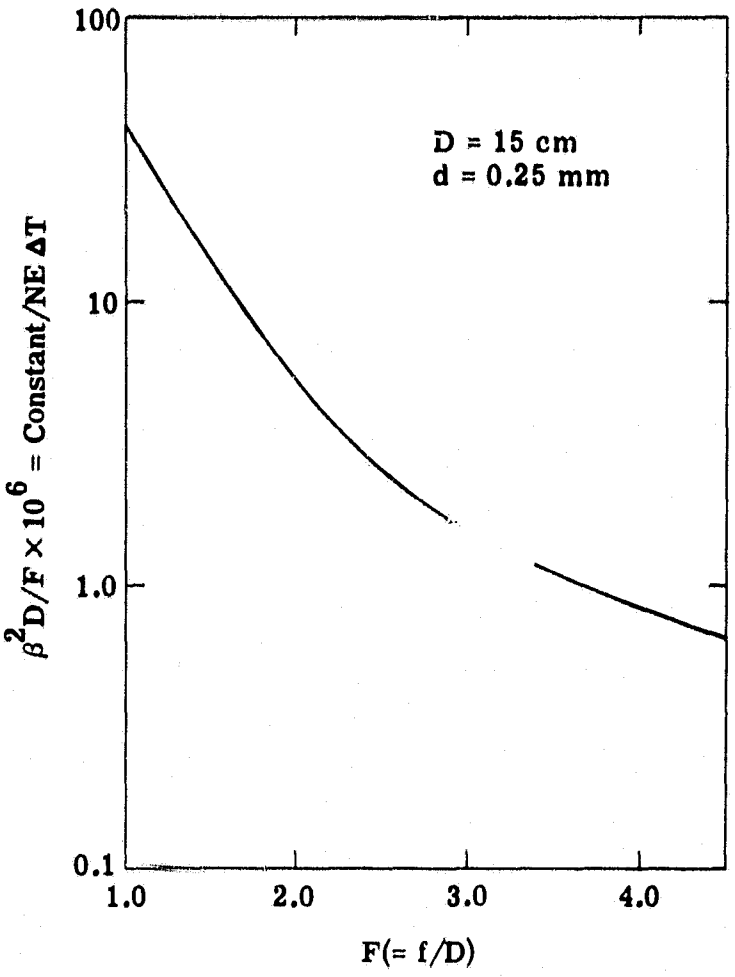


FIGURE 4. NE ΔT VERSUS f NUMBER. The NE ΔT is 1°K for a target temperature of 200°K.

recorder has a ten-bit dynamic range, then $\beta^2 D/F = 3 \times 10^6$ gives essentially full coverage of the sunlit side of the moon (from 100° to 200°K) with an NE ΔT ≦ 1°K. Using figures 3 and 4 would call for F = 2.4, and thus $\beta$ = 0.7 milliradians. Similarly, with $\beta^2 D/F = 64 \times 10^{-6}$, full coverage of the moon's dark side from 0° to 220°K could be obtained, with NE ΔT ≦ 1°K for all temperatures greater than 130°K. Here it would seem desirable to fix F at 2.4 so that the same optics may be used, and to choose that value of $\beta$ which would give the desired performance. Thus,

$$\beta^2 = \frac{64 \times 10^{-6}}{D/F}$$

or

$$\beta = 3.2 \text{ milliradians}$$

### 3.1.3. PERFORMANCE CONSIDERATIONS

3.1.3.1. Spectral Bandwidth. The spectral bandwidth of the scanning radiometer is selected to eliminate, as far as possible, reflected solar radiation and to conform to the wavelength limitations of practical detector-cooler combinations.

It is impossible, of course, totally to eliminate the reflected solar radiation on the sunlit side of the moon. On the dark side, it is not unreasonable to leave the short wavelength region unfiltered for the cold side detector. On the other hand, the sunlit side poses problems for the hot side detector. A reasonable criterion would be to require that the signal-to-noise ratio generated by the reflected sunlight $(SNR]_{solar}$ should be less than unity. In figure 5, $SNR]_{solar}$ is plotted against $\lambda_0$ (where $\lambda_0$ is the short wavelength cutoff) for the hot side radiometer. It may be observed that $\lambda_0 > 5\ \mu$ gives $SNR]_{solar} < 1$, which is the desired result. On this basis, $5\ \mu \leq \lambda \leq 13.5\ \mu$ was chosen as the wavelength region for the hot side sensor and $\lambda \leq 13.5\ \mu$ was chosen for the cold side sensor.

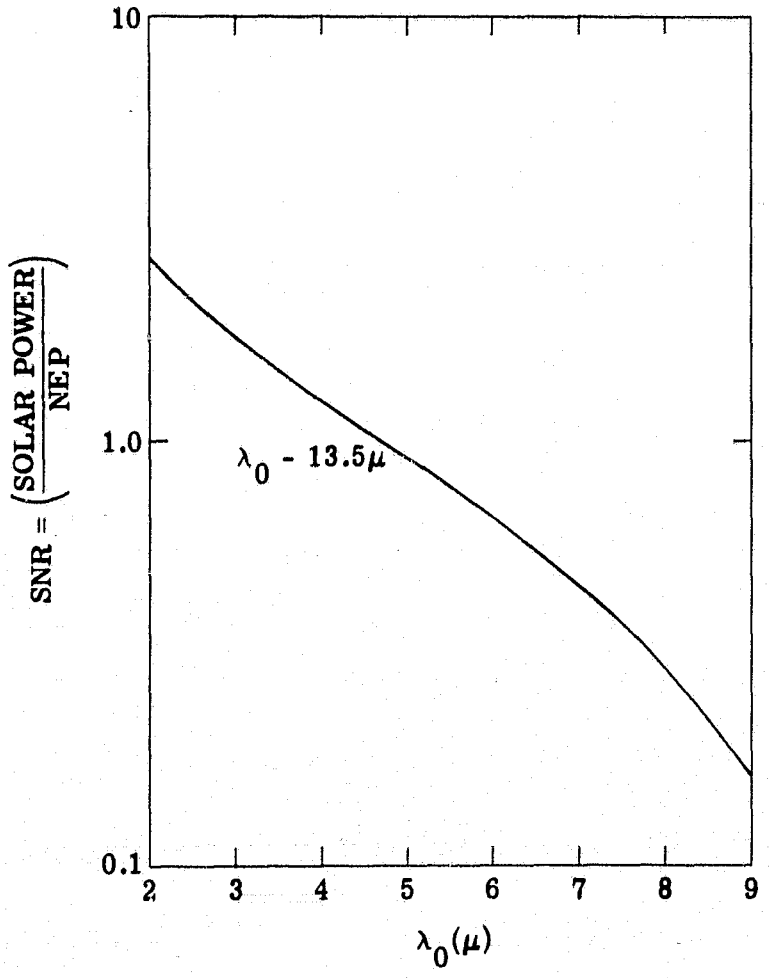


FIGURE 5. REFLECTED SOLAR RADIATION SNR VERSUS SHORT-WAVELENGTH CUTOFF

3.1.3.2. Sensitivity. The radiometer will possess two channels, one for measurements below 220°K and the other for measurements from 200° to 400°K, with the NE$\Delta$T $\leqq$ 1.0°K for all temperatures exceeding 130°K (see fig. 6). Complete parameters are as follows:

| Parameter | Cold Side | Hot Side* |
|---|---|---|
| resolution $\beta$ | 3.2 milliradians | 0.7 milliradians |
| wavelength region $\Delta\lambda$ | 0-13 $\mu$ | 5-13 $\mu$ |
| rotation rate r | 6.6 r/sec | 30 r/sec |
| electronic bandwidth $\Delta$f | 6.5 kHz | 135 kHz |
| information content | 10 bits/word | 10 bits/word |
| dwell time | 485 $\mu$sec | 23 $\mu$sec |
| f number F | 2.4 | 2.4 |
| collecting aperture D | 15 cm | 15 cm |
| NE$\Delta$T | (see fig. 6) | (see fig. 6) |

For a more detailed discussion of the factors which bear upon radiometer performance, see appendix II.

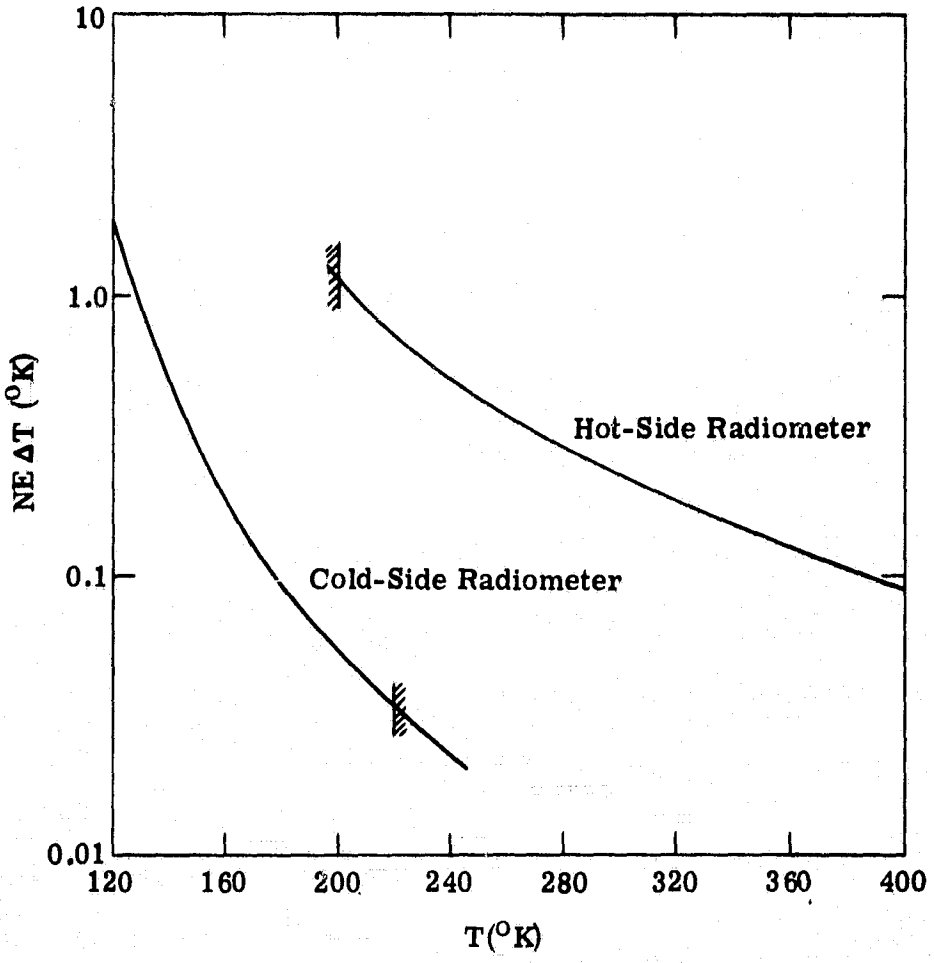


FIGURE 6. NE$\Delta$T VERSUS SOURCE TEMPERATURE

*This system is also recommended for terrestrial orbital experiments.

3.1.3.3. Electronic Bandwidth. The electronic bandwidth of the preamplifier system must be flat for all frequencies from well below the scan rate r to the frequency corresponding to the element rate $\left(\frac{1}{2} \times \frac{2\pi r}{\beta}\right)$. Thus

$$\Delta f \cong r(\pi/\beta - 1)$$

Since $\pi/\beta \cong 10^3$ in all cases, the bandwidth may be taken as $\pi r/\beta$. This is the value used in the calculations in this report. Utilizing the contiguity relation, this becomes:

$$\Delta f = \frac{\pi(v/h)}{\beta^2}$$

In figure 7, $\Delta f$ has been plotted against $\beta$ for the v/h for typical earth and lunar orbits.

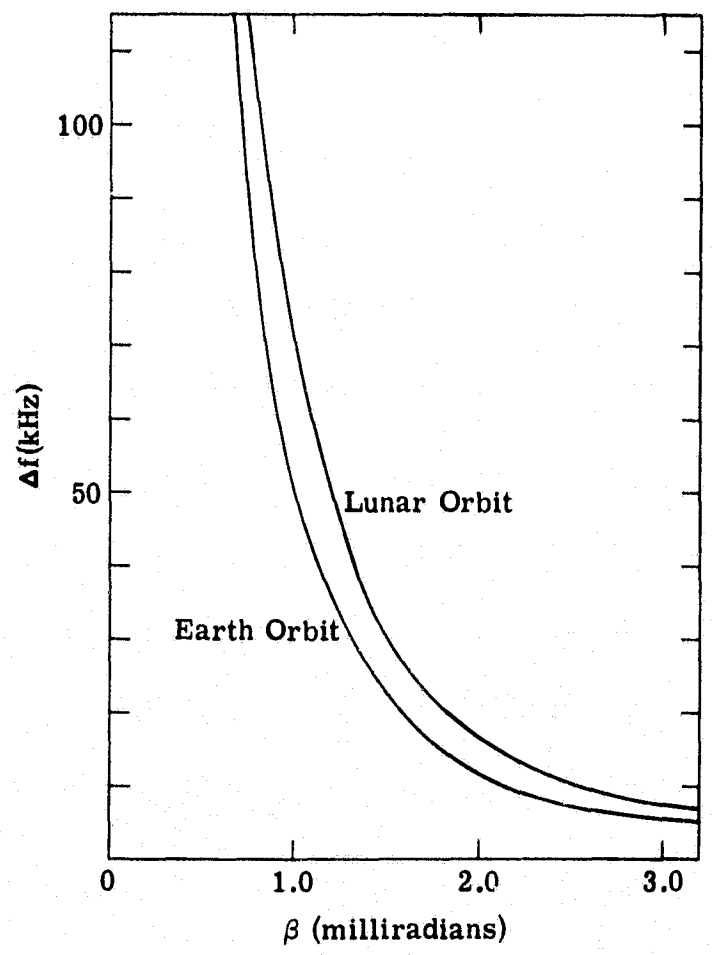


FIGURE 7. ELECTRONIC BANDWIDTH REQUIREMENT

3.1.3.4. Drum Assembly and Drive. The actual construction details of the drum assembly are not specified here, but there are several mechanical considerations which, because of their nature, should at least be mentioned. Centrifugal loading produced by rotation will cause the

scanning M1 mirror to bend. This bending must be limited in order to obtain the desired resolution, and the mirror should be made to have as high a stiffness-to-weight ratio as is practicable. Of the known and available materials, beryllium has by far the highest stiffness-to-weight ratio and appears to be the obvious choice for this mirror. The use of honeycomb or similar type of construction results in much higher stiffness-to-weight ratios than those obtained using a solid type of construction, but mirrors using honeycomb construction frequently lack the stability required for high resolution optical components, especially under conditions involving varying mechanical and temperature stresses. The scanning mirror should therefore be constructed of solid beryllium. The other two mirrors inside the scanning drum are not nearly as critical with respect to the stiffness-to-weight ratio, but in order to minimize the weight and to obtain the best possible match in thermal expansion coefficients, these mirrors, as well as the entire drum assembly, should also be made of beryllium. The remaining optical components, along with the supporting mechanical structure, might best be constructed using other materials, but because the operating temperature will almost certainly vary considerably, careful consideration must be given to the various thermal properties.

Although three separate driving motors are shown in figure 1, it may be possible as well as desirable to eliminate one or two of these. The calibration and chopper drives must be synchronized with the scanner drum in both speed and phase, but the speeds might, for practical reasons, be made integral multiples. Thus, the use of separate motors for each of these two drives would require angular position sensors and servo controls for each motor. Such motor drives are readily available, and their use would simplify the mechanical design, but probably at the expense of reduced efficiency and reliability. If a single motor were used, the scanner drive motor could be moved to the other end of the scanner drum and a belt employed to drive the drum. However, a direct coupling between the drum and the shaft-angle encoder should be retained in order to monitor the scan angle as accurately as possible.

## 3.2. MULTISPECTRAL SCANNING RADIOMETER

3.2.1. GENERAL. In section 2, it was shown that, in addition to the high resolution thermal scanner, there was need for spectral analysis of the radiation from all areas of the terrestrial or lunar surface. It was shown also that the wavelength range of such observations should be as wide as practicable. For terrestrial radiation, this range is limited by atmospheric absorption to 0.33 to about 13.5 $\mu$. Since the moon does not have an appreciable atmosphere, it would be desirable to extend the range to at least 30 $\mu$ in order to detect all appreciable thermal emission. The feasibility of using a scanner-spectrograph combination to obtain spectral and spatial information in one operation has been discussed in an earlier

report [2]. A preliminary design study for a system with a specific airborne application has also been completed [4].

Early in the present study, some work was done on alternative methods, in particular, methods using filtered detector arrays. With the latter, a modified scanning system is necessary to insure that each detector element scans the same scan line and that appropriate delays are put into each signal channel so that all the signals from a given target element are time coincident. However, the relatively low throughput of the K mirror (i.e., the necessity of using only high f numbers) was discouraging, and the principal result of this phase of the study was to emphasize the relative advantages of the scanner-spectrograph approach. We were further persuaded by the development of the folded-spectrograph optical system [4] which appears to resolve the problems of spectrograph optical design discussed in reference 1.

3.2.2. THE SCANNER-SPECTROGRAPH DESIGN. In developing an instrumental design for a specific purpose, it is necessary to consider both the requirements of the user and engineering feasibility. For space experiments, it is not possible to exactly specify either user requirements or engineering constraints. Few, if any, users know the optimum spectral or spatial resolution for given tasks; moreover, at the present time, the weight, space, and power available for experimental packages has not been specified. Thus, in practice, the development of specifications and designs has been carried out by trial and error in order to find the optimum solution.

In reference 2, the primarily short wavelength (0.33 to 2.5 $\mu$) requirements of the agriculturalists and the primarily long wavelength (8 to 14 $\mu$) requirements of the geologists are considered separately, and separate scanner-spectrograph designs are developed. These two system designs are found to be incompatible, since the short wavelength system had a much finer spatial resolution. It is pointed out, however, that a combined system would be quite feasible if a compromise were made with respect to the spatial resolution.

The advantages of using the widest possible wavelength coverage have since become apparent. Specifically, since the correlation between reflected and thermal spectra is not known, it should be studied for all classes of targets and backgrounds, and this can only be done satisfactorily by using a system which makes simultaneous and spatially coincident measurements covering both wavelength ranges. Thus, when the study reported in reference 4 was begun, consideration was restricted to a combined system with a spatial resolution of 2 to 3 milliradians. An optical system was designed using a rather large rock salt prism in a folded on-axis spectrograph. This design makes possible spectral resolution which is adequate for users specifically

interested in the visible and near visible regions. The resolution in the thermal infrared is probably more than adequate for users interested in temperature and certain emittance effects, though only adequate for the least stringent requirements of geologists and mineralogists concerned with restrahlen spectra of terrestrial or lunar rocks and soils. The design is so flexible, however, that it is recommended for intial use in spaceborne infrared experiments. In fact, finer spectral resolution over a limited spectral range could readily be obtained by making relatively minor changes in one or more of the following: image slicer, detector array, dispersing element, rotational speed of scan mirror, or entrance slit size. Of these, only the cooled detector arrays are inherently expensive and complex. The effect of changing the dispersing element is shown in figure 8.* Changes in spectral resolution resulting from changes in entrance slit size can be inferred directly because the resolved intervals are directly proportional to the slit width.

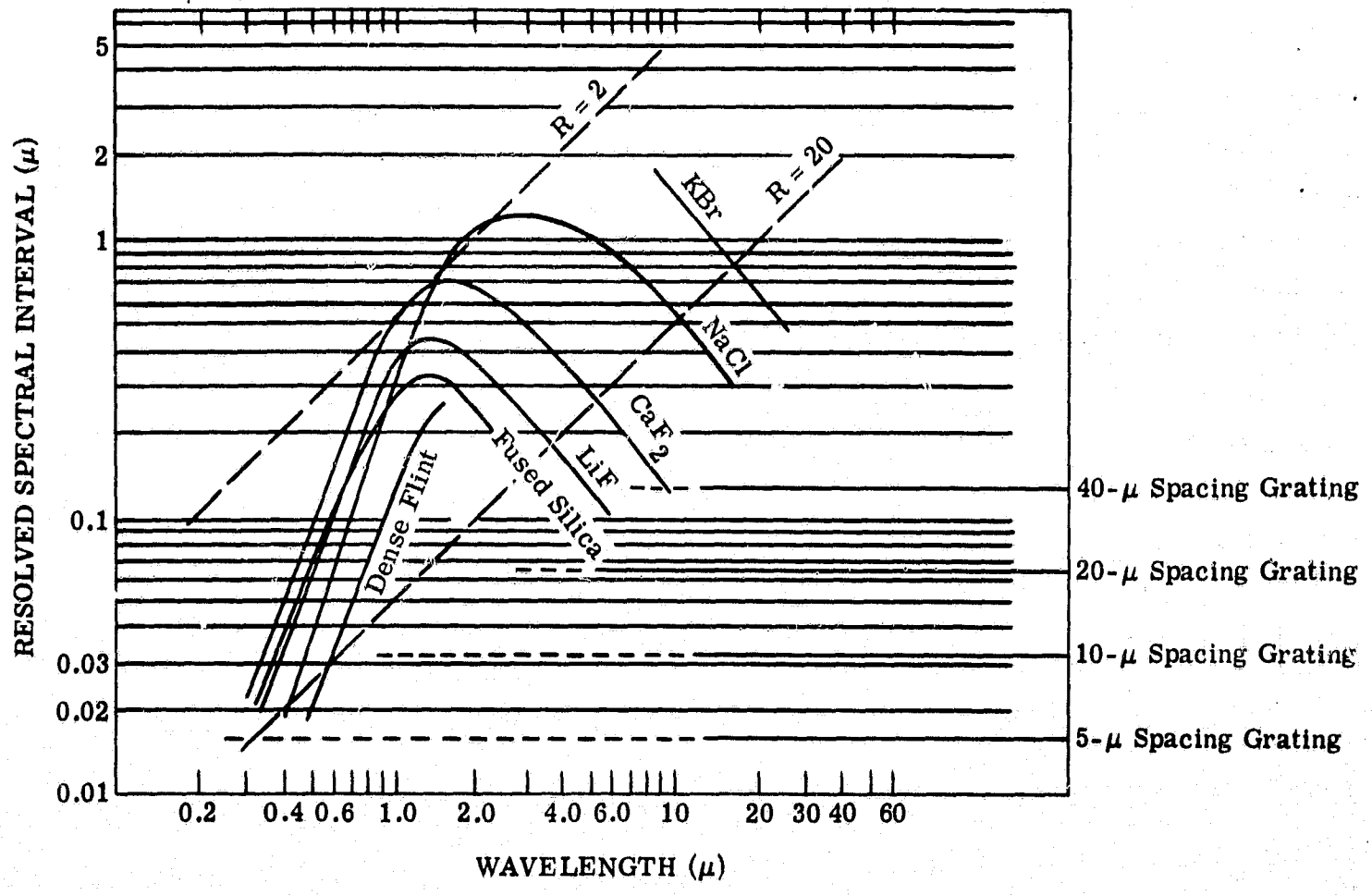


FIGURE 8. SPECTRAL RESOLUTION FOR VARIOUS DISPERSING ELEMENTS

*This figure is identical to figure 6, page 13, of reference 2, with the exception of a scale change which takes into account the new basic specifications.

The design of the folded-spectrograph system specifies 29 channels, but this number could be somewhat increased or decreased by making suitable changes in the detector arrays and image slicers. However, it should be noted that increasing the number of channels increases the data bulk and compounds the problems of data analysis and processing. This suggests that it would be inadvisable to carry out initial space experiments with the highest possible spectral resolution across the entire spectrum. A system with a relatively small number of channels covering the 0.33- to 13.5-$\mu$ band could be used for initial experiments. Higher resolution instruments with proportionately narrower spectral ranges could then be used for subsequent experiments which would be more specialized. In this way, the problem of handling the data would not be magnified when higher resolutions were used.

A preliminary design sketch for a 3-milliradian, 0.33- to 13.5-$\mu$ scanner-spectrograph is shown in figure 9.* No doubt several engineering changes will have to be made to make this system suitable for space operation; but most of these are dealt with in section 4. The present discussion is limited to a very brief description.

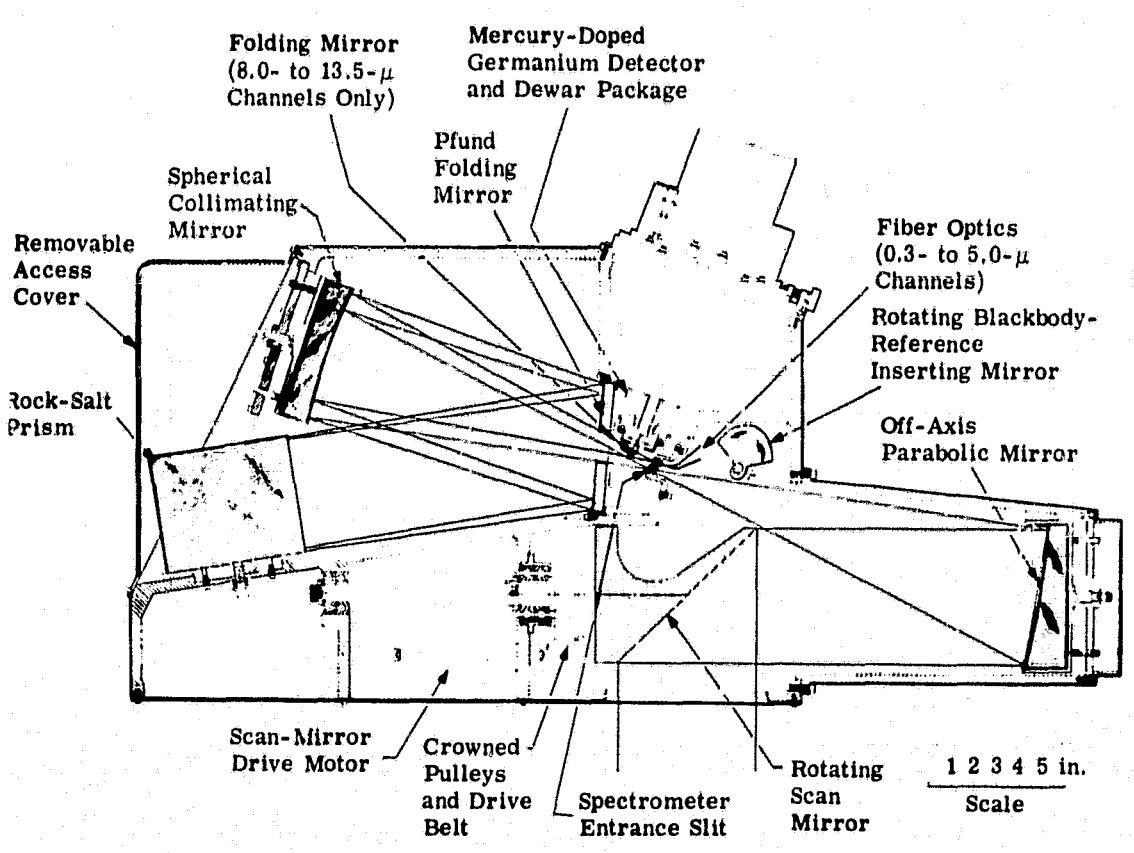


FIGURE 9. THE SCANNER-SPECTROGRAPH

*This sketch was originally prepared under another contract and is copied directly from the final report (ref. 4, p. 15), which also contains a detailed description of the design and the rationale for its selection.

The spectrometer entrance slit near the center of the diagram lies at the focal point of the off-axis parabolic mirror and thus defines the solid angle of the instantaneous FOV of the system. The rotating scan mirror causes this instantaneous FOV to scan a line on the surface beneath the scanner. As the vehicle moves across the surface, successive scans cover the adjacent and parallel strips normal to the vehicle's motion. The radiation entering the spectrometer is collimated and passed to the rock salt prism by the Pfund mirror. The rear face of the 30° prism is silvered, and the prism positioned so that the dispersed radiation returns to the Pfund mirror and thus to the collimating mirror. This mirror focuses the dispersed beam into a spectrum whose length is normal to the plane of the diagram and passes through the diagram just above the entrance slit. Figure 10 shows the wavelength distribution of the spectrum (ref. 4, p. 11). The spectrum is sliced by folding mirrors and a fiber optics array and transferred to an array of detectors. The only detector package shown in figure 9 is the mercury-doped germanium array, which covers the 8- to 13.5-$\mu$ region of the spectrum. (The cryogenic system would undoubtedly be modified in the space version—see sec. 4.3). The location of the shorter wavelength detectors is less critical because of the flexible fiber-optic relay system which can be used at these wavelengths. Radiation from thermoelectrically controlled blackbody reference sources would be reflected into the beam by means of the rotating mirror for calibration of the longer wavelength detectors. Standardized quartz-iodide lamps would be mounted on the scanner housing beside the scan mirror for calibration of the shorter wavelength detectors. Because of the absence of windage in the high vacuum of space, a much smaller and less powerful scan-mirror drive motor than the one considered in reference 4 would suffice. To minimize bearing and drive problems (see sec. 4.1), the motor should probably be made integral with the scan mirror shaft.

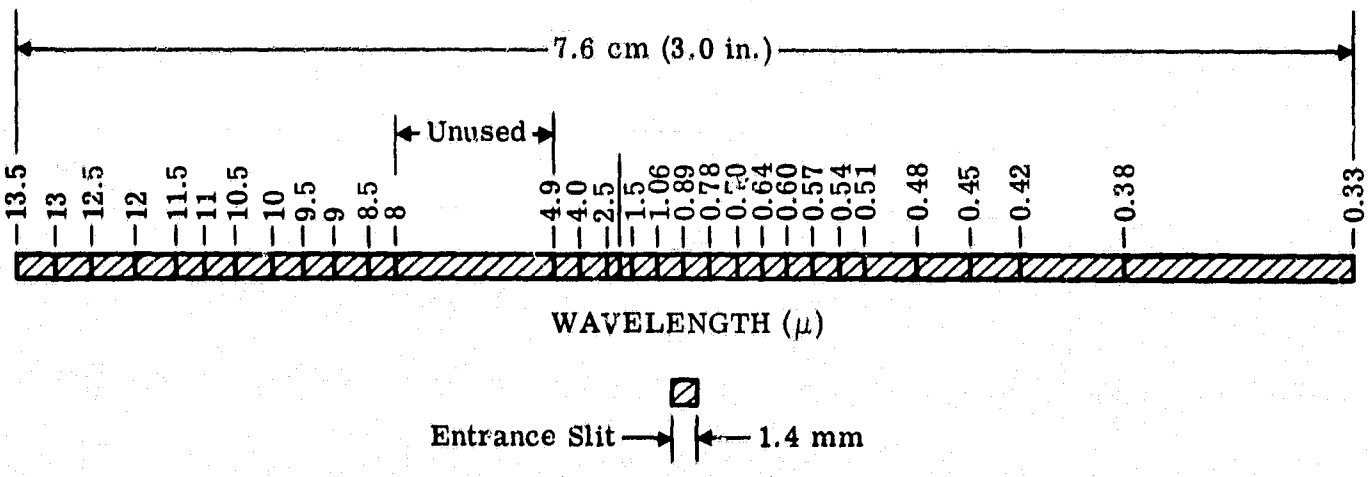


FIGURE 10. SPATIAL DISTRIBUTION OF THE SPECTRUM IN THE SCANNER-SPECTROGRAPH

## 3.3. SPECIAL PURPOSE SCANNING RADIOMETERS

The scanning radiometers described in the previous sections are general purpose scanners in the sense that they are based on compromises which produce results valuable to experimenters from any of several disciplines. The analysis of results obtained with such devices will probably indicate the need for special purpose scanners. Two specialized requirements are already apparent and are discussed briefly below. Since the detailed requirements for specialized scanners will become clearer as experimental work proceeds, and particularly when the results of early experiments are analyzed, they are considered here in a preliminary way only.

3.3.1. LUNAR COLD-SIDE RADIOMETRY. It is recommended in section 3.1.1 that a large area detector be incorporated in the medium resolution scanning radiometer to enable scientists to make measurements on the cold side of the moon. Recent estimates of the surface temperature, based on measurements from the earth, suggest that the cold side is colder than has been supposed, perhaps as cold as 70°K. If this is true (and a definitive answer presumably will become available from the results of experiments on the lunar surface within the next few years), the medium resolution radiometer probably will not be capable of making completely satisfactory measurements on the cold side. We can see this by examining the performance curves derived in appendix II. (The rationale for the preparation of these curves was based upon previous estimates of minimum cold side temperatures on the order of 120°K.) In particular, consider the high sensitivity channel of the medium resolution radiometer. Here $\beta$ is 3 milliradians, the aperture D is 16 cm, and F is 2.25. Thus,

$$\frac{\beta^2 D}{F} = 64 \times 10^{-6}$$

which corresponds to the most sensitive system considered. At a target temperature of 120°K, the NE$\Delta$T in this system is 2°K and is increasing rapidly with falling target temperature. In fact, it is clear that the NE$\Delta$T will be on the order of 100°K when the target temperature drops to the temperatures of interest (around 70°K). A two-orders-of-magnitude improvement is required, which could be achieved by increasing the resolution to 30 milliradians (nearly 2°). This instantaneous field, however, would not be compatible with the design described in section 3.1.1.

A more promising approach would be to use a longer wavelength detector such as zinc- or copper-doped germanium. This would involve a more elaborate cryogenic system than the one required for the mercury-doped detector of the medium resolution radiometer. It would also be desirable to cool the optics in order to minimize radiation noise caused by the small but not

negligible emissivity of the reflecting and obscuring surfaces. If a calibrated system is needed in order to make better estimates of surface temperatures, it would also be desirable to make this system more elaborate and capable of calibration at low temperatures. A useful and highly sensitive scanning radiometer designed along these lines appears to be practicable.

3.3.2. VERY HIGH RESOLUTION SCANNING RADIOMETER. The medium resolution scanning radiometer discussed in section 3.1.1 has a nominal angular resolution of 0.7 milliradians. From a $10^6$ ft orbit, this system should achieve a ground resolution of about 700 ft. As was shown in section 2.1, many experiments in orbital remote sensing of the earth's surface require considerably better ground resolution. Considering the sensitivity curves derived in appendix II, $\beta$ could be reduced to 0.35 milliradians (for d = 16 cm, F = 2.25) and still achieve an NE $\Delta$T of about $1^{\circ}$ at a target temperature of $280^{\circ}$K. However, even for this small gain in spatial resolution, serious practical difficulties arise. For example, the new parameters imply a faster rotation rate for the scan mirror, an increased information rate and data bulk, and probably a larger and heavier instrument. In fact, in order to obtain a worthwhile increase in spatial resolution, it would probably be necessary to use larger entrance apertures and multiple detectors. In order to maintain reasonable data bulk and limit mechanical complexity, it would also be desirable to limit the total FOV. Two approaches seem feasible:

(1) A linear array of detectors would be used in the focal plane of an optical mechanical scanner so that several adjacent lines were scanned at the same time. By limiting the total field and using either multiple scan mirrors or a nodding scan mirror, it would be possible to achieve reasonably high efficiency (duty cycle) while avoiding insuperable mechanical scanning problems.

(2) No mechanical scanning would be used. A fan-shaped FOV would be formed by placing a linear array of detectors in the focal plane of a suitable wide angle optical system. This FOV would be projected onto the ground to form a line perpendicular to the motion of the vehicle. The elements of this line would scan parallel strips on the ground as the vehicle moved along its path. The multiple parallel outputs of the detector array could then be processed to form a strip map.

The difficulty in 2 would be in fabricating and cooling the detector array and in packing and wiring the preamplifiers in such a way as to avoid cross talk and undue obstruction of the optics. Recent improvements in detector and cryogenic technology place the array and cryogenic problems well within the possibility of solution. Detector manufacturers claim that arrays containing hundreds of detector elements are now practicable. Similarly, recent progress in microelectronics had made it possible to have very small arrays of preamplifiers.

With both approaches, however, there appears to be considerable difficulty in introducing a satisfactory calibration system, but considering the requirements for high resolution scanners, accurate radiance calibration is probably of secondary importance.

# 4
# TECHNICAL PROBLEM AREAS

## 4.1. GENERAL

The most fundamental limitation of a passive electro-optical measurement system is the so-called photon noise in the radiant beam at the entrance aperture. The SNR determined by this effect can be written*

$$SNR = \tau P_S \sqrt{\frac{qt}{P_T}}$$

where $\tau$ = the transmission of the optical system

$P_S$ = the rate of arrival of signal photons at the entrance aperture

$P_T$ = the total rate of arrival of the photons at the detector

$q$ = the detective quantum efficiency of the detector

$t$ = the duration of the measurement

$\tau$, P, and t are determined by the design of the equipment and its mode of operation, while q is an intrinsic property of the detector over which the experimenter has no control. In practice, the SNR will be degraded in the amplifying and recording processes. At the present time, detectors are capable of q's of between 0.1 and 0.5 over most of the wavelength range of interest. A technical problem area is a set of closely related engineering problems which may prevent the limit imposed by the selected design parameters and best available q's from being approached in the practical application. Such problem areas fall into one or more of the following categories:

(1) The problems which exist whether or not the equipment is operated in a spacecraft or aircraft. This category covers two specific problems:

(a) The design must be optimized in order to make the best possible use of the best available detectors. The SNR produced by a scanner of given basic specifications will depend on its optical and electronic efficiencies. The design and fabrication should ensure maximization of these efficiencies.

*This equation is based on classical statistics. Strictly speaking, integrals over wavelength $\tau_\lambda P_\lambda q_\lambda$ should be used in deriving this expression, leading to a more complex result. However, the simple expression given fills the needs of the present discussion.

(b) Most scanners whose outputs are strip maps produce maps which are distorted in various ways, particularly at the edges. Often such distortions are of little consequence, but decisions must be made as to whether and to what extent they should be avoided or corrected.

(2) The problems which arise because of the logistics of space flight, especially those associated with data storage and transmission.

(a) Because of the extended duration of orbital flights and the vast area that can be covered, considerable quantities of data can be collected on a single flight. Recording all of this data may involve the use of an appreciable weight and volume of tape or film, and telemetry of the data to the ground may involve major problems. Returning the recorded data to earth may well tax the recovery system. Thus, inflight editing or some form of preprocessing to reduce data bulk would be desirable.

(b) There are weight and space limitations imposed on equipment by space vehicle logistics, but this problem seems to be relatively well understood, and the solutions and compromises required appear to be a matter of straightforward engineering. On the other hand, the need for very high reliability of every system, subsystem, and component must not be forgotten.

(3) The problems, created or greatly magnified by the orbital properties of satellites, which arise because of the distance from the surface under observation.

(a) The resolved length of a given angular resolution depends upon the distance; for example, a system with a 1 milliradian resolution gives a resolved length of 1 ft if used from an aircraft flying at 1000 ft. On the other hand, from a typical $10^6$-ft earth orbit, the resolved length is 1000 times greater, or 1000 ft. This should not be regarded primarily as a problem, however, but rather taken as an indication that it is unlikely that the value of orbital remote sensing can be directly inferred from the value of conventional airborne remote sensing. A well known illustration of this is the great meteorological importance of photographs of cloud formations taken from satellites; these photographs display weather patterns which cannot easily be pieced together from localized data gathered in more conventional ways.

(b) A very real problem in this category arises from the rapidity with which the temperature and solar illumination of the earth's or moon's surface changes as the satellite passes above these surfaces. For example, on a low inclination earth orbit, conditions change from twilight to midday in about 20 min; on a similar lunar orbit, the surface temperature may change by 200°C in about the same time. In aircraft operation, it is

usually possible to use fixed channel gains and biases and not impair the efficiency of the dynamic range of the recording technique; in other cases, it is possible to have operators set up the gains and biases during a preliminary pass over the target, knowing that surface conditions will not change materially during the interval between passes. Since neither of these possibilities exists in orbital operation, it will be necessary to use either preprogramming or some form of automatic gain control (AGC). It will also be necessary to use highly viable radiative calibration and referencing techniques in order to obtain absolute values for the radiances observed.

(4) The problems which result directly from the orbital environment, such as those associated with using bearings and lubricants in high vacuum and designing stable cryogenic systems for the infrared detectors which will operate reliably in a weightless environment. (It is interesting to note that operation in the high vacuum of space will have at least one important advantage: the windage problems associated with high speed mirror rotation in air will disappear. For this reason, and because of the difficulty of providing safe and efficient windows, the possibility of operating the scanners inside a manned orbiting laboratory is not considered in this report.)

The following sections treat specific problem areas in detail.

## 4.2. BEARINGS

It is well known that it is impractical to use conventional bearing and lubrication techniques in an outer space environment. We studied this problem by surveying the relevant literature and visiting the Lubrication and Wear Branch of the NASA Lewis Research Center.* The following discussion is based primarily on information gained during this visit.

Our purpose here is to relate the current state of bearing technology to anticipated space experiments which would utilize optical-mechanical scanning components. The following operating conditions would apply:

(1) Vacuums as low as $10^{-6}$ Torr (earth orbits) and/or $10^{-11}$ Torr (lunar orbits)

(2) 15-day missions with continuous operation

(3) Balanced heavy loads

(4) DN ≅ 50,000 mm-rpm (D is the bearing bore diameter, N is the rpm)

One of the questions about vacuum conditions frequently posed is, How can one visualize the effects of reduced vacuum upon a bearing? Two factors are significant in relation to the

*The visit was arranged by Edward E. Bisson of the Fluid Systems Components Division. Donald H. Buckley of the Space Environmental Lubrication Section and Herbert W. Scribbe of the Bearings Branch were also very helpful.

life of a bearing in a vacuum: the evaporation of the lubricant and the oxidation of the metallic surface.

The evaporation rate of a substance depends largely upon the mean-free path of the surrounding environment. At extremely high pressure, very few molecules escape from the substance because of the effective barrier imposed by the environmental medium. As the pressure is decreased, molecules begin easily to escape and significant evaporation occurs. By the time the pressure is down to $10^{-6}$ or $10^{-7}$ Torr, there is so little resistance that the evaporation rate becomes constant (functionally dependent upon molecular attractions, temperature, and other determinants of cohesiveness). An example of this is the evaporation rate curve for teflon shown in figure 11.

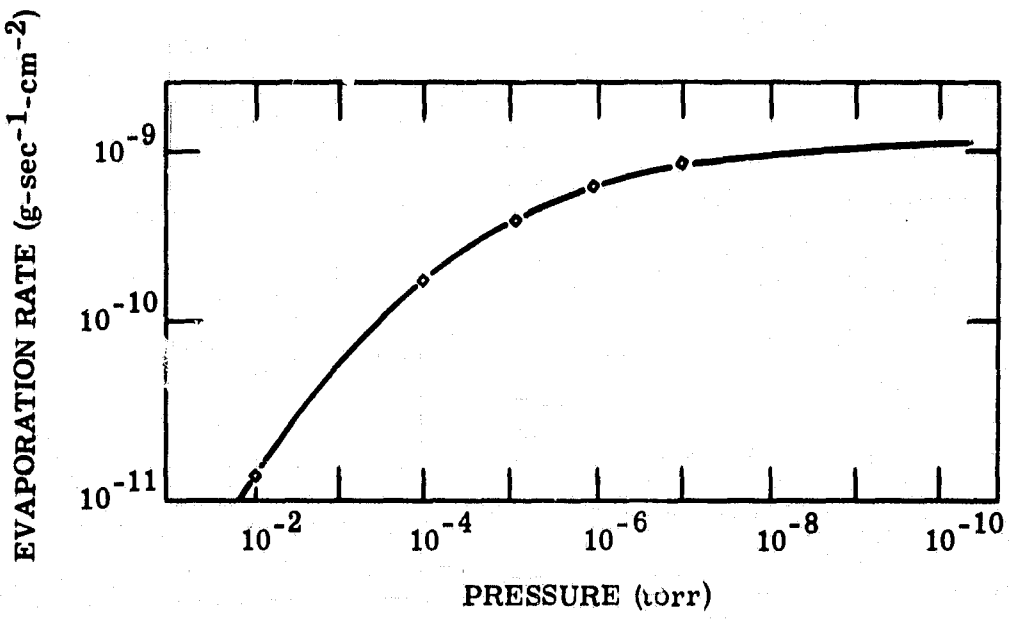


FIGURE 11. EVAPORATION RATE OF A TEFLON SURFACE

The oxidation of the metallic surface in turn depends upon two factors: the oxidation rate of an undisturbed surface (as a function of the partial pressure of oxygen) and the cleaning effect of the rolling elements. The first is shown in figure 12. The second will, of course, depend upon the application. In practice, it has been found that oxidation is not a problem with continuously operating rolling-element bearings if the rate of formation of oxide is less than 1 Å/min* which occurs at about $10^{-7}$ Torr (fig. 12). It should be noted that certain oxides, such as FeO and $Fe_3O_4$, are beneficial, but normal $Fe_2O_3$ is harmful because of its mechanical properties.

*It may prove desirable to provide an inert gas atmosphere for the bearings prior to the achievement of orbit.

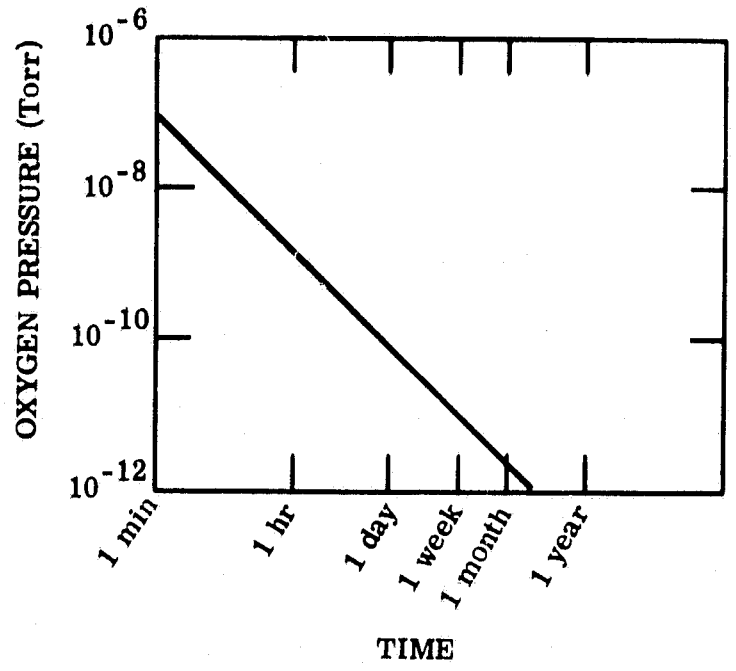


FIGURE 12. TIME FOR THE FORMATION OF A 1-Å LAYER OF FeO ON IRON

Another difficulty presented by vacuum conditions is the build-up of heat caused by the lack of conductive and convective energy exchange with the environment. Adequate heat dissipation can be accomplished by radiation using specially designed heat reservoirs with large exposed radiating surfaces.

A temperature rise in a bearing can be expected to reduce its operating clearances. Initial clearances must be enlarged in order to prevent subsequent seizing if a heat concentration is anticipated. In some cases, this could conflict with the necessity for precise alignments in certain optical instruments, but this is not expected to be a problem in a scanner because of the large separation between the support bearings.

Because of our application, the people at NASA Lewis tended to downgrade the value of hydrocarbon lubricants since vaporized lubricants may contaminate the optical surfaces. Although they have done considerable work on conventional hydrocarbon lubricants, the Lewis researchers are concentrating upon solid films because of their advantages with regard to bearing speed and bearing life. Certain space missions, however, have been carried out using liquids and greases as lubricants [6]. In fact, Bisson finds that this approach is feasible for medium duration missions [7].

In a vacuum, metallic surfaces are outgassed and tend quickly to become chemically clean. In the absence of protective oxide layers, contacting surfaces tend to adhere, i.e., to "cold-

weld." If there is not sufficient driving torque to break this weld, a catastrophic failure of the bearing will occur. On the other hand, if sufficient torque is available to shear the weld junctions and keep the bearing operating, the resulting rapid wear will shorten the bearing life considerably.

The purpose of a lubricant is, in part, to prevent cold-welding by dispersing a low-shear-strength film between all metallic contact points; shearing then occurs in the soft layer only, and damage to the basic metal is minimized. In the past, oil and grease films were used; today the emphasis is on metallic coatings or dry lubricant coatings which serve as the low-shear-strength interface. Researchers have found that vacuum-deposited gold and binder-free molybdenium disulfide ($MoS_2$) perform this role best. The effectiveness of these substances is a function of the tenacity with which they adhere to the base materials. Great adhesiveness of gold layers has been accomplished by cleaning the base material through ion bombardment in a vacuum and then depositing the film on the clean surfaces. This process appears to produce a molecular bond not unlike a cold-weld; $MoS_2$ however, is brushed into the surface after cleaning. Good results have been achieved with $MoS_2$ plus a sodium silicate binder applied with an air-brush to depths of a few Angstroms. Friction-and-wear measurements under vacuum conditions ($p < 10^{-6}$ Torr) have to date indicated that $MoS_2$ is the better of the two solid-film lubricants; intermittent-operation lifetimes of 250 hr and more have been experienced without failure or apparent increases in driving torque at DN ≅ 50,000 mm-rpm.

Where a binder or liquid lubricant has been used, there has been a tendency toward accumulation of residue in the bearing. This can cause roughness, high loads, and premature failure of the bearings. With greases, accumulation occurs when the oil has vaporized and only the soap or thickener is left, both of which do not lubricate. This problem has been circumvented in some instances by using oil-impregnated reservoirs with no thickeners. Similarly, elimination of the binders in solid lubricants disposes of the problem of the binder coagulating, which is detrimental to the bearing. As indicated above, $MoS_2$ can now be applied without a binder where formerly it was necessary to mix the lubricant with a phenolic resin, silicone, or silicate. At one time, so much difficulty was encountered because of build-up of the binder that $MoS_2$ was rejected as a useful lubricant. Metal films, if not applied in such a way as to produce effective cohesion, can flake and cause problems. Improvements in application techniques and reduction of the film thickness (0.0003 in. for gold film) seem to go far toward eliminating flaking and subsequent failure.

The following may be concluded from our discussion of bearings:

(1) Any problems likely to be encountered in lunar orbits will also be encountered in earth orbits.*

(2) Care must be taken so that the heat sinks and radiating surfaces are adequate for complete heat dissipation, since there will be no convection.

(3) Clearances must be adequate for avoidance of seizure of the equilibrated bearing.

(4) Hydrocarbon lubricants may be undesirable because of contamination of the scanner components. This, however, can usually be avoided through careful shielding of the system.

(5) Cold-welding and subsequent destruction of the bearings may only be avoided by maintaining at all times a protective low-shear-strength coating of all contacting metals.

(6) Accumulations of nonlubricating residues (soap, thickener, or binder) must be avoided for successful bearing operation.

(7) At the present time, the use of hydrocarbon lubricants with labyrinth seals to prevent undue loss and shields to prevent contamination of the optics appears to be a reliable solution to the bearing problem. The use of solid lubricants does not appear to have the demonstrated reliability necessary for consideration in the immediate future.

## 4.3. DETECTOR OPTICS AND SHIELDING

The ultimate limit to the SNR of an optical sensor is given by

$$\mathrm{SNR} = \tau P_S \sqrt{\frac{qt}{P_T}}$$

(see sec. 4.1). Thus, to obtain the best possible SNR, a detector with the best available quantum efficiency q should be used; the ratio of the signal photon rate $P_S$ to the total photon rate from all sources $P_T$ should be maximized, and all other sources of noise should be kept negligible compared to the radiation noise considered in the above equation. These conditions are not necessarily independent and, particularly at very low light levels, the magnitude of the radiation noise will also be very low and some other form of noise will inevitably predominate.

*At a 300-mi altitude, the mean-free-path is about 20 mi. Molecular collisions are very infrequent at orbital altitudes.

It is now possible to obtain detectors with values of q within a factor of about four of its ideal value of unity for the whole wavelength range from 0.33 to 35 $\mu$, though it may be necessary to use cold filtering to achieve this at some wavelengths. At those wavelengths at which thermal radiation can be ignored (generally <4 $\mu$), $P_0$ can be made essentially zero by the use of appropriate stops and light shields which insure that no radiation reaches the detector except that associated with the signal. At longer wavelengths where the emitted radiation from the optics and its surroundings cannot be ignored, stops and shields are effective only if they can be maintained at a temperature low enough so that the effective power they radiate to the detector is small compared with the signal power. In some cases, this can be done readily by designing the optical system in such a way that the effective aperture stop is close enough to the detector that it can be conductively coupled to the cryostat and insulated from its warmer surroundings by putting it inside the vacuum space of the dewar. In fact, provision of such stops as part of the detector package is now commonplace. It should be noticed, however, that the optical components are themselves sources of radiation because of their temperature and their generally small, but always finite, emittance. Mirrors, for instance, always have an emittance of a few percent, and if several mirrors are used in series, the emittance of the optical train is likely to be appreciable. (The simplest scanner will have two or three reflecting surfaces, while a scanner-spectrograph is likely to have ten or more.) This emittance is, according to Kirkoff's Law, equivalent to the absorption of the optical train which, of course, will also attenuate the signal. Unless the optical train is appreciably warmer than the target, this attenuation of the signal will have a greater effect on the SNR than will the noise resulting from the radiation emitted by the optics. Thus, while it will always be advantageous to keep the optical system as cool as practicable, it is probably only for measurements on the cold side of the moon that the radiation emitted by the optics is likely to have an important effect on the SNR.

It is also possible and desirable to reduce radiation noise by optical filtering. Again, this is straightforward except where thermal radiation is important, in which case radiation emitted or reflected into the beam by the filter becomes significant. To avoid this problem, more and more infrared packages are being supplied with optical filters built into the package in such a way that the temperature of the filter is maintained close to that of the (cooled) detector. Here it should be noticed that a spectroscopic dispersing system is not, in general, effective in restricting the wavelength range of operation from the point of view of reducing radiation noise. The action of the prism or grating will restrict radiation reaching the detector and originating at the target to a narrow wavelength band. However, radiation from the interior of the monochromator will reach the detector at all other wavelengths. For example, in a properly aligned

prism monochromator, the rays with wavelengths inside the band passing through the prism and reaching the detector will have come through the entrance slit. For wavelengths on either side of the passband, the rays will have originated from the inside of the jaws of the entrance slit, and for other wavelengths, the rays will have come from other parts of the inside of the monochromator, including the prism itself for those wavelengths at which the prism material absorbs. Thus, while a spectrograph may be the best way efficiently to separate the required wavelength bands for multispectral sensing, it may still be desirable to have each element of the detector array cold-filtered to maximize the SNR. Again, such filtering will inevitably attenuate the signal radiation to some extent. It will usually be impractical to provide each element of the detector array with individual filters. Thus, design of this part of the system will require close cooperation between the optical designer and the detector and filter suppliers.

Another related factor is detector size. If an infrared detector is limited by current noise, as many of them were until relatively recently, it is desirable to make the size of the detector as small as is compatible with an efficient optical design. This is done by making the f number of the radiant cone falling onto the detector as small as possible. However, if the radiation noise predominates, the SNR will be independent of the detector size, and, provided the efficiency of the cold shielding and filtering is unchanged, the number at the detector will become non-critical. This can facilitate greatly the optical design. Unfortunately, low radiation densities on large detectors result in high detector impedance, and the problem of coupling the pre-amplifiers to the detectors is compounded. Thus, the electronics designers may also have to be involved in the design of the detector optics to insure optimum performance. The problem of preamplifier design is dealt with in section 4.5.

## 4.4. CRYOGENIC SYSTEMS

Many of the infrared detectors which might be used in scanner applications require cooling to very low temperatures. Various methods have been used to achieve these low temperatures for laboratory and for airborne applications, all of which involve, to varying degrees, logistic, maintenance, and reliability problems. Cryogenic systems were studied in the light of our own experience, through a literature survey, and through discussions with a number of organizations which have had relevant experience.

Two cryogenic techniques have been used effectively in other applications. These are the thermoelectric technique and cooling by radiative coupling with space (as with the InSb detector used in the Nimbus High Resolution Scanner). Unfortunately, these appear to be inappropriate in that they are incapable of reaching sufficiently low temperatures. For use out to 13.5 $\mu$ it is necessary to employ Ge:Hg detectors which require temperatures below 35°K and, for

longer wavelength operations, even lower temperatures. These temperatures are well below the practical limits for either technique. One of the techniques might, however, be considered if less extended long-wavelength coverage was considered adequate.

Three classes of cryogenic systems should, however, be considered, two of which are open-cycle systems and the other a closed-cycle system. In a closed-cycle system, a working fluid is continuously cycled thermodynamically so that no working fluid is lost. In an open-cycle system, the working fluid is allowed to go to waste after being used in an open cycle to remove heat from the detector.

4.4.1. CLOSED-CYCLE SYSTEMS. A closed cycle system is defined as one in which the working fluid is conserved and whose supply does not present a logistics problem. However, current systems designed for airborne used have shown poor reliability and require considerable power (typically several kW for 25°K systems), the production of which is a problem in space operation. Since all this power is converted to heat, dissipating it is a further problem. Most experts, however, seem convinced that these problems will be overcome relatively quickly and that such systems will eventually be preferred for space flight operation, particularly for extended-duration flights. Information on various closed-cycle systems is readily available in the manufacturers' literature, and so will not be discussed further here.

4.4.2. OPEN-CYCLE SYSTEMS. The two classes of open-cycle systems are based on the storage and sublimation of solidified gases and on the storage of cryogenic fluids.

4.4.2.1. Sublimation Coolers. This system has been developed on a proprietary basis by the Aerojet-General Corporation [8, 9]. A storage dewar is filled with a liquified gas such as hydrogen or neon, and the pressure over the liquid is reduced by pumping so that some liquid evaporates, and the remainder is cooled and ultimately solidifies. Much care is necessary in order to obtain a high density solid, but Aerojet claims that this can be done. (Alternatively, the fluid could be solidified by passing liquid helium through coils in the dewar tank, but designing a coupling system for the necessary transfer tubing which did not introduce a major heat leak would be very difficult.) The temperature of the solid can be controlled by maintaining a constant (low) pressure over the solid. This is a simple operation in space, but would require vacuum pumping during the prelaunch hold. The heat from the detectors would be transferred to the solid by means of a flexible conductor.

The obvious advantage of this system is that a solid can be restrained more easily than a fluid under zero gravity conditions. At the present time, however, it is by no means clear what

would happen to the subliming solid and whether it would remain in good thermal contact with the conduction path to the detector. The manufacturer claims that, on the basis of laboratory experiments and theoretical analysis, an efficient and practical system for space use can be made. However, it would appear that preliminary space experiments with such systems would be desirable before considering them for use as a vital part of other experiments.

4.4.2.2. Fluid Storage System. The simplest method of obtaining low temperatures in the laboratory is to use bulk-stored liquids. The object to be cooled is mounted in the vacuum space of a dewar and cooled by thermal conduction to the liquid inside the dewar. This technique has also gained wide acceptance for use with experimental airborne systems, since many engineers regard it as more reliable and convenient than closed-cycle coolers. For space applications, two problems arise: (1) a large weight of liquid is required to maintain cooling over an extended period; (2) it is difficult to vent the exhaust gas in a zero-g environment without venting liquid. Garrett AIResearch* claims that 2 could be, and has been, solved. They maintain that it is possible to arrange a long vent tube between the inner and outer walls of the storage dewar, and to valve the two ends of the tube in such a way that liquid will never leave the valve at the outer end. This method has, in fact, been used in a space experiment to cool a Ge:Hg detector [10]. For longer duration space flights, however, the Garrett engineers feel that an alternative system might be preferable. In the life-support systems designed and manufactured by Garrett for the manned space-flight programs, liquified gases are stored in the supercritical state by injecting heat from an electric heating coil when necessary. In this way, the pressure in the tank is maintained above the critical pressure so that the fluid in the tank has only one phase. Thus, if venting is necessary or if fluid is withdrawn, there is no possibility of high density liquid being ejected and low density gas being left in the tank. Gas stored in this way would not be useful directly for cryogenic purposes; since the volume and pressure are maintained constant, the temperature of the fluid varies considerably as the contents of the tank are depleted and is generally higher than the required temperature. However, since high pressure gas could be obtained from the tank at any time, it would be possible to use an open-cycle Joule-Thompson cooler to obtain the required low temperature.

4.4.3. CONCLUSIONS. There is no doubt that the problems associated with the cooling of an infrared detector array involved in an orbital experiment can be solved. At the present time, a fluid storage open-cycle system is indicated, though this conclusion may well have to be

*We are indebted to R. S. Hunt of Garrett AIResearch for arranging a visit and several very valuable discussions with the staff.

changed in the light of developments in closed-cycle and sublimation techniques. The selection of working fluid and the trade-offs between subcritical and supercritical storage will have to be decided on the basis of detailed studies of specific mission requirements.

## 4.5. PREAMPLIFIERS

The outputs of the sensitive radiation transducers with which we are concerned are invariably at very low, voltage levels, and preamplifiers must be used which are capable of amplifying these signals to levels at which they can be conveniently transferred and used. Ideally, the design and construction of these preamplifiers should be such that the noise which they add to the detector output is small compared to the noise output of the detector. At the same time, the preamplifier bandwidth should be large enough that the signal is not distorted. In some applications, vacuum tubes rather than solid-state first stages have been used to avoid the increase in rms noise which occurs at very low frequencies in solid-state devices. However, field-effect transistors (FET) may be used to overcome this difficulty since selected FET's appear to be at least as good for this purpose as the best selected vacuum tubes.

Another important problem is the need to prevent high frequency roll-off at too low a frequency since this will spoil the along-the-line resolution of the scanner. The roll-off frequency required is $\pi(V/H)/\beta^2 n$ (see ref. 2 and app. II). The roll-off frequencies involved in the systems described in sections 3.1 and 3.2 are 135 kHz and 9 kHz respectively. Solid-state preamplifiers with the required characteristics are well within the state of the art, [4], though to reach 135 kHz it might be necessary to use a cryogenically cooled FET for the first stage, as described by Pullan [11]. The difficulty of reaching a given roll-off frequency will increase with the resistance of the detector since this increases the resistance-capacitance (RC) time-constant produced by the resistance of the detector and load resistor together with the stray and input capacity of the first stage. Reducing the resistance of the load will reduce the RC time-constant but will also create a mismatch which alters the signal, so that reducing the resistance of the load below some optimum value will only make the overall SNR worse. The FET can be mounted inside the dewar envelope so that it is very close to the detector (to reduce stray capacitance to a minimum) and cooled (to reduce its noise). Other types of transistors do not operate at such reduced temperatures and cannot be used in this way.

The impedance of modern solid-state infrared detectors varies approximately inversely with the effective photon flux received. Thus, when such detectors are efficiently shielded spatially and/or spectrally from extraneous radiation, resistances may become very high (see ref. 12, p. 81). This problem would be particularly acute in a scanner designed as suggested in section 3.3.1 for observing the cold side of the moon. A rather complicated trade-off would

have to be carried out to choose system parameters which would enable optimum usage of the available components and techniques.

## 4.6. AUTOMATIC GAIN AND LEVEL CONTROL

The limited dynamic range inherent in the electrical components of a radiometric measurement system must be considered in designing such a system. Because certain types of noise and measurement errors tend to remain nearly constant regardless of the level of the signal, it is generally desirable to keep the signal levels as large as possible in order to obtain the most accurate measurements. However, when the signal levels become too high, saturation may occur, causing large errors. Therefore it is evident that, where the input signal level varies greatly over an extended period of operation, some means of controlling the internal signal levels is desirable. Two kinds of automatic control will be needed; these will be referred to as automatic level control (ALC) and automatic gain control (AGC).

Figure 13 is a simplified block diagram showing the essential components involved in the processing of the signal between the detector preamplifier and the transmitter. To simplify the following discussion, it will be assumed that all channels employ ac coupling, and that the dynamic ranges are centered about zero. Where these assumptions are not fulfilled in actual practice, the same conclusions may nevertheless be reached using the same line of reasoning with minor modifications.

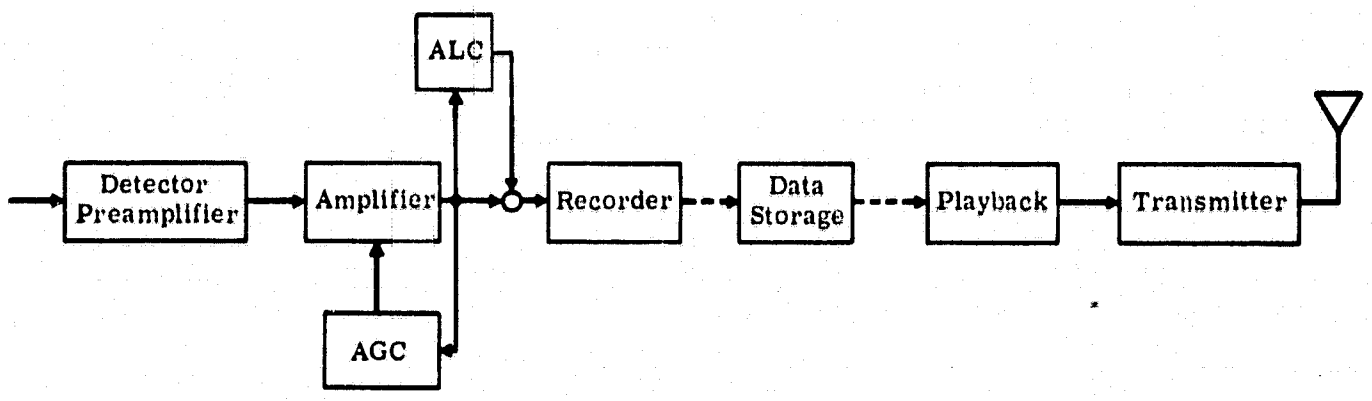


FIGURE 13. SPECTROMETER/RADIOMETER ONBOARD DATA PROCESSING

Figure 14 shows a simplified waveform of the electrical output from the preamplifier over one revolution of the scanner. A distinction is made in this figure between the average output level and the average signal level. The average output level is the average value of the output over a complete revolution of the scanner, while the average signal level is the average value of the output over the ground-scanning portion of the cycle. These two values will almost

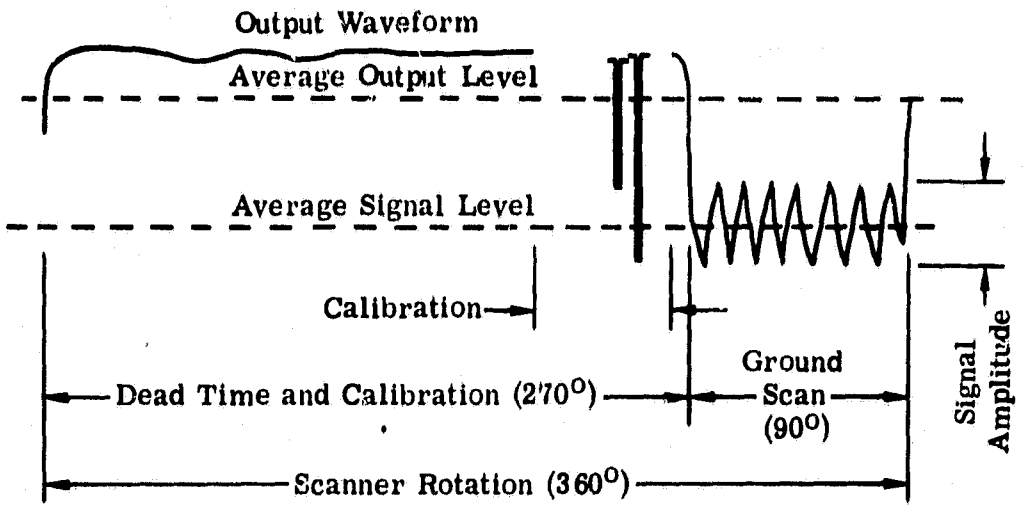


FIGURE 14. PREAMPLIFIER OUTPUT

always be different, because during most of the dead time the scanner will be looking at the inside of the housing, which will generally have a different radiance than the ground. This difference may be expected to fluctuate considerably, and may at times be quite large compared to the overall signal amplitude. Unless some special provision is made, the average output level will become the zero level in an ac-coupled system, and, in regard to the output waveforms shown, it may be seen that the zero level will require a dynamic range much larger than the signal amplitude. Thus, some means would have to be provided to make the average signal level the zero level for the tape recorder in order to achieve efficient use of the available dynamic range of the recorder. It is the purpose of ALC to provide such control.

One method of accomplishing ALC would be to ascertain the zero signal level by sampling only the signal portion of the output and then add to the entire output signal a dc voltage (or current, as appropriate) equal to the difference between the average signal level and the average output level. It is this method that is shown in figure 14. A necessary feature of any ALC method is that it does not make any changes in level during the period of time between the start of calibration and the end of the ground scan which follows; otherwise, the calibration will be destroyed.

Two different criteria may be used to determine the amount of gain desired between the preamplifier and the tape recorder. The first gives the minimum value of gain required to provide an overall SNR which is effectively detector-noise limited; use of this minimum value of gain will result in a system having the best possible sensitivity. The second gives the maximum value of gain which may be used without exceeding the dynamic range of the recorder; use of this maximum value of gain will result in the complete utilization of the available dy-

namic range. It may be seen that, using the above definitions for the desired minimum and maximum gains, it will be possible for the minimum value to exceed the maximum. In addition, when the two values are equal, the system will have the smallest dynamic range consistent with the best possible sensitivity.

If the system sensitivity is to be limited only by detector noise, it follows that any noise introduced after preamplification must be negligible. Although there are numerous potential noise sources between the preamplifier and the transmitter, only the tape recorder requires special consideration as long as reasonable care is taken in the design of the remaining components. The minimum amplification desired between the detector preamplifier and the recorder may be determined from a knowledge of the equivalent rms noise of the recorder-playback (referred to its input) a. d the rms noise output from the preamplifier. To determine exactly how low the recorder noise must be, relative to the detector-preamplifier noise, before it may be considered negligible requires a somewhat arbitrary decision, but as long as the input power of the recorder-playback equivalent noise is less than one-fifth the noise power from the detector and preamplifier at the recorder input, the increase in noise due to the recorder will be less than ten percent, which should be acceptable. Since the detector noise will vary with changes in background temperature, signal level, and other conditions (recorder noise cannot be expected to change in the same manner) this minimum value of amplification may be expected to change significantly. This would indicate the desirability of an AGC amplifier between the preamplifier and the recorder.

The maximum desirable value of gain may be determined from a knowledge of the maximum signal amplitude and the saturation level for the recorder-playback, assuming that the other components involved have a range large enough to handle the signals involved. Since it should be a relatively simple matter to establish this maximum value, it will not be discussed any further.

With minimum and maximum values of signal amplification established, the operating range, or tolerance, for the AGC stage is also established. The methods most commonly employed for controlling AGC amplifiers utilize the maximum signal levels and would thus be most suitable for limiting the maximum gain. In this particular application, however, it would be much more desirable to operate at or near the minimum value, for the following reasons:

(1) Changes in amplifier gain should be made only during dead time, when neither calibration nor ground scanning is taking place; otherwise the calibration will be invalid. The gain would thus remain fixed during a given ground scan and the associated calibration period.

(2) If the gain is to be set at a maximum value, this must be done on the basis of a predicted maximum signal. Without going into detail on how such a prediction may be made, it

may easily be seen that the occurrence of an unexpectedly large signal could result in saturation and the loss of what might be few but nevertheless very important data points. Of course, it would still be possible for such saturation to occur if the AGC amplifier were operating at the minimum value of gain, but in such a case it could hardly be considered a fault in the AGC.

(3) It is conceivable that practical considerations may dictate the use of a recorder whose dynamic range may not be large enough to handle the complete range of signals which would occur in a system with an AGC based on the minimum gain criterion.

Under such conditions, the best AGC would probably be one which limits gain to a value within the dynamic range of the system, at the expense of system sensitivity whenever necessary. Thus we feel that the best AGC, using the normal predictive mode of control, should operate at the minimum value of gain necessary to realize the best possible sensitivity whenever the signal level is low enough, and at the maximum value compatible with the dynamic range of the system whenever the signal levels become too large.

Because of the nature of the signals involved, most applications require the use of predictive control for AGC, but for this particular application, such control need not be relied upon. Instead, a second detector could be used to prescan the field of view of the scanner, and the signal obtained could be used to control AGC. Such a method has the advantage of allowing the use of maximum gain compatible with the dynamic range of the system, and, at the same time, of virtually eliminating the possibility of unexpected saturation. There is, of course, the obvious disadvantage that an additional detector and preamplifier will be required, but this disadvantage might be at least partially offset by the fact that these could also serve as an alternate in case the primary detector or preamplifier should fail. Whether or not these advantages would be sufficient to justify the additional cost involved would be difficult to determine from information presently available, but the possible use of such a method should at least be worth future consideration.

As an alternative to a strict AGC system, it would be possible to record the output signal on several tapes or parallel tape channels. These parallel signals could then be read and analyzed in near-real time to determine which should be transferred to the permanent record. The other signals would be discarded and the tape reused. (It would be possible to pack the useful data efficiently by avoiding the situation in which sections of tape are left empty during the dead time of the scan in the same operation.)

### 4.7. CALIBRATION

An object portrayed in an image will be distinguishable only if the relevant area of the image shows brightness contrast relative to the surroundings. If objects are to be recognized by their

shape, then there is no need to establish an exact relationship between image brightness and target brightness. Correct relative brightnesses may aid identification, and in photography will make the "picture" look realistic, but it is often unnecessary to have an absolute calibration of image brightness in terms of target radiance or apparent radiance. (The target radiance may be attenutated by absorption and scattering or increased by emission and scattering in the path. The resulting radiance at the measuring instrument uncorrected for these path effects is usually referred to as "apparent" radiance.) On the other hand, in many scientific applications, it is important to know the radiance level represented by each possible image intensity level.

Existing remote sensing scanners were not designed with built-in calibration, and attempts to add calibration systems have often been unsatisfactory largely because of the mechanical difficulty of incorporating the calibration sources and optical systems. As is well known, accurate radiometric techniques are very complex and require great care. The main problem in designing an inflight calibration system for a spaceborne radiometer is in preventing the inaccuracies which result from changes in the performance of components because of the space environment. Such calibration would, of course, be a relatively simple matter if the radiometer could be relied upon to retain its calibration over an extended period of operation, but experience has shown that this is not the case. Thus, it becomes necessary to recalibrate the radiometer at frequent intervals in order to maintain its accuracy. Such frequent calibrations require special design considerations in such applications as the present, where the radiometer operation cannot be interrupted to perform the calibrations; here, calibration must be accomplished during the very short intervals between successive scans.

In the following sections, we consider the calibration of thermal systems, i.e., calibration at those wavelengths (greater than, say, 4 $\mu$) at which reflected solar energy is negligible, and the calibration of shorter wavelength systems.

4.7.1. THERMAL RADIOMETER CALIBRATION. In order to obtain an accurate calibration, we must insert a calibrated source of radiation into the field of view of the detector in such a way as to retain, as nearly as possible, the same optical efficiency and the same numerical aperture as in the scanner. Calibrated sources of radiation are readily available in the form of blackbodies, so that this requirement is easily fulfilled. In the scanning radiometer described in section 3.1.1, for example, the numerical aperture is determined by mirror M5 for both the scanning and calibrating operations, and it is evident that the numerical apertures will be the same. However, since here, and in general, not all of the mirrors used are the same, it cannot be guaranteed that the optical efficiency will be the same, but it is probable

that if the same number of mirrors are used and if they are made as much alike as possible, any errors resulting from the use of different mirrors should be relatively small. Changes in mirror reflectivity due to aging seldom introduce errors which exceed two or three per cent under normal conditions, and for mirrors with an initial reflectivity approaching unity, such changes would introduce errors of approximately the same magnitude. Furthermore, since the two separate mirror systems would be operating in the same environment, changes in reflectivity for all mirrors should be nearly the same if the same materials are used, and any errors resulting from changing reflectivities should be considerably smaller than the changes themselves.

Although the most desirable method of calibration would be the one which yielded a continuous curve of radiance versus detector output, such a curve would be difficult to obtain with the scanner in operation. In the interest of simplicity, only a limited number of points on this curve might be provided, but this should be adequate as long as there are not discontinuities or abrupt changes in the calibration curve. The number of calibration points which should be provided will depend on the range of radiation levels (or surface temperatures) for which calibration is required. Successive points which differ by a factor of 2 in radiant flux emitted within the spectral region of interest, i.e., in the 8- to 14-$\mu$ region, should be adequate. Thus, if the hottest blackbody is at a temperature of 400$^{o}$K, these criteria would require additional blackbodies at temperatures of approximately 335, 285, 250, 220, and 200$^{o}$K

Perhaps a better alternative would be to use two temperature-controlled blackbodies. Thermoelectric coolers have been used successfully in airborne systems to control the temperature of calibration sources over adequate temperature ranges. The power required would not be excessive, though probably not negligible compared with that required for a complete scanner in a space environment. Dissipating the waste heat would be a minor engineering problem. The temperature of the two sources would be controlled so that the signals they produced would bracket the levels present in the video signal at the time. The temperature of the surface being overflown can vary quite rapidly, particularly on the moon when the system is traversing the terminator, but if the calibration sources are kept small, there should be no difficulty in changing their temperatures quickly. The actual temperatures of these blackbody sources would have to be measured with a contact thermistor or a resistance thermometer and recorded with the other housekeeping data.

If the optical path of the calibration system is not identical with that of the radiometer, the mirror surfaces in the two paths may differ in temperature. Since the mirrors have small but finite emittances, this may present a problem. In normal applications, this effect can often be ignored since the mirror and the objects being scanned are at roughly the same temperature;

thus, in an efficient mirror system, the reflected radiation exceeds the self-emitted radiation by perhaps an order of magnitude or more. However, where the objects being scanned are much colder than the mirrors, the self-emitted radiation may easily exceed that which is reflected. This condition will probably exist when the coldest portions of the lunar surface are being scanned. Temperatures down to about 100°K or lower are expected, though, for practical reasons, the radiometer mirrors will be at temperatures in the vicinity of 250° to 300°K. Assume a hypothetical case in which the mirror system has a 90% reflectance (10% emissivity) and a temperature of 250°K, while the surface temperature is 100°K and has an emissivity of 100%; then the radiation in the 8- to 14-$\mu$ region incident to the detector from the mirror system will exceed that from the surface by a factor of approximately 160. Under such operating conditions, the substitution of a mirror system whose reflectance differed from that of the first by only 1.0% would result in a change in radiation to the detector equivalent to that which would occur if the surface temperature changed by approximately 30°K. Or, if the mirror systems had exactly the same values of reflectance, a 1°K difference in their temperature would be equivalent to a change in surface temperature of approximately 14°K.

It should now be quite evident that any calibration system which uses different mirrors for the scanning and calibrating functions cannot provide an accurate calibration where the surface temperatures are far below those of the mirrors, unless both the temperatures and reflectances can be precisely matched (apparently a hopeless task). It would thus appear that the only practical method of instrument calibration under such conditions is the use of the same optical system as for scanning. However, several serious problems would still remain. This method requires a calibrated radiation source whose area must exceed, if only slightly, the area of the scanning aperture. Though a source of this size is neither readily available nor simple to construct, it could no doubt be constructed. In order to be effective, however, the temperature of this source would have to be near that of the surface being scanned, i.e., in some cases below 100°K. Maintaining a source of this size at such a low temperature would require a considerable amount of cooling. If the temperature inside the scanner housing is 250°K, the cooling load required to compensate for radiant heating alone would exceed 3 W. Using a liquid oxygen coolant, this radiant heating would require one liter of coolant for every 18 hours of operation, or approximately 20 liters for a 15-day mission. Add to this the coolant necessary to compensate for conduction heating of the blackbody and the losses through the cryostat, and it may be seen that use of this method of calibration to obtain accurate measurements of very low surface temperatures will result in a considerable increase in the size and weight of the system. However, it does appear that such calibration could be practical if it is felt that the need for quantitative data justifies the cost. In fact, it seems necessary to develop a highly

specialized scanning radiometer to make accurate measurements on the coldest parts of the moon (see secs. 2.1 and 3.3). It would probably be necessary to cool the optics of this instrument, and the very low temperature reference sources could no doubt be incorporated into the system used for this purpose.

4.7.2. SHORTER WAVELENGTH CALIBRATION SYSTEMS. Much of the above discussion of thermal calibration applies for the wavelength range below, say, 4 $\mu$, where thermal radiation can be ignored relative to reflected radiation. There are, however, two important differences, both of which will generally result in simplification:

(1) Any black surface will have essentially zero radiance over these wavelengths and can be used as one reference source. The inside of the case around the scanning mirror is often used in this way. Further, for any likely ambient temperature, emission from the mirrors can be ignored.

(2) Radiant sources such as hot tungsten filaments, though poor approximations of the spectrum of reflected sunlight, have very much higher radiances (radiance = watt-cm$^{-2}$-steradian$^{-1}$-$\mu^{-1}$).

As a result of 2, it is possible to produce signals of the appropriate magnitude using small area sources and without collimating. In fact, for The University of Michigan flight programs, satisfactory short wavelength calibration has been obtained by mounting quartz-iodine lamps in the walls of the scan mirror housing with baffles to limit the angular extent of the calibration signal. Since these lamps run at temperatures lower than those characteristic of solar radiation, it is necessary to use two or three lamps with varying power to give appropriate signals across the whole wavelength range. Because of uncertainty in both the temperature and geometry of the filaments, the lamps cannot be considered as primary standards. However, with appropriate monitoring of the electric power drain, they form excellent internal standards and are themselves calibrated when the whole instrument is calibrated during laboratory tests. Unfortunately, the power requirements for this system (~150 W) are somewhat excessive for spacecraft use, from the points of view of both provision and dissipation. It would probably be better to modify this system by using very low power tungsten lamps to illuminate a diffusing plate and then to collimate the radiation from these plates. The optical system for introducing calibration signals described in section 3.1.1 would be ideal in this case.

## 4.8. MULTISPECTRAL DATA HANDLING

Some of the many alternative paths by which the scanner's multispectral data may be handled to give processed or reduced data at an earth-based station are shown in figure 15.

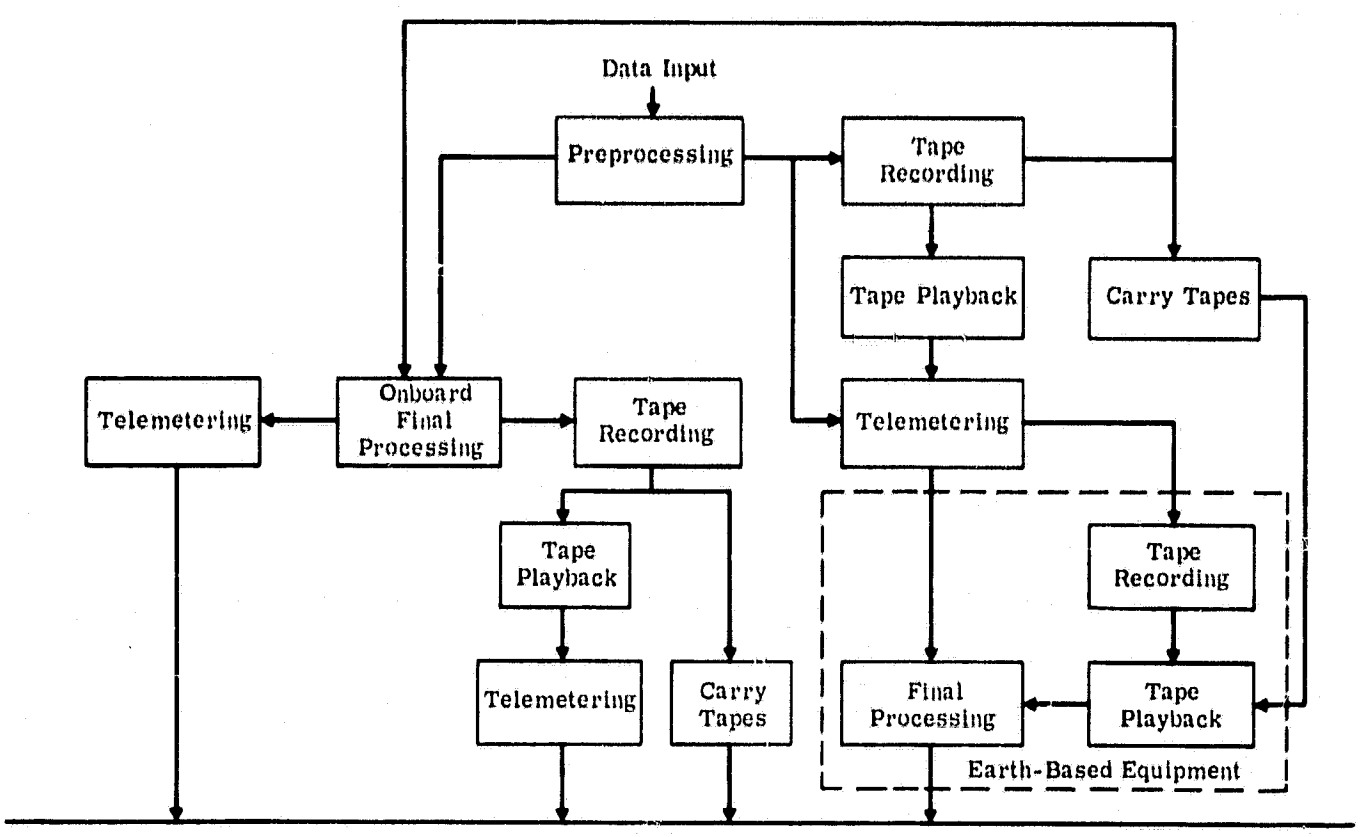


FIGURE 15. DATA-HANDLING FLOW CHART

After preprocessing, there is the choice of performing the final processing on board or transmitting the data to the earth for final processing. If final processing is performed aboard the satellite, the resulting data may be transmitted to the earth station by radio telemetry as it is produced, or it may be recorded on magnetic tape. The tape-recorded data may then be transmitted by radio telemetry at a more convenient time, or the tapes may physically be carried back to the earth when the mission is completed. If the data is transmitted to the earth by radio telemetry, the received signals may be transmitted to the processor as they are received, or they may be tape recorded for processing at some later time.

Thus, there are several choices to be made concerning the way to choose an optimum path for the data to follow in order to become available in processed form at the earth station. In the following sections, these choices are discussed in more detail and a recommended data-handling path is derived.

4.8.1. DATA PREPROCESSING. Data preprocessing consists in modifying the signals from the multispectral scanner so that they are in a form suitable for tape recording, transmitting by radio telemetry, or driving the processor. In general, preprocessing involves amplification and, possibly, addition of a bias voltage to the signal from each scanner channel so that the

resulting signal will cover a voltage range which matches the input requirements of the equipment which that signal is to drive. For example, if FM tape recording is to be the next step after preprocessing, the preprocessing equipment would produce signals covering the range from -1.4 to +1.4 V, the normal range of an FM tape recorder. The design of the preprocessor, then, is somewhat dependent upon the path chosen (fig. 15).

The levels of the signals from the multispectral scanner will have a large dynamic range, since they depend upon the illumination or the temperature of the material being scanned as well as upon its nature. Therefore, it would be undesirable to use a fixed setting of gain and bias for each channel. If the settings were made so that the strongest signals from the scanner did not produce excessive voltages at the outputs of the preprocessor, the weaker signals from the scanner would not be sufficiently strong to be useful. If, on the other hand, the gains in the preprocessor were adjusted to give usable outputs from the weaker scanner signals, the stronger signals would overload the equipment. In each case, the gains and biases used in the preprocessor should be set according to the nature of the material being scanned and its illumination. These controls could be set manually by operators, or equipment could be included which would set them automatically, but either way it will be necessary to consider the setting of the controls as essential information to be used in the final processing of the data. Thus, if the preprocessed data is to be recorded on magnetic tape, the settings of the gain and bias controls in the preprocessor should also be recorded.

4.8.2. FIRST STEP AFTER PREPROCESSING. As shown in figure 15, the preprocessed data could be given final processing aboard the satellite, or could be transmitted to the earth for final processing. The data in final processed form might be a map showing the location of some specific terrain feature, such as wheat fields, or they might be numerical, showing, for example, the statistical distribution of wheat fields. Transmission of such data to a ground station would be simple compared with transmission of the preprocessed data, since the bulk would have been greatly reduced. If the purpose of the mission were to search for and map the locations of a few specific types of terrain feature, the onboard final processor would be adequate, but it would probably not have sufficient flexibility for general use. Although an optimum form of final processor has not yet been developed, it is likely that the design of such a processor will be based on a statistical description of the spectrum of the terrain feature to be mapped (see ref. 4). This processor will use a large quantity of analog computing equipment. If integrated circuitry were used and the processor were simplified to a specialized rather than a general purpose device, it might be possible to reduce its weight and power requirements sufficiently to permit its use aboard a satellite. However, the weight and power con-

sumption would still be quite large, and the system would be limited to specific uses. A ground-based processor, on the other hand, could be made as flexible as desired, since the weight and power restrictions would be much less severe.

Another disadvantage of the satellite-carried final processor is that only a very small percentage of the information content of the multispectral scanner's output data would be utilized, and the remainder would be discarded. If the tape-recorded multispectral data were available for use with a ground-based processor, it could be "played through" the processor again and again, with the processor set up for identifying and passing a set of signals for a different kind of material with each pass of the tape. Of course, if the data for the multispectral scanner were first recorded on magnetic tape and the tape-recorded data given final processing aboard the satellite, this disadvantage would be overcome, but this would require that both the final processor and wideband tape recording and playback equipment be installed in the satellite. In addition, operating this equipment would require considerable attention from the crew.

Therefore, in consideration of the present state-of-the-art in analog computing and tape recording, and in view of the desirability of reducing the duties of the crew of a satellite, it is recommended that the final processing of the multispectral scanner data be performed at an earth-based station rather than on board the satellite.

4.8.3. TAPE RECORDING VERSUS DIRECT TELEMETERING. As shown in figure 15, the preprocessed data could be telemetered directly to the earth, or it could be tape recorded initially and transmitted later. The principal advantage of direct transmission of the data by radio telemetry would be to eliminate the tape recording equipment in the satellite, thereby reducing the weight and power consumption. However, in order to permit the gathering and transmitting of scanner data under all conditions, it appears that intermediate tape recording would be necessary at times. For example, if the satellite were not in the line of sight of any radio telemetry receiving stations or relay stations, it would be impossible to transmit data directly, but the scanner data gathered at that time could be recorded and transmitted later when the satellite would be in a more favorable position to communicate with the receiving stations.

Another disadvantage of direct radio telemetry of the scanner data is that in the event that noise, interference, or an equipment malfunction caused the data to be received imperfectly, those data would be irretrievably lost, whereas if the data were tape recorded, they could be retransmitted if necessary. It therefore appears evident that the preprocessed data should be recorded magnetically on board the satellite.

4.8.3.1. Type of Recording. Up to this point, it has been assumed that if the data are to be recorded, it will be on magnetic tape. There are, of course, other media for recording data, one of which is photographic film. An efficient method of recording on film would be to record each scanner channel as a strip map of the area being scanned, using film density recording. This would involve a cathode ray tube and an optical system for each channel, and, with suitable arrangement, it should be possible to record the strips representing 30 channels side by side on 70-mm film. Although it should be possible to obtain sufficient resolution by this method if good optical systems and a high resolution film are used, the density of the recorded film would not bear a linear relationship to the magnitude of the recorded signals. Since the final data processor operates electronically, it would be necessary to have a playback apparatus which scanned the film strips and electronically reproduced the original signals which had been recorded. Because of the nonlinear relationship between exposure and film density, and because of the dependency of density upon the film processing, it would be extremely difficult, or perhaps impossible, to recover the recorded signals with sufficient fidelity to permit satisfactory final processing. Thus, although film density recording would permit recording more data in a smaller space, it would not be a satisfactory means of recording the preprocessed multispectral data because of the difficulty involved in accurately recovering the signals in electrical form for final processing. Of course, the data could be stored on the film as a multiple track FM system, similar to that used for magnetic tape, but the density of stored information would not be as great and certainly would not be as noise free as magnetic tape.

Magnetic tape recording possesses two further advantages: (1) tapes may be reused; (2) no special developing equipment is required (as it is for photographic film). If the data recording method is restricted to magnetic tape, there is still a decision to be made as to whether analog FM or some form of digital coding should be used. Direct recording would not be satisfactory since the frequency of response of a direct recorded system does not include dc, and the output level is not consistent but depends upon the condition of the tape, how often it has been played back, etc.

Either analog FM or some form of digital recording would meet the accuracy requirements, but FM recording would be superior in terms of bandwidth and relative information capacity. One way of rating the information capacity of a recording system is to determine the number of recorded cycles per channel per inch of tape length and multiply this by the number of channels per inch of tape width to obtain the capacity in cycles per square inch. Table I (taken from ref. 13, p. 72) compares the relative information capacity of magnetic tape for the various recording methods. Since the publication of this data in 1961, there have been many advances in the design of tape recorder heads for FM use. At present, it is possible to obtain recorders

TABLE I. THE RELATIVE INFORMATION CAPACITY OF MAGNETIC TAPE

| Recording Method | Capacity (cycles per square inch) |
|---|---|
| Direct recording | 32,000 to 160,000 |
| Wideband FM | 2880 |
| Pulse duration modulation | 864 |
| Digital | 896 |

with direct record/reproduce bandwidths of 1.5 MHz and FM record/reproduce bandwidths of 500 kHz at tape speeds of 120 in./sec. For 14 channels on a 1-in. tape, the tape information capacity for such machines is

$$\frac{1{,}500{,}000}{120} \times 14 = 175{,}000 \text{ cycles per square inch for direct record/reproduce}$$

and

$$\frac{500{,}000}{120} \times 14 = 58{,}000 \text{ cycles per square inch for FM record/reproduce}$$

The information capacity for digitally encoded data on magnetic tape, however, does not appear to have been enlarged. Therefore, it seems apparent that analog FM recording on magnetic tape is the best choice for a preprocessed data recording system at the present time.

4.8.3.2. Information Rate of the Scanner. In order to obtain a lower bound on the rate at which magnetic tape must be used, it is necessary first to obtain the rate at which the scanner produces information. Assume the scanner rotates at 500 rpm and has a resolution of 3 milliradians. It has been shown (ref. 4, p. 35) that a scanner with a 3-milliradian resolution rotating at 2000 rpm would require a bandwidth of 35 kHz if the rise time is the time required to scan one resolution element (3 milliradians). Therefore, the same scanner operating at 500 rpm, or 1/4 of 2000 rpm, would require only 1/4 of 35 kHz, or 8.75 kHz. A bandwidth of 10 kHz per channel should be more than adequate. The total information rate for 30 scanner channels would be 30 × 10 or 300 kHz.

4.8.3.3. Tape Speed. If the tape could record 58,000 cycles per square inch, it would be used at a minimum rate of 300,000/58,000 = 5.2 square inches per second. This would suggest a tape speed of 7.5 in./sec for 1-in. tape or 15 in./sec for 1/2-in. tape. These figures do not allow, however, for frequency separation between multiplexed signals on each channel. It has been shown [4] that the 2000-rpm scanner data could be recorded on 1-in. tape at 120 in./sec. The 500-rpm scanner's outputs could therefore be recorded on 1-in. tape at 120/4 or 30 in./sec or on 1/2-in. tape at 60 in./sec.

The satellite will carry a scanning infrared radiometer with a single channel output at a maximum bandwidth of 200 kHz. Recording a wideband signal of this type by analog FM techniques requires a tape speed of at least 60 in./sec. A single tape recorder, using 1/2-in. tape and operating at 60 in./sec. A single tape recorder, using 1/2-in. tape and operating at 60 in./sec, could record the output of the scanning radiometer as well as the 30 channels from the multispectral scanner. A possible assignment for the 7 tracks on the 1/2-in. tape would be as follows:

| Tape Track No. | Use |
|---|---|
| 1 | audio, synchronization signals, general information |
| 2 | six scanner channels (multiplex) |
| 3 | six scanner channels (multiplex) |
| 4 | six scanner channels (multiplex) |
| 5 | six scanner channels (multiplex) |
| 6 | six scanner channels (multiplex) |
| 7 | scanning radiometer channel |

The multiplex channels use the inner tracks of the tape, where tape contact with the recording head is more reliable. Since each scanner channel requires 10 kHz, and each track is capable of recording up to 250 kHz, there should be no problem in multiplexing six of the 10-kHz channels on a track with 250-kHz capability. In fact, other channels could be added, if necessary.

4.8.3.4. Tape Requirements. At 60 in./sec, a 3600-ft reel of magnetic tape would provide 12 min of recording time. Thus, with continuous recording, the tape consumption would be 5 reels per hour. For a fourteen-day mission with continuous recording of data, the tape requirements would be 1680 reels. If each reel weighed 2 lb, the total weight of recording tape required would be 3360 lb, somewhat in excess of 1 1/2 tons. The weight cost for data storage on tape on board the satellite would be 10 lb/hr. Sufficient storage for 10 hr (100 lb of tape) would not be an excessive amount of weight to carry, but since 10 hr is slightly less than 3% of the total time in a 14-day mission, it seems unlikely that it would be sufficient for storage of all data gathered during the mission, even with very selective editing.

On the other hand, if the recorded data were transmitted by radio telemetry to the earth station on a regular schedule, the tapes could be erased and reused indefinitely, and the 10 hr of storage time would probably be sufficient. It is recommended, therefore, that the preprocessed multispectral data be tape recorded and that the recorded data be transmitted to the earth station by radio telemetry on a regular schedule so that the tapes may be reused for recording further data. The large amount of tape required for recording even a moderate

percentage of the total amount of data practically eliminates the possibility of tape recording all the data that is physically to be carried back to the earth upon completion of a mission.

4.8.3.5. Number of Tape Recorders. If each reel of tape holds only 12 min of data, it will be impossible, with a single tape recorder, continuously to record data from the scanner for intervals exceeding 12 min. Scanner data generated during the time interval when the recorder is being reloaded will be lost unless the operator switches to a second stand-by recorder while changing tape on the first. In addition, a tape-playback unit is needed for reproducing the tape for radio telemetry transmission to the earth. Thus, ideally, the tape equipment aboard the satellite should consist of two tape decks for recording and one for playback, although one of the recording tape decks could be used for playback for radio transmission when the scanner data is not being recorded. However, only one set each of record and reproduce electronics would be needed.

4.8.3.6. Ground Equipment. It would be possible directly to process the signals as they are received at the earth station, but this would involve most of the disadvantages of processing aboard the satellite, such as loss of information and inflexibility. It would be better to record the received signals so that they could be processed later in as many ways as desired. In short, it seems advisable to use an intermediate tape-recording apparatus to store data when contact with the ground cannot reliably be maintained and to transmit the multispectral data to the earth station via radio telemetry as continuously as possible whenever the communications channel is reliable. A block diagram of the suggested data transmitting system is shown in figure 16. Note that the output of the preprocessing block goes directly to the telemetering transmitter as well as to the tape recorder. This permits direct telemetering of data whenever conditions are favorable, thereby eliminating the tape-record-take-playback sequence in the data handling.

## 4.9. IMAGE DISTORTIONS

Though the plane mirror is the only optical element capable of creating a perfect image, camera systems have been developed in which the distortions are negligible both from an aesthetic and a practical viewpoint. On the other hand, strip maps produced from a mechanical scanner output are often noticeably distorted, particularly toward the edges of the map. While this effect may be an annoyance to an inexperienced viewer, it is rarely of much practical importance. We proceed briefly to discuss the various effects involved and the circumstances under which correction of such effects would be desirable.

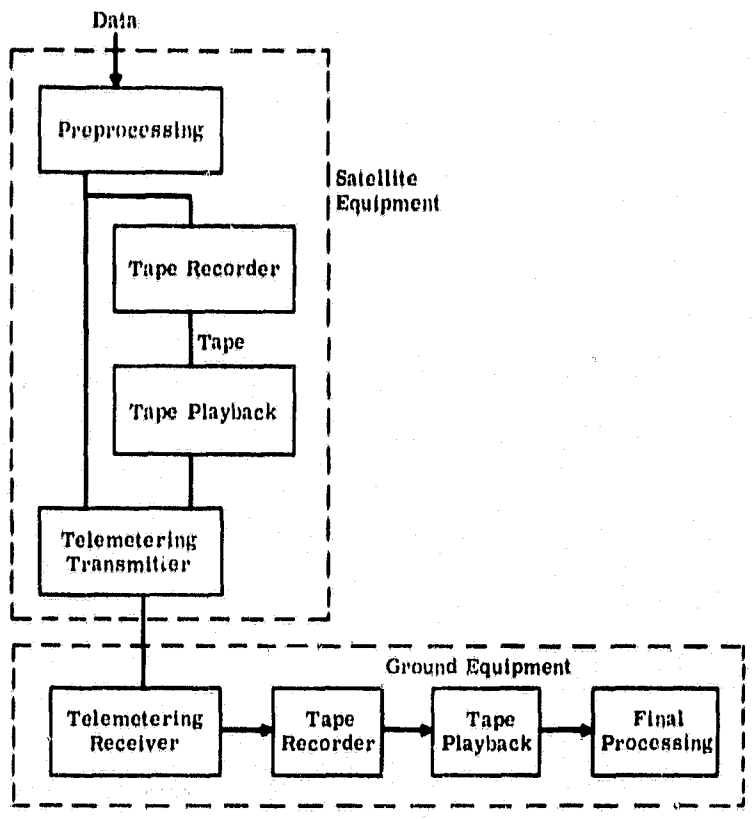


FIGURE 16. DATA TRANSMITTING SYSTEM

As a general rule, any combination of scanning and processing will produce a final image which is not a perfect reproduction of the target scene. Factors which can produce infidelity in the finished product include

(1) Variations in altitude of the vehicle or target scene

(2) A recording method which is not a true analogue of the scanning method

(3) Variations in attitude of the scanning vehicle

Some of these difficulties are discussed in references 14 and 15, so they will not be dwelt upon at length in this study. It is, of course, possible to correct 1 through electronic means and stereoscopic presentation. 2 may be alleviated electronically or by using analog display techniques [14]. 3 may be corrected by gyrostabilization and by using electronic techniques.

Priorities in geometric correction techniques must depend upon the function which is to be served by the survey. Highly accurate correction is needed for mapping applications where large geometric distortions would be detrimental to the mission. On the other hand, no correction is needed to obtain an inventory of lunar materials. Moderately good correction would, however, be needed to correlate lunar or terrestrial materials with gross surface features (eg., maria or craters on the moon and natural topological features on the earth). Better correction is required where the detailed study of surface composition, temperature, etc., is demanded.

4.9.1. NO CORRECTION OF DISTORTIONS. The rule in optical-mechanical scanning has been to accept geometric distortions in imagery as a necessary evil. Since previous target areas have been mapped accurately by other means, there has been little demand for true geometric fidelity as long as gross features exist for identification of the target area. The following refers to the factors listed in section 4.8.

Many geometric distortions of type 2 can be made tolerable by the use of suitable overlays [15]. Where distortions of types 1 and 3 can be minimized (through altitude and attitude control), such an approach is acceptable. This technique reduces system complexity, but makes interpretation more difficult. In defense of the technique, one can argue (with merit) that interpretation is no problem because this is the type of approach which has been used for years in infrared image interpretation. It should also be noted that distortions of type 2 are small for view angles close to the nadir and become very large close to the horizon. For most purposes, they can be ignored for nadir angles of less than $40^{o}$ or $45^{o}$.

4.9.2. MODERATE CORRECTION OF DISTORTIONS. The equations presented in reference 14 may be used to derive approximations for making moderate corrections. The use of gyrostabilized platforms or gyroreferenced systems would minimize any distortions caused by attitude variations.

4.9.3. ACCURATE CORRECTION OF DISTORTIONS. Extreme accuracy in mapping the lunar terrain would require the following:

(1) Sensitive gyrostabilization of either the platform or the synchronization system

(2) An analog recording device (ref. 14, p. 3)

(3) Continuous v/h measurement and speed control

4.9.4. CONCLUSIONS. Since primary mapping applications are likely to be carried out photographically, some geometric distortion in the infrared imagery can be tolerated. Unless the widest possible coverage is mandatory, it will be wise to restrict the part of the scan used to $\pm 40^{o}$ or $\pm 45^{o}$ from the nadir. In this way, distortions resulting from a recording method which is not a true analogue of the scanning method will be slight, and data bulk will be reduced. For earth orbits, this will also avoid problems in correcting for atmospheric effects which become much more marked at the shallow view angles where the atmospheric path is longest. It will be necessary, of course, to stabilize the scanner or compensate the image if the orbiting vehicle itself is unstable enough to affect the image.

## Appendix I
## CORRECTING IMAGE ROTATION

One of the characteristics of scanners which use a scanning mirror rotating about the optical axis of the collector is that the instantaneous FOV rotates as the scan mirror rotates. This rotation is undesirable in certain applications, particularly where several detectors are used in an array and it is desired that all detectors trace the same ground path. Scanners which use a mirror rotating about an axis perpendicular to the optical axis do not cause the FOV to rotate, but they require fairly complex relay optics which tend to limit their usefulness to applications involving relatively low resolution. Thus, it would be desirable to provide some means of correcting for the FOV rotation in scanners which use a mirror rotating about the optical axis.

One method is to use a K mirror, shown in figure 17. The K mirror consists of three plane mirrors, and when it is rotated about the optical axis, the image rotates in the same direction and at twice the mirror speed. To eliminate image rotation, the K mirror must rotate in the direction opposite to the rotation of the scanning mirror and at half the speed. K mirrors have

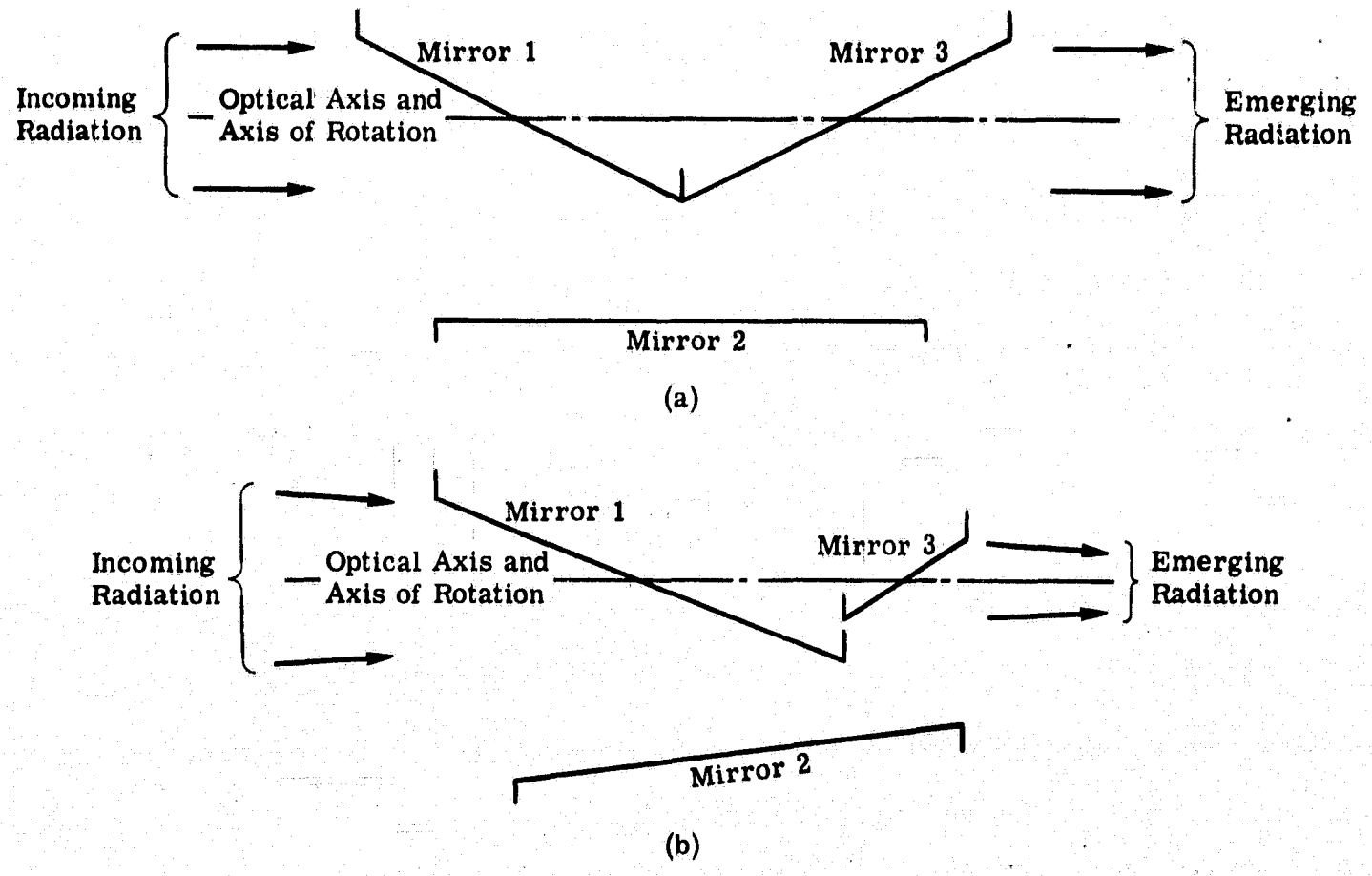


FIGURE 17. K-MIRROR CONFIGURATIONS. (a) Symmetrical K-mirror. (b) Asymmetrical K-mirror.

been used in a variety of applications, but in the vast majority, the mirrors have had a symmetrical configuration in which the first and third plane mirrors intersect the optical axis at the same angle, while the second plane mirror is parallel to the optical axis (fig. 17a). Although this configuration might appear to be a logical choice where the light is collimated, it becomes readily apparent after a few sample ray traces that an asymmetrical configuration is better where there is converging radiation. Thus, in determining an optimum configuration for the K mirror, a more general model should be considered (fig. 17b). The symmetrical K mirror is a special case of the general asymmetrical configuration.

It may be seen from figure 17 that, for a given configuration of the K mirror, there is a maximum angular convergence for the light beam which, if exceeded, will result in the loss of some incoming light. This convergence will in effect establish a limiting f number for the focusing optics, and since this is a very important parameter for the optical system, the applicability of the K mirror will depend upon the maximum angular convergence. Thus it is necessary to determine the relationships between the important dimensions of the K mirror in order to decide whether or not the use of a K mirror is possible, and if so, what its optimum dimensions shall be. The relationships which exist between the various dimensions of the K mirror may be determined by tracing the two extreme rays and the central ray through the mirror system. These relationships are illustrated in figure 18. The nomenclature used in the following analysis is also defined in this figure.

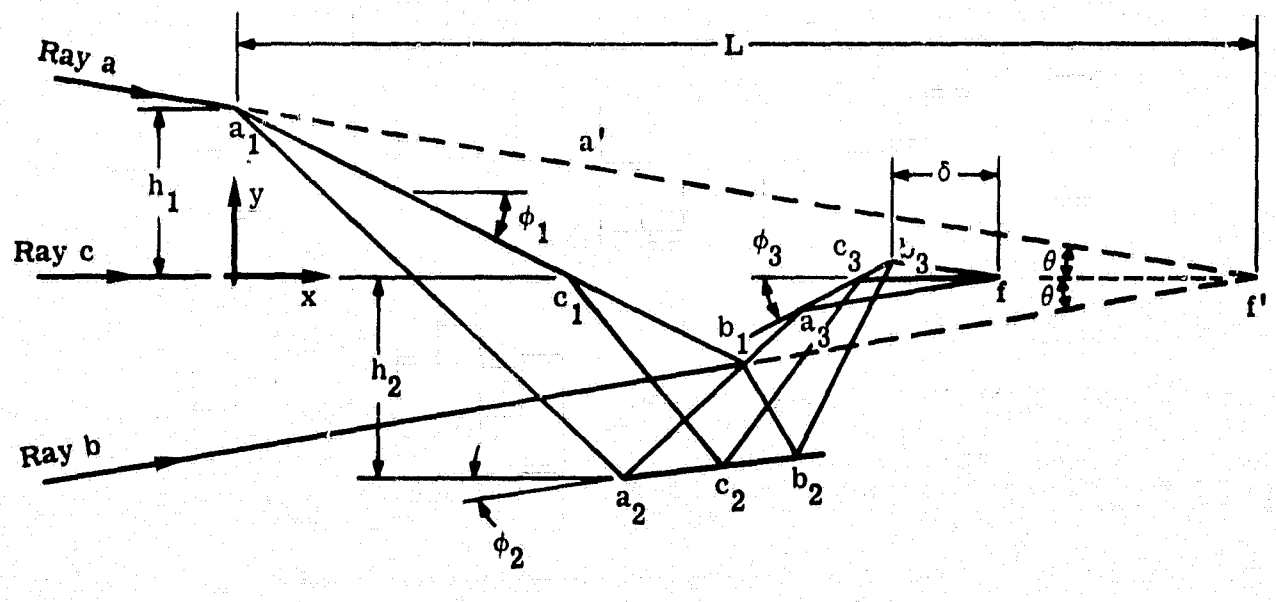


FIGURE 18. K-MIRROR GEOMETRY USED TO DERIVE OPTIMUM CONFIGURATIONS

The equation of the line segment $\overline{a_1 b_1}$, representing mirror 1, is

$\overline{a_1 b_1}$: $$y = h_1 - x \tan \phi_1$$

and the equation of the line representing ray b and its extension b' is

$\overline{b_1 f'}$: $$y = x \tan \theta - h_1$$

The intersection of the two lines $\overline{a_1 b_1}$ and $\overline{b_1 f'}$ gives

$$x_{b_1} = \frac{2h_1}{\tan \theta + \tan \phi_1}$$

$$y_{b_1} = \frac{\tan \theta - \tan \phi_1}{\tan \theta + \tan \phi_1} h_1$$

The line segment $\overline{a_1 a_2}$ is given by the equation

$\overline{a_1 a_2}$: $$y = h_1 - x \tan (2\phi_1 - \theta)$$

and since by definition $y_{a_2} = h_2$,

$$x_{a_2} = \frac{h_1 - h_2}{\tan (2\phi_1 - \theta)}$$

and

$$y_{a_2} \equiv h_2$$

Proceeding formally, the following equations may be written:

$\overline{b_1 a_2}$: $$y - h_2 = \frac{y_{b_1} - y_{a_2}}{x_{b_1} - x_{a_2}} \left( x - x_{a_2} \right)$$

$$\phi_2 = 1/2 \left[ \tan^{-1} \left( \frac{y_{b_1} - y_{a_2}}{x_{b_1} - x_{a_2}} \right) + \theta - 2\phi_1 \right]$$

$\overline{a_2 b_2}$: $$y - h_2 = x \tan \phi_2$$

$\overline{b_1 b_2}$: $$y - y_{b_1} = \left( x_{b_1} - x \right) \tan (2\phi_1 + \theta)$$

$$x_{b_2} = \frac{y_{b_1} + x_{b_1} \tan (2\phi_1 + \theta) - h_2}{\tan \phi_2 + \tan (2\phi_1 + \theta)}$$

$$y_{b_2} = h_2 + x_{b_2} \tan \phi_2$$

$\overline{c_1 c_2}$:
$$y = -\left(x - x_{c_1}\right) \tan 2\phi_1$$

$$x_{c_1} = \frac{h_1}{\tan \phi_1}$$

$$x_{c_2} = \frac{x_{c_1} \tan 2\phi_1 - h_2}{\tan \phi_2 - \tan 2\phi_1}$$

$$y_{c_2} = h_2 + x_{c_2} \tan \phi_2$$

$\overline{c_2 c_3}$:
$$y - y_{c_2} = \left(x - x_{c_2}\right) \tan 2(\phi_1 + \phi_2)$$

$$x_{c_3} = \frac{x_{c_2} \tan 2(\phi_1 + \phi_2) - y_{c_2}}{\tan 2(\phi_1 + \phi_2)}$$

$$y_{c_3} \equiv 0$$

$\overline{a_3 b_3}$:
$$y = \left(x - x_{c_3}\right) \tan (\phi_1 + \phi_2)$$

$\overline{b_2 b_3}$:
$$y - y_{b_2} = \left(x - x_{b_2}\right) \tan (2\phi_1 + 2\phi_2 + \theta)$$

$$x_{b_3} = \frac{y_{b_2} + x_{c_3} \tan (\phi_1 + \phi_2) - x_{b_2} \tan (2\phi_1 + 2\phi_2 + \theta)}{\tan (\phi_1 + \phi_2) - \tan (2\phi_1 + 2\phi_2 + \theta)}$$

$$y_{b_3} = \left(x_{b_3} - x_{c_3}\right) \tan (\phi_1 + \phi_2)$$

$\overline{b_3 f}$:
$$y - y_{b_3} = \left(x_{b_3} - x\right) \tan \theta$$

$$x_f = \frac{y_{b_3} + x_{b_3} \tan \theta}{\tan \theta}$$

$$\delta \equiv x_f - x_{b_3}$$

Given the above relationships, there remains the problem of finding an optimum configuration so that for a given angle $\theta$ and the required minimum value of $\delta$, the best possible configuration for the K mirror may be found. Since the K mirror will probably be used in conjunction with either a Cassegrain or Newtonian type of telescope, both of which are shown in figure 19, it seems reasonable to assume that the optimum configuration will be the one which minimizes the ratio of $h_1/\delta$, because it is the value of $h_1$ which determines the central obscuration of the primary mirror. As an extreme example, it would obviously be impossible to use a K mirror if the minimum value of $h_1$, for given values of $\delta$ and $\theta$, were equal to or exceeded the radius of the primary mirror. Having established this criterion, the solution of the above equations for $\phi_1$ and $h_2$ which gives a minimum value of $h_1/\delta$ for a given value of $\theta$ must be found. Because of the transcendental functions contained in the equations, the only practicable means of solution appears to be trial and error.

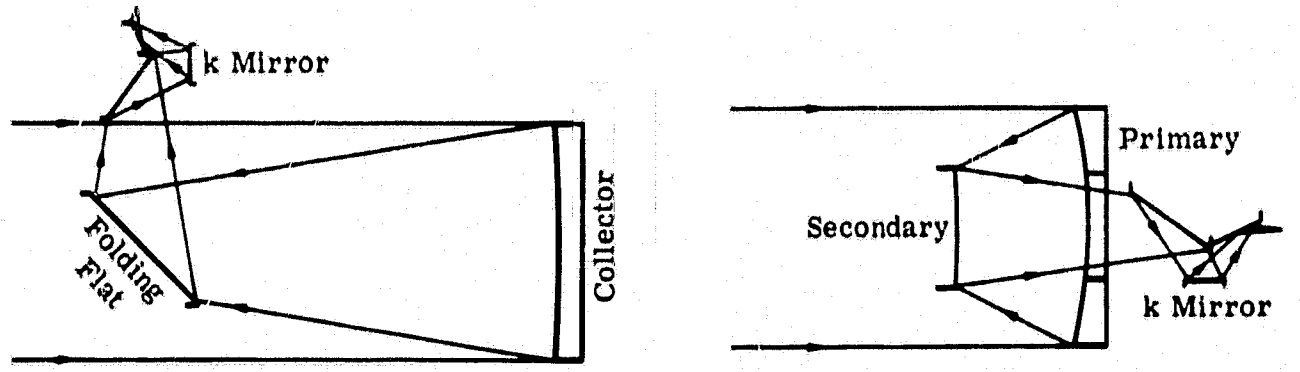


FIGURE 19. LOCATION OF THE K-MIRROR. (a) Using Newtonian optics. (b) Using Cassegrain optics.

Solutions obtained for various values of $\theta$ are shown in figure 20. It should be mentioned that because the value of $h_1/\delta$ did not change rapidly with small changes (from their optimum values) in $\phi_1$ and $h_2$, the values obtained for these quantities were not as accurate as those for $h_1/\delta$. However, from a practical point of view, this condition is actually desirable because it means that although the solutions obtained may be in slight error, the values of $\phi_1$ and $h_2$ are not critical, thus allowing for increased manufacturing tolerances.

To illustrate how the results of these calculations may be applied in practice, we assume that an optical system having an aperture of 100 mm and effective focal length of 250 mm is specified, and that a 0.25 × 4-mm detector array is required. In addition, a minimum end clearance between the K mirror and detector array of 6 mm is required in order to eliminate interference between the K mirror and the dewar. Figure 21 shows the geometry for this example. Since the dimension $\delta$ in figure 18 implies the use of a detector which is infinitesimal, an equivalent value of $\delta$ must be determined for the present example where the detector dimen-

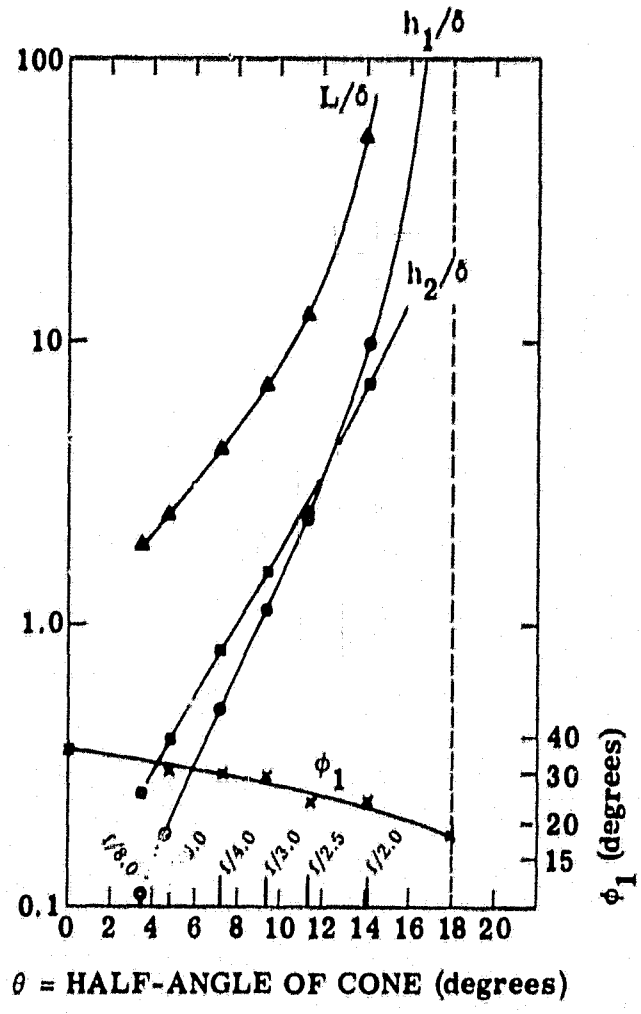


FIGURE 20. DIMENSIONS OF THE OPTIMUM K-MIRROR

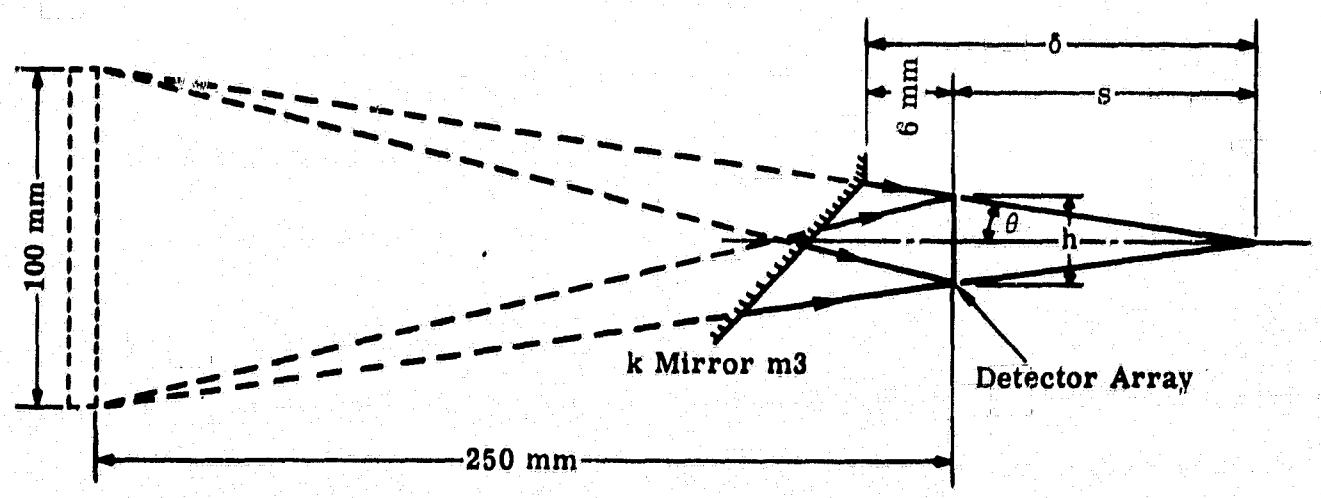


FIGURE 21. K-MIRROR GEOMETRY CONSIDERED FOR A 250-mm FOCAL LENGTH SYSTEM

sions are not negligible. The dimension h in figure 21 represents the maximum linear dimension of the face of the detector array. It is evident that the value of h need never exceed the diagonal for a rectangular detector array, though it may be appreciably less in certain applications. The length of the diagonal is used in the following derivation:

$$h = \sqrt{(1/2)^2 + 4^2} = 4.03 \text{ mm}$$

and from figure 21,

$$100(250 + s) = h/s = 4.03/s$$

which gives

$$s = 10.5 \text{ mm}$$

so that

$$\delta = 6 + 10.5 = 16.5 \text{ mm}$$

The angle of convergence of the extreme rays is

$$\theta = \arctan \frac{100/2}{250 + s} = 10.85^{o}$$

Using this value for $\theta$, the curves in figure 20 give

$$h_1/\delta = 2.06$$

$$h_2/\delta = 2.37$$

$$L/\delta = 10.7$$

Thus, for $\delta = 16.5$ mm,

$$h_1 = 34.0 \text{ mm}$$

$$h_2 = 39.1 \text{ mm}$$

$$L = 176.5 \text{ mm}$$

The optical path length which must be accomodated by the K mirror is L - s = 176.5 - 10.5 = 166 mm, and although it would be possible to provide a free optical path of this length with a reflective optical system of 250 mm focal length, the central obscuration would of necessity be very high, thereby indicating the impracticability of using a K mirror. However, if a refractive optical system were used, a K mirror might be feasible, although it would be quite large.

As may be seen from the above calculations, the size of the K mirror may be reduced by decreasing the value of $\delta$, which may be accomplished by decreasing the value of h. This could,

of course, be done by decreasing the size of the detector array, but that would require that either the number or the size of the detectors be reduced, and this would significantly alter the nature of the problem. However, the value of h may also be reduced by properly phasing the scanning and K mirrors, provided the total scan angle is less than $360^{\circ}$. We illustrate this by using the previous example but now limiting the total angular FOV of the scanner to not more than $60^{\circ}$. A $60^{\circ}$ field of view will require a scan mirror rotation of $30^{\circ}$ on either side of the center, so that the K mirror rotation will be $15^{\circ}$ on either side of the center. By aligning the K mirror in such a way that the plane of symmetry is perpendicular to the long side of the detector array when in the central position, the value of h may be reduced significantly, as shown in figure 22. From this figure,

$$\frac{h}{2} = \frac{4}{2} \sin 15^{\circ} + \frac{1/2}{2} \sec 15^{\circ} = 0.509 + 0.259 = 0.768$$

$$h = 1.536 \text{ mm}$$

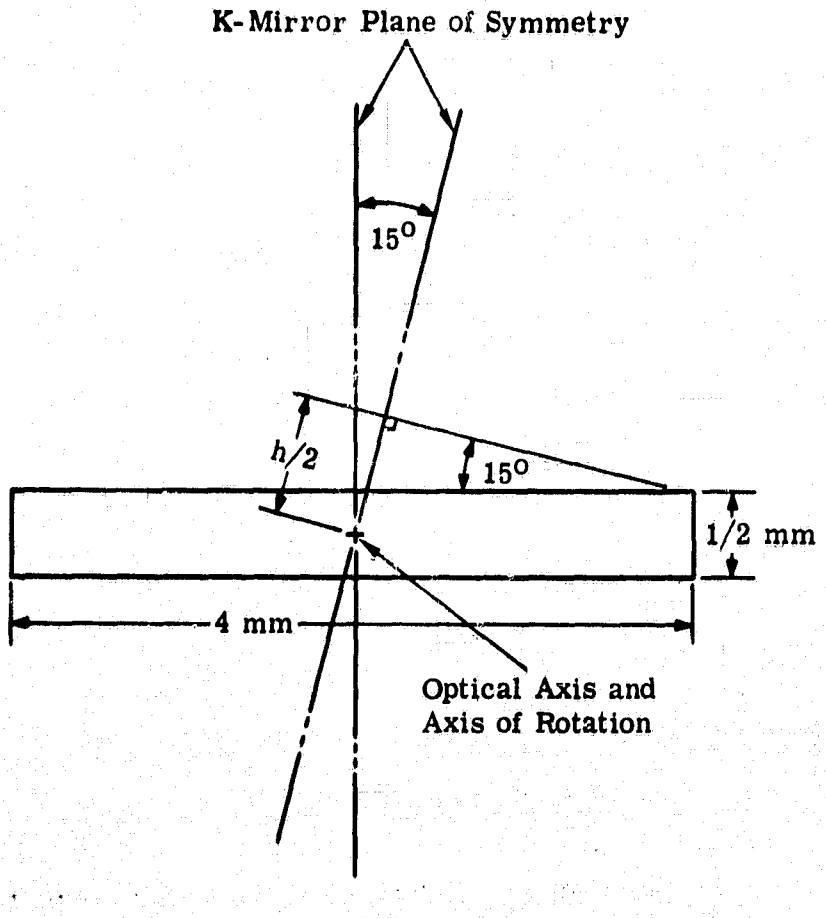


FIGURE 22. END VIEW OF THE DETECTOR ARRAY

Using this new value of h and proceeding as in the previous examples gives

$$s = 3.9 \text{ mm}$$

$$\delta = 6 + 3.9 = 9.9 \text{ mm}$$

$$\theta = 11.1^{\circ}$$

From figure 21,

$$h_1/\delta = 2.3$$

$$h_2/\delta = 2.55$$

$$L/\delta = 11.6$$

so that for $\delta = 9.9$ mm,

$$h_1 = 22.8 \text{ mm}$$

$$h_2 = 25.3 \text{ mm}$$

$$L = 114.9 \text{ mm}$$

For this example, the free optical path length which must be passed through the K mirror is 114.9 - 3.9 = 111 mm, a value significantly less than that required for the previous example. Figure 23 shows a K mirror combined with a Cassegrain telescope, which meets the require-

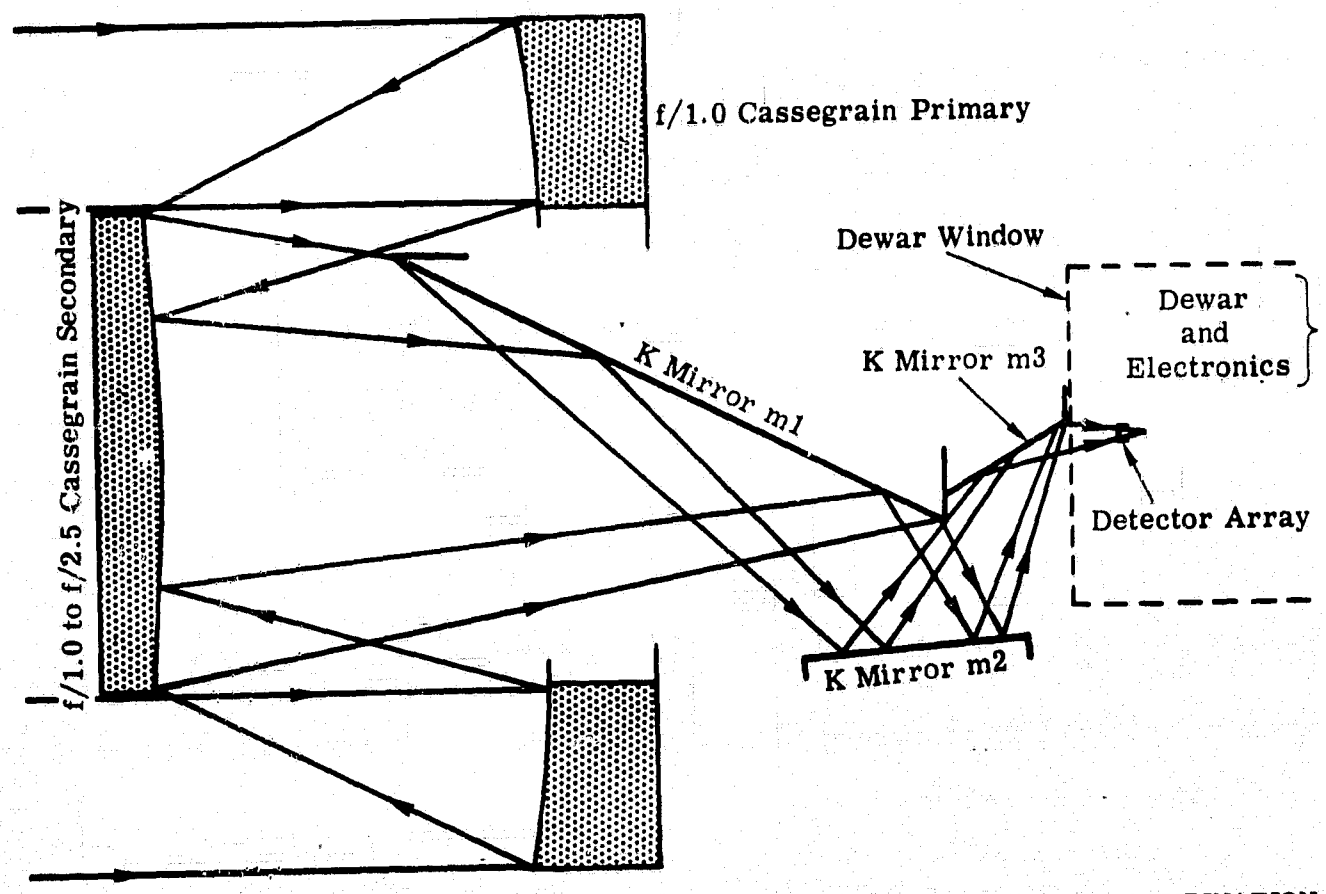


FIGURE 23. OPTICAL LAYOUT FOR THE K-MIRROR AND FOLDED-TELESCOPE COMBINATION

ments of the above example. As may be seen from this figure, using the K mirror requires a configuration resulting in a central obscuration of approximately 58 mm, which reduces the area of the collecting aperture approximately 34%. Although this obscuration exceeds that which is normally present in Cassegrain telescope designs, whether it would be considered excessive would depend upon the application and the alternatives available to the designer.

We conclude that while the asymmetric K-mirror is more versatile than the usual symmetrical version, it is still a bulky device and restricts the telescope with which it is used to relatively narrow field angles. Thus, with the establishment of the feasibility of the scanner-spectrograph approach to multispectral scanning, it seems unlikely that the K-mirror approach is desirable or necessary.

## Appendix II
## SCANNER PERFORMANCE RELATIONS

In reference 2, expressions for the performance of generalized scanners are derived. These enable the user to compute the SNR resulting from changes in target radiance. Calculations of radiance changes produced by given temperature differences are somewhat time-consuming. To avoid the need for them, we have extended the calculations in [2] so that the SNR can now immediately be calculated in terms of temperature differences. We have also changed some of the notation and omitted some of the geometrical relationships which are dealt with in detail in [2], but which are now regarded as obvious.

### II.1. NOMENCLATURE

$\beta$ = the system resolution (radians)

$c_2$ = the blackbody constant (1.44 cm $^{o}$K)

D = the diameter of the collecting optics (cm)

$D^*_\lambda$ = the detectivity at wavelength $\lambda$ (cm-Hz$^{1/2}$/W)

d = the detector diameter (cm)

$\epsilon$ = the emittance of the radiation source

f = the focal length of the collecting optics (cm)

F = the f number of the optics at the detector

$\Delta f$ = the information bandwidth of the system electronics = $\frac{\pi(\text{rpm})}{\beta(60)}$

h = the altitude of the observation platform (ft)

$\lambda$ = the wavelength (cm)

$N_\lambda$ = the spectral radiance of the radiation source (W-steradian-cm$^{-3}$)

$\sigma$ = the signal efficiency

SNR = the signal-to-noise ratio

T = the temperature of the radiation source ($^{o}$K)

$\tau$ = the total transmission (optical efficiency)

v = the velocity of the observation platform (ft/sec)

## II.2. GEOMETRICAL CONSIDERATIONS

Suppose a source at a temperature T, with an emittance $\epsilon$, radiates into a steradian a quantity of power equal to $\epsilon N_\lambda$ per unit area and wavelength interval. Then the total power collected by the optical system is

$$\text{Power} = \epsilon N_\lambda \, \delta\lambda \tau \frac{(\beta h)^2 \frac{\pi D^2}{4}}{h^2}$$

$$= \frac{\pi}{4} \tau \epsilon N_\lambda \, \delta\lambda \beta^2 D^2$$

The SNR produced in the electronics is

$$\text{SNR} = \frac{\text{Power}}{\text{NEP}}(\sigma)$$

where NEP is the noise equivalent power of the detector. But $\text{NEP} = \frac{\delta\sqrt{\Delta f}}{D^*_\lambda}$; therefore we can write

$$\text{SNR} = \frac{\pi \tau \epsilon D^*_\lambda N_\lambda \, \delta\lambda \beta^2 D^2 \sigma}{4d\sqrt{\Delta f}}$$

The following geometrical relation between the detector size and the parameters of the optical system can be used to simplify this expression:

$$d = \beta F D$$

also

$$\Delta f = \frac{\pi(\text{rps})}{\beta} = \frac{\pi(\text{v/h})}{\beta^2}$$

Thus,

$$\text{SNR} = \frac{\sqrt{\pi} \tau \epsilon D^*_\lambda N_\lambda \, \delta_\lambda \beta^2 \sigma D}{4F\sqrt{\text{v/h}}}$$

## II.3. SENSITIVITY OF NARROW WAVELENGTH BAND SYSTEMS

Since N is a function of T, the sensitivity of the system to small changes in source temperature and emittance can be found by differentiating:

$$d(SNR) = \frac{\sqrt{\pi}\tau D_\lambda^* \delta\lambda \beta^2 \sigma D}{4F\sqrt{v/h}} (\epsilon dN_\lambda + N_\lambda d\epsilon) \qquad (1)$$

Using Planck's equation

$$N_\lambda = \frac{\lambda^{-5} c_1}{e^{c_2/\lambda T} - 1}$$

and differentiating we find

$$\frac{\partial N_\lambda}{\partial T} = - \frac{c_2 N_\lambda}{\left(e^{c_2/\lambda T} - 1\right)\lambda T^2}$$

Provided $\delta\lambda$ is small so that $N_\lambda$ does not change significantly within the range $\delta\lambda$, we can put

$$d(SNR) = \frac{\sqrt{\pi}\epsilon D_\lambda^* N_\lambda \delta\lambda \beta^2 \sigma D}{4F\sqrt{v/h}} \left( \frac{C_2}{\psi \lambda T^2} dT + \frac{d\epsilon}{\epsilon} \right)$$

where $\psi = 1 - e^{c_2/\lambda T}$.

For the range of wavelengths ($\lambda < 13\mu$) and temperatures ($T < 400^\circ K$) with which we are concerned, $\lambda T \leqq 3c_2$, so that if we make $\psi = 1$, the error in d(SNR) will be less than 5%. Making this assumption and making d(SNR) equal to unity, we find that the NE $\Delta T$ is given by

$$NE\,\Delta T \equiv \frac{4F\sqrt{v/h}}{\sqrt{\pi}\sigma\tau\epsilon D_\lambda^* N_\lambda \delta\lambda \frac{c_2}{\lambda T^2} \beta^2 D}$$

and the noise-equivalent emittance difference (NE $\Delta\epsilon$) by

$$\frac{NE\,\Delta\epsilon}{\epsilon} \equiv \frac{4F\sqrt{v/h}}{\sqrt{\pi}\sigma\tau\epsilon D_\lambda^* N_\lambda \delta\lambda \beta^2 D}$$

Comparing the two equations we see that

$$\frac{NE\,\Delta\epsilon/\epsilon}{NE\,\Delta T} = \frac{c_2}{\lambda T^2} = \frac{1}{60}$$

for $\lambda = 10\ \mu$

$T = 300^{O}K$

## II.4. TRADE-OFF CURVES FOR NARROW WAVELENGTH BAND SYSTEMS

The NE $\Delta T$ and NE $\Delta\epsilon/\epsilon$ relationships in section II.3 lend themselves well to parametric representation, as follows:

Let

$$K = \frac{\sqrt{\pi}}{4}\frac{\sigma\tau\epsilon c_2}{\sqrt{v/h}}$$

$$\theta \equiv \frac{\beta^2 d}{F}\frac{\delta\lambda}{\lambda}$$

$$\phi \equiv D^*_\lambda N_\lambda$$

In terms of these parameters,

$$\text{NE}\ \Delta T = \frac{T^2}{K\theta\phi}$$

$$\frac{\text{NE}\ \Delta\epsilon}{\epsilon} = \frac{c_2}{\lambda T^2}(\text{NE}\ \Delta T)$$

The trade-off curves, then, are presented as NE $\Delta T$ and NE $\Delta\epsilon/\epsilon$ versus $\lambda$ with $\theta$ as a parameter (see fig. 24). Notice that a different set of curves is required for each target temperature, and that these expressions are only valid for narrow wavelength intervals.

## II.5. SENSITIVITY OF EXTENDED WAVELENGTH INTERVAL SYSTEMS

For extended wavelength intervals, it becomes necessary to integrate the right-hand side of equation 1, giving*

$$d(\text{SNR}) = \frac{\sqrt{\pi}}{4}\frac{D^*_{\lambda_0}\beta^2\sigma D}{\lambda_0 F\sqrt{v/h}}\int_{\lambda_1}^{\lambda_2}\tau\epsilon\lambda\left(\frac{\partial N_\lambda}{\partial T}dT + \frac{d\epsilon}{\epsilon}N_\lambda\right)d\lambda$$

*Since the detector will detect quanta of energy, the following should hold:

$$D^*_\lambda = \frac{\lambda}{\lambda_0}D^*_{\lambda_0}$$

This equality has been substituted in (1) prior to integration. While it does not hold exactly in practice, its use gives a more accurate result than the more usual assumption that $D^*_\lambda$ is a constant (see fig. 25).

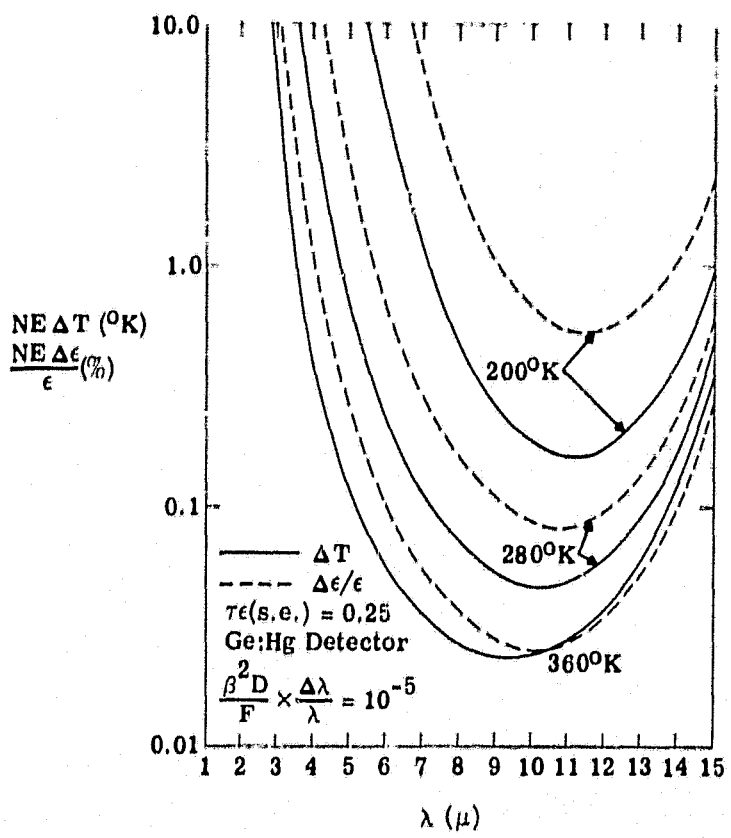


FIGURE 24. PERFORMANCE CURVES FOR NARROWBAND SPECTROMETRIC SCANNERS. $\beta$ = 3 milliradians, D = 15 cm, F = 1.0, and $\Delta\lambda/\lambda$ = 1/13.5.

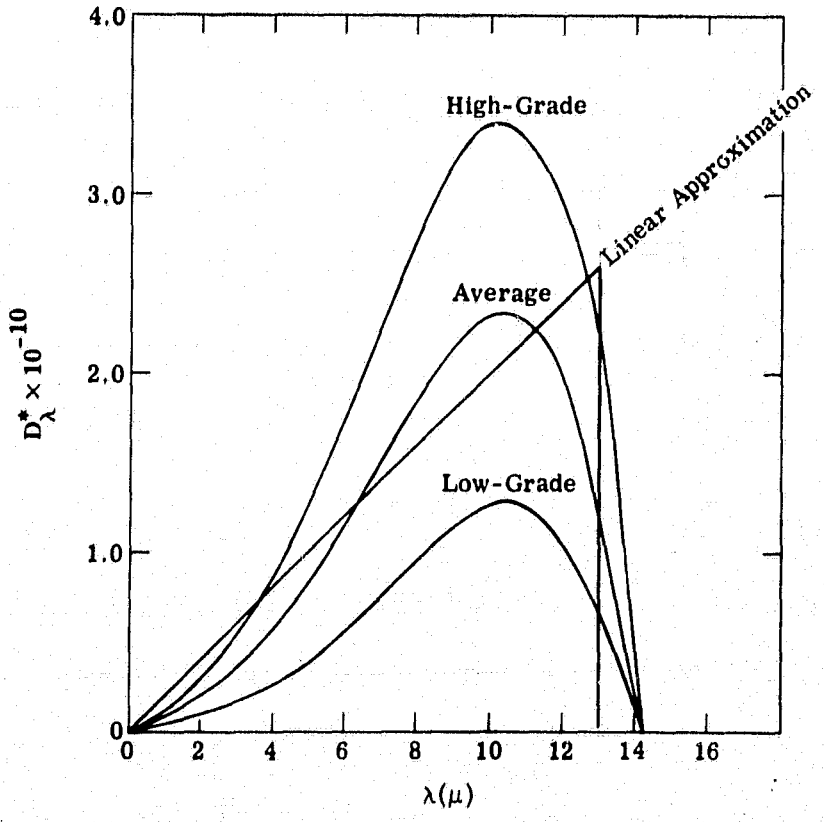


FIGURE 25. SPECTRAL RESPONSE OF TYPICAL Ge:Hg DETECTORS

This can be rewritten

$$d(SNR) = \frac{\sqrt{\pi}}{4} \frac{D^*_{\lambda_0} \beta^2 \sigma D}{\lambda_0 F \sqrt{v/h}} \overline{\tau\epsilon} \left[ dT \frac{\partial}{\partial T} \int_{\lambda_1}^{\lambda_2} \lambda N_\lambda \, d\lambda + \frac{d\epsilon}{\epsilon} \int_{\lambda_1}^{\lambda_2} \lambda N_\lambda \, d\lambda \right]$$

This may be written as

$$d(SNR) = \frac{\sqrt{\pi}}{4} \frac{D^*_{\lambda_0} \beta^2 \sigma D}{\lambda_0 F \sqrt{v/h}} \overline{\tau\epsilon} \left\{ dT \left( \frac{C_2}{T^2} N \Delta f \right) + \frac{d\epsilon}{\epsilon} [N \Delta(\lambda g)] \right\}$$

where $ng = \int_0^{\lambda} \frac{\lambda N_\lambda \, d\lambda}{N}$ and $nf = \frac{T^2}{c_2 N} \frac{\partial g}{\partial T}$; g and f have been computed for appropriate ranges of $\lambda$ and T, and the results are given in table II and figure 26. Now

$$NE \, \Delta T = \left\{ \frac{\partial(SNR)}{\partial T} \right\}^{-1}$$

and

$$\frac{NE \, \Delta\epsilon}{\epsilon} = \left\{ \epsilon \frac{\partial(SNR)}{\partial \epsilon} \right\}^{-1}$$

From the preceding, these are seen to be

$$NE \, \Delta T = \frac{4F\sqrt{v/h}}{\sqrt{\pi \tau\epsilon} D^*_{\lambda_0} \beta^2 D\sigma \left( C_2 / \lambda_0 T^2 \right) N \Delta f}$$

and

$$\frac{NE \, \Delta\epsilon}{\epsilon} = \frac{C_2}{T^2} \frac{\Delta f}{\Delta(\lambda g)} \Delta T$$

The total range of the system SNR will be limited by the information capacity of the recording or telemetry device. Thus, a given detector signal channel is limited as to the range of target temperatures which it can observe.

If the system has an information range capacity of b bits, then the maximum SNR ratio will be $2^b$ (b need not be an integer). If $\partial(SNR)/\partial T$ were constant with T, then the total temperature range of the system would be $\Delta T \approx (SNR)_{max}$. The actual case is not as simple. The

TABLE II. g(x) AND f(x) FOR $0.01 \leq x \leq 0.20$, WHERE $x = \frac{\lambda T}{C_2}$

| x | g(x) | | f(x) | |
|---|---|---|---|---|
| 0.01 | 5.844 | -39 | 5.904 | -39 |
| 0.016 | 2.792 | -23 | 2.838 | -23 |
| 0.02 | 3.861 | -18 | 3.940 | -18 |
| 0.03 | 2.022 | -11 | 2.086 | -11 |
| 0.04 | 3.620 | -8 | 3.776 | -8 |
| 0.042 | 1.032 | -7 | 1.077 | -7 |
| 0.044 | 2.660 | -7 | 2.782 | -7 |
| 0.046 | 6.277 | -7 | 6.592 | -7 |
| 0.048 | 1.380 | -6 | 1.452 | -6 |
| 0.050 | 2.802 | -6 | 2.956 | -6 |
| 0.052 | 5.405 | -6 | 5.715 | -6 |
| 0.054 | 9.877 | -6 | 1.047 | -5 |
| 0.056 | 1.723 | -5 | 1.830 | -5 |
| 0.058 | 2.882 | -5 | 3.068 | -5 |
| 0.060 | 4.643 | -5 | 4.955 | -5 |
| 0.064 | 1.093 | -4 | 1.172 | -4 |
| 0.068 | 2.303 | -4 | 2.471 | -4 |
| 0.072 | 4.426 | -4 | 4.791 | -4 |
| 0.076 | 7.878 | -4 | 8.568 | -4 |
| 0.080 | 1.315 | -3 | 1.437 | -3 |
| 0.084 | 2.076 | -3 | 2.279 | -3 |
| 0.088 | 3.127 | -3 | 3.450 | -3 |
| 0.092 | 4.520 | -3 | 5.010 | -3 |
| 0.096 | 6.360 | -3 | 7.086 | -3 |
| 0.100 | 8.530 | -3 | 9.550 | -3 |
| 0.105 | 1.20 | -2 | 1.35 | -2 |
| 0.110 | 1.62 | -2 | 1.84 | -2 |
| 0.115 | 2.13 | -2 | 2.43 | -2 |
| 0.120 | 2.72 | -2 | 3.12 | -2 |
| 0.125 | 3.39 | -2 | 3.92 | -2 |
| 0.130 | 4.14 | -2 | 4.81 | -2 |
| 0.135 | 4.96 | -2 | 5.81 | -2 |
| 0.140 | 5.85 | -2 | 6.89 | -2 |
| 0.145 | 6.802 | -2 | 8.072 | -2 |
| 0.150 | 7.681 | -2 | 9.370 | -2 |
| 0.155 | 8.868 | -2 | 1.067 | -1 |
| 0.160 | 9.960 | -2 | 1.205 | -1 |
| 0.165 | 1.108 | -1 | 1.350 | -1 |
| 0.170 | 1.223 | -1 | 1.500 | -1 |
| 0.175 | 1.334 | -1 | 1.651 | -1 |
| 0.180 | 1.456 | -1 | 1.811 | -1 |
| 0.185 | 1.575 | -1 | 1.971 | -1 |
| 0.190 | 1.692 | -1 | 2.133 | -1 |
| 0.195 | 1.809 | -1 | 2.297 | -1 |
| 0.20 | 1.925 | -1 | 2.461 | -1 |

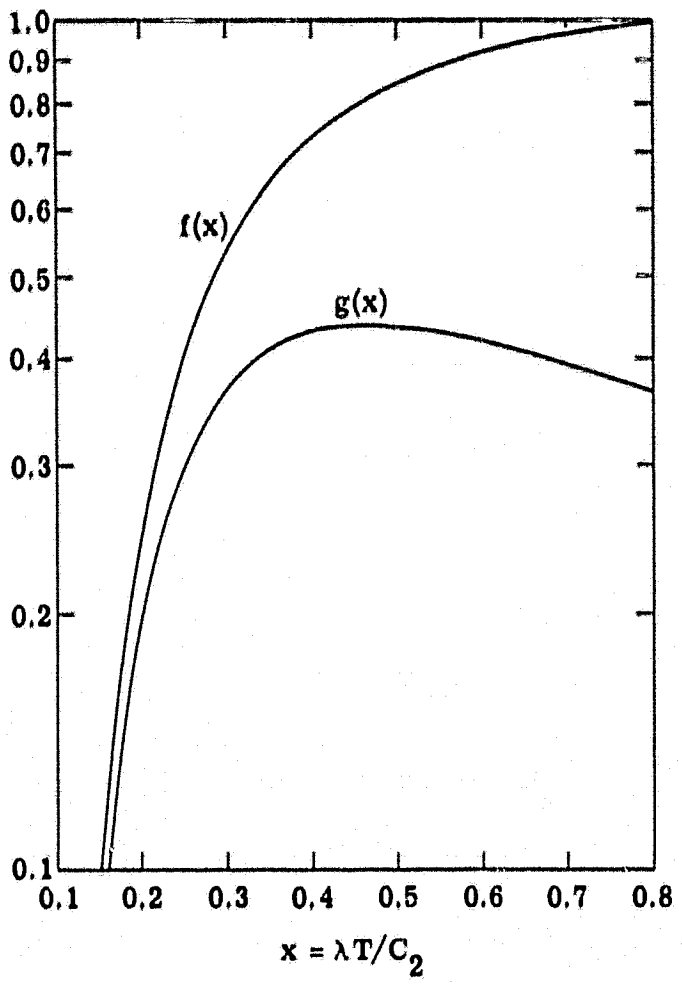


FIGURE 26. g(x) AND f(x) FOR $0.16 \leqq x \leqq 0.80$.

true dynamic range is computed as follows: the power impinging upon the detector is given by

$$P\alpha \int_{\lambda_1}^{\lambda_2} \lambda N_\lambda d\lambda$$

The total range of power which may be measured by the system may be written

$$\Delta P = NEP \times (SNR)_{max}$$

Choosing some temperature $T_0$ as the design temperature,* this becomes

$$\Delta P = \left.\frac{\partial P}{\partial T}\right|_{T_0} NE\,\Delta T\Big|_{T_0} \times (SNR)_{max}$$

*Design temperature is that target temperature for which the NE ΔT is some specified value (e.g., $0.1^{\circ}K$).

Thus,

$$\Delta\int_{\lambda_1}^{\lambda_2}\lambda N_\lambda\,d\lambda = \left[\int_{\lambda_1}^{\lambda_2}\lambda\frac{\partial N_\lambda}{\partial T}\bigg|_{T_0}d\lambda\right]\mathrm{NE}\,\Delta T\Big|_{T_0}\times(\mathrm{SNR})_{max}$$

or

$$\Delta[\Delta(\lambda Ng)] = \Delta\left(\frac{c_2 N_0}{T_0^2}f_0\right)\mathrm{NE}\,\Delta T_0\times 2^b$$

The dynamic temperature limits, as functions of $T_0$ and b, are shown in figures 27 to 29 for the 5- to 13-$\mu$ region (within the temperature range $120^\circ K \leq T \leq 400^\circ K$).

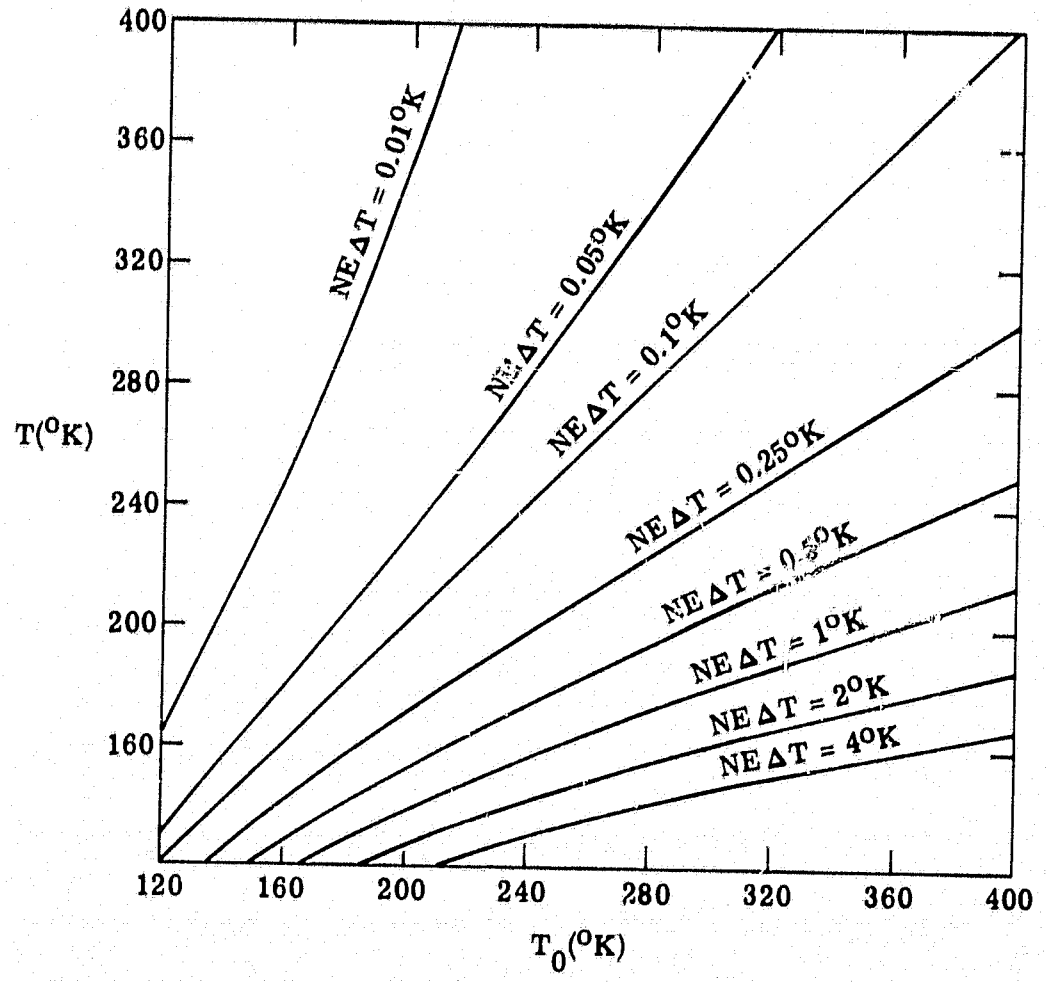


FIGURE 27. NE ΔT VERSUS TEMPERATURE FOR A 5- TO 13-$\mu$ SYSTEM ($NE\,\Delta T_0 = 0.1^\circ K$)

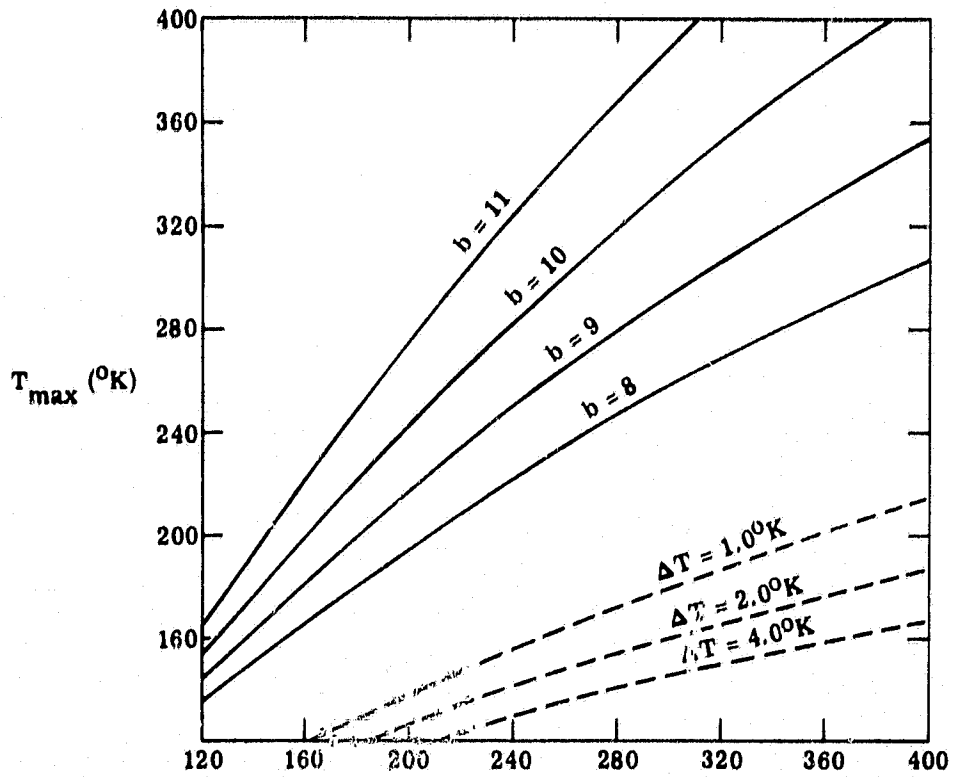


FIGURE 28. DYNAMIC RANGE CURVES FOR A 5- TO 13-$\mu$ SYSTEM ($T_{min}$ = 120$^o$K)

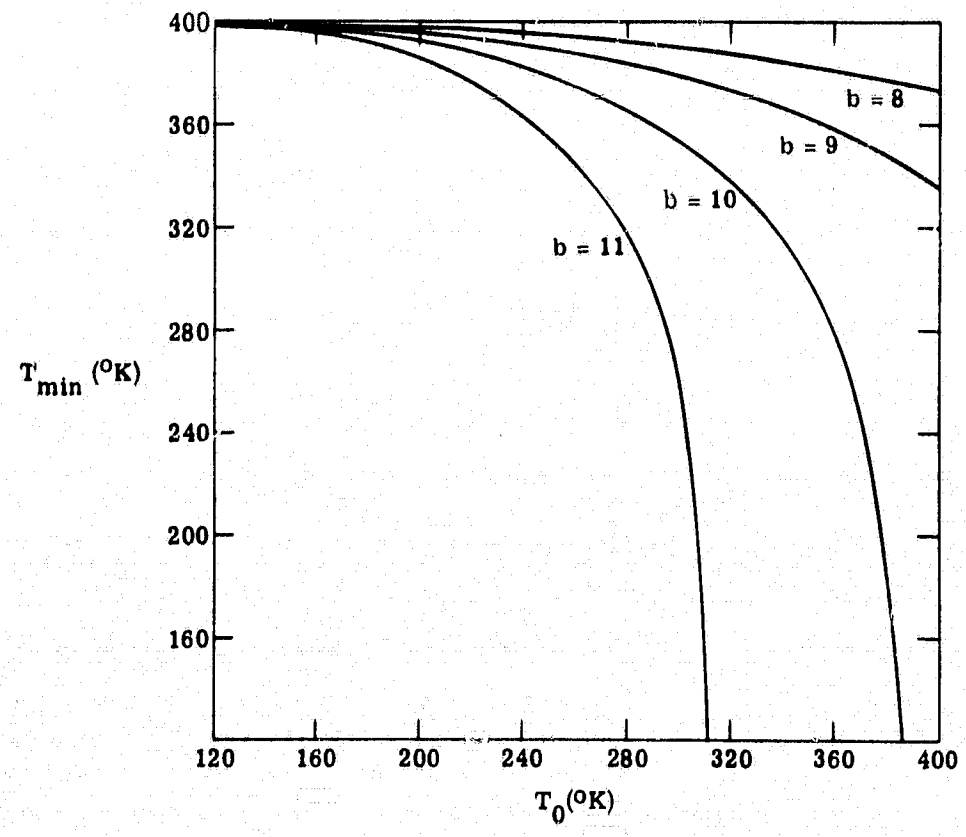


FIGURE 29. DYNAMIC RANGE CURVES FOR A 5- TO 13-$\mu$ SYSTEM ($T_{max}$ = 400$^o$K)

## II.6. TRADE-OFF CURVES FOR EXTENDED WAVELENGTH INTERVAL SYSTEMS

The trade-off curves for the extended (5 to 13$\mu$) wavelength system show NE $\Delta$T versus target temperature with $\beta^2$D/F as a parameter in figures 30 and 31. The dynamic range limitations

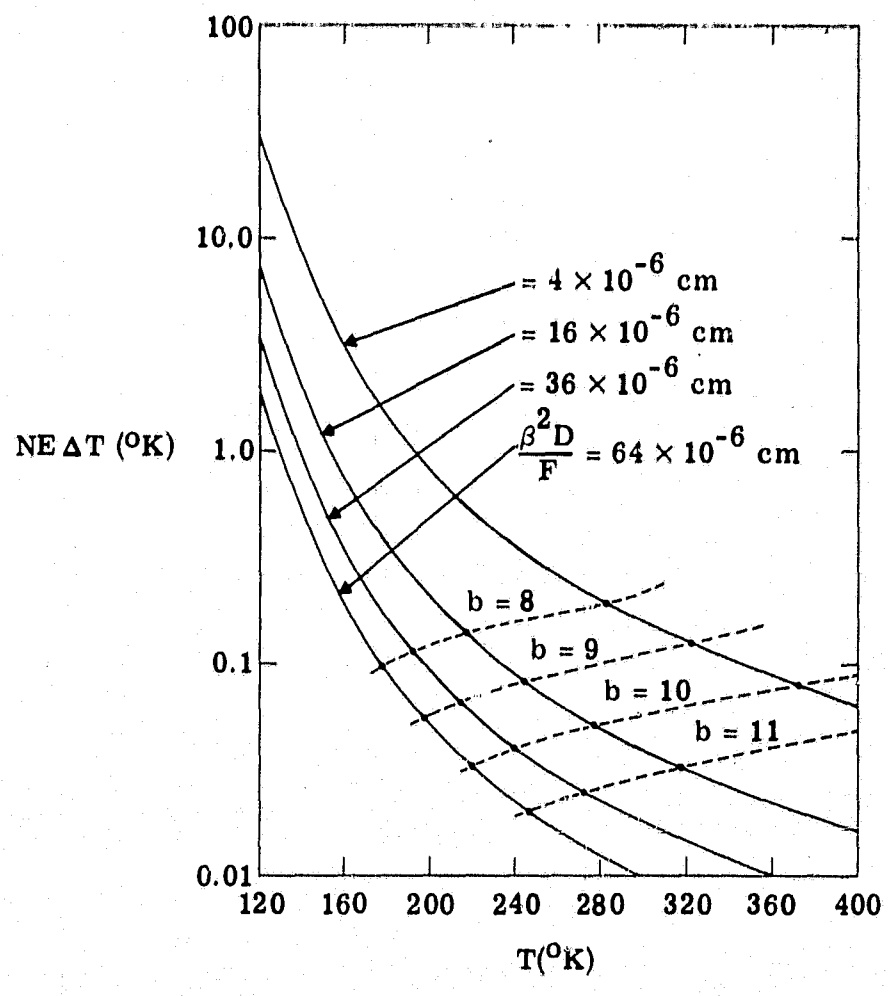


FIGURE 30. NE$\Delta$T VERSUS TEMPERATURE FOR A COLD-SIDE DETECTOR (5 TO 13 $\mu$)

for various values of b are indicated by the dashed lines. Note that NE $\Delta$T $\alpha$ $\beta^2$D/F. Following are some examples which explain the curves:

(1) It is desirable to have a single-channel (one detector) system capable of sensing the entire lunar surface. A 10-bit A/D converter is available. From figure 31, it can be seen that the dashed curve for b = 10 (bits) becomes asymptotic to a $\beta^2$D/F curve at $\beta^2$D/F = $3 \times 10^{-6}$ cm. Assuming a 6-in., f/5 system, this means that $\beta$ will be 1 milliradian. Examples for the NE $\Delta$T follow:

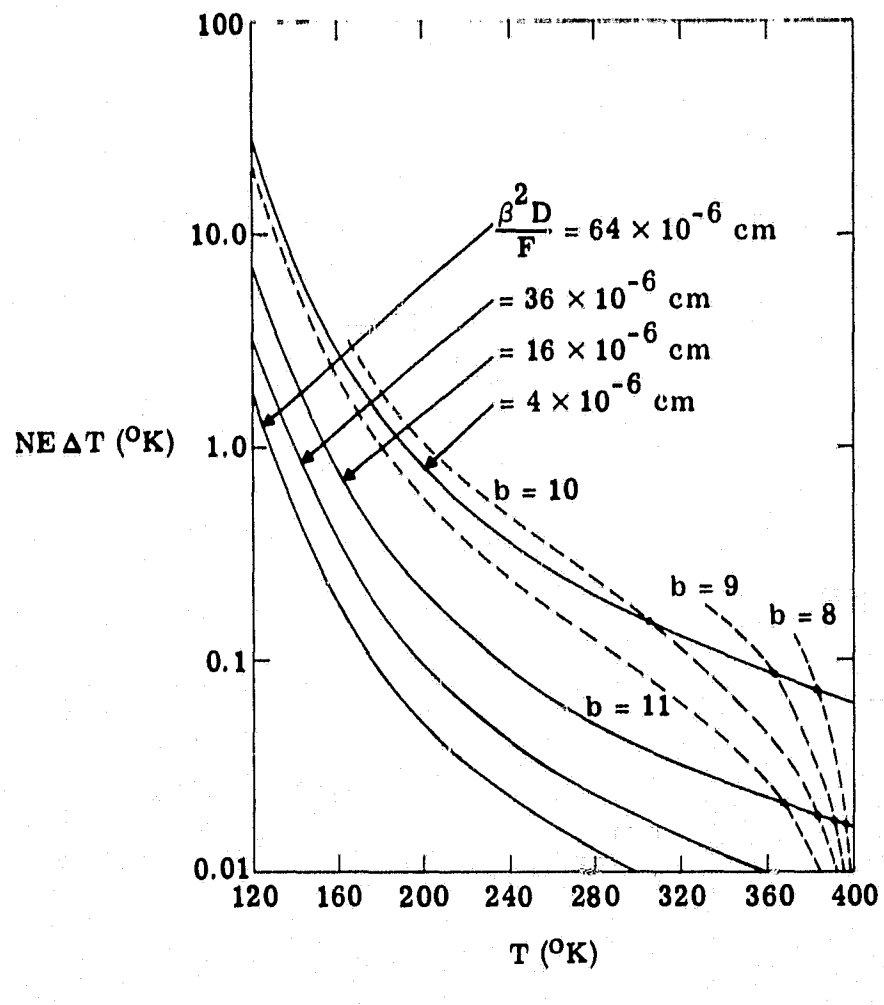


FIGURE 31. NE ΔT VERSUS TEMPERATURE FOR A HOT-SIDE DETECTOR (5 TO 13 $\mu$)

| T (°K) | NE ΔT (°K) |
|---|---|
| 120 | ~40 |
| 160 | 3.6 |
| 200 | 1.0 |
| 240 | 0.47 |
| 280 | 0.32 |
| 320 | 0.17 |
| 360 | 0.11 |
| 400 | 0.08 |

(2) A scanner which will have an NE $\Delta T \leqq 1^{\circ}K$ for $120^{\circ}K \leqq T \leqq 400^{\circ}K$ is required. This must be accomplished with no more than two detectors and have $b \leqq 10$. From figure 31 it is clear that the hot-side detector must be limited to $T \geqq 200^{\circ}K$, with parameters and performance

as in 1. The cold-side detector must have $\beta^2 D/F \cong 128 \times 10^{-6}$ cm. Extrapolating the b = 10 curve, it appears that it will be possible to handle all information from $120^{\circ}$ to $200^{\circ}$K, thereby covering the full temperature range. Again, assuming d = 6 in. and f/5 optics, $\beta \cong 6.6$ milliradians. The performance will be as follows:

| Cold Side | | Hot Side | |
|---|---|---|---|
| T($^{\circ}$K) | NE $\Delta$T($^{\circ}$K) | T($^{\circ}$K) | NE $\Delta$T($^{\circ}$K) |
| 120 | 1.0 | 200 | 1.0 |
| 160 | 0.1 | 240 | 0.47 |
| 200 | 0.03 | 280 | 0.32 |
| | | 320 | 0.17 |
| | | 360 | 0.11 |
| | | 400 | 0.08 |

(It should be understood that these curves are predicated upon linear gain factors and full utilization of the dynamic content of the signal, i.e., one bit corresponds to an SNR of 1. Using logarithmic amplifiers or degrading the digital resolution, it would be possible to carry more dynamic temperature range but with degraded temperature resolution. In regions where the NE $\Delta T < 0.1^{\circ}$K, this may be desirable and hence might warrant future consideration.)

## II.7. PHOTOMULTIPLIER SYSTEMS

The power incident upon the photocathode surface of the photomultiplier is represented by

$$P_\lambda = 0.25\tau\beta^2 D^2 (\rho_\lambda H_\lambda \delta\lambda)$$

where $P_\lambda$ = the diffuse reflectance of target

$H_\lambda$ = the solar radiant flux at the target plane ($w/cm^2/\mu$)

The SNR for a narrow wavelength range is given by

$$(SNR)_\lambda = \frac{\sigma \Delta P_\lambda}{(P_N)_\lambda}$$

Assuming that the photomultiplier is shot-noise limited, the NEP is

$$(P_N)_\lambda = \sqrt{\frac{2e\,\Delta f}{R_c}\sigma P_\lambda}$$

where $e = 1.6 \times 10^{-19}$ (coulombs)

$\Delta f$ = the bandwidth = $\pi(v/h)/\beta^2$

$R_c$ = the cathode radiant sensitivity (amps/W)

The SNR then, if given by

$$\text{SNR} = \Delta\rho_\lambda \beta^2 D \sqrt{\frac{1}{8\pi e} \frac{\tau\sigma}{v/h} \frac{R_c H_\lambda \delta_\lambda}{\rho_\lambda}}$$

For the case at hand, the following parameters apply:

$D = 15$ cm

$\beta = 3$ milliradians

$v/h = 1/40$ sec$^{-1}$

$\rho_\lambda = 0.25$

$\delta\lambda = \lambda/R$

$\sigma\tau = 0.25$

The noise-equivalent reflectance difference for this case, then, is represented by

$$\text{NE}\,\Delta\rho_\lambda = 2.35 \times 10^{-6} \sqrt{\frac{R}{R_c H_\lambda \lambda}}$$

## Appendix III
## THE EFFECT OF USING A RECTANGULAR ENTRANCE SLIT IN A SCANNER-SPECTROGRAPH

In the discussions of scanner-spectrograph design in references 2 and 4 and in section 3.2 of this report, attention has been confined to the square entrance slit. This is the obvious choice, since the shape of this slit and the optical aberrations determine the instantaneous FOV of the scanner, and it is a usual and convenient practice to make this FOV either round or approximately square. However, the throughput of a spectrograph of a given size is usually a maximum when the entrance slit is long relative to its width. If this entrance slit were used in a scanner-spectrograph with the long dimension of the slit perpendicular to the scan line, the resolution along the lines would be appreciably finer than the line widths. The resolutions along the lines could easily be degraded by appropriate electronic smoothing to give equivalent resolution in the two directions. Under certain circumstances, this system could be advantageous (see ref. 2, p. 38). An analysis of the effect on system performance of a rectangular entrance slit and electronic smoothing has been carried out. Though nonsquare entrance slits have not been recommended, the analysis is given here for completeness and possible future reference.

Assume that the size of the ground resolution element is increased by a factor a in the direction parallel to the flight direction by elongations of the slit and by a factor b in the

orthogonal direction by electronic smoothing. The first step in determining the effect of changing the instantaneous FOV is to develop equations that specify the size of several elements of the spectrometer. Figure 32 shows a top and a side view of the system. We use the term "width" for the x dimension and "height" for the y dimension. The slit height $y_s$ is determined by

$$\frac{y_s}{F_1 D_1} = \beta_y$$

$$y_s = F_1 D_1 \beta y$$

$$y_s = F_1 D_1 \beta x$$

The slit width $x_s$ is

$$\frac{x_s}{F_1 D_1} = \alpha_x \qquad (2)$$

$$x_s = F_1 D_1 \alpha_x$$

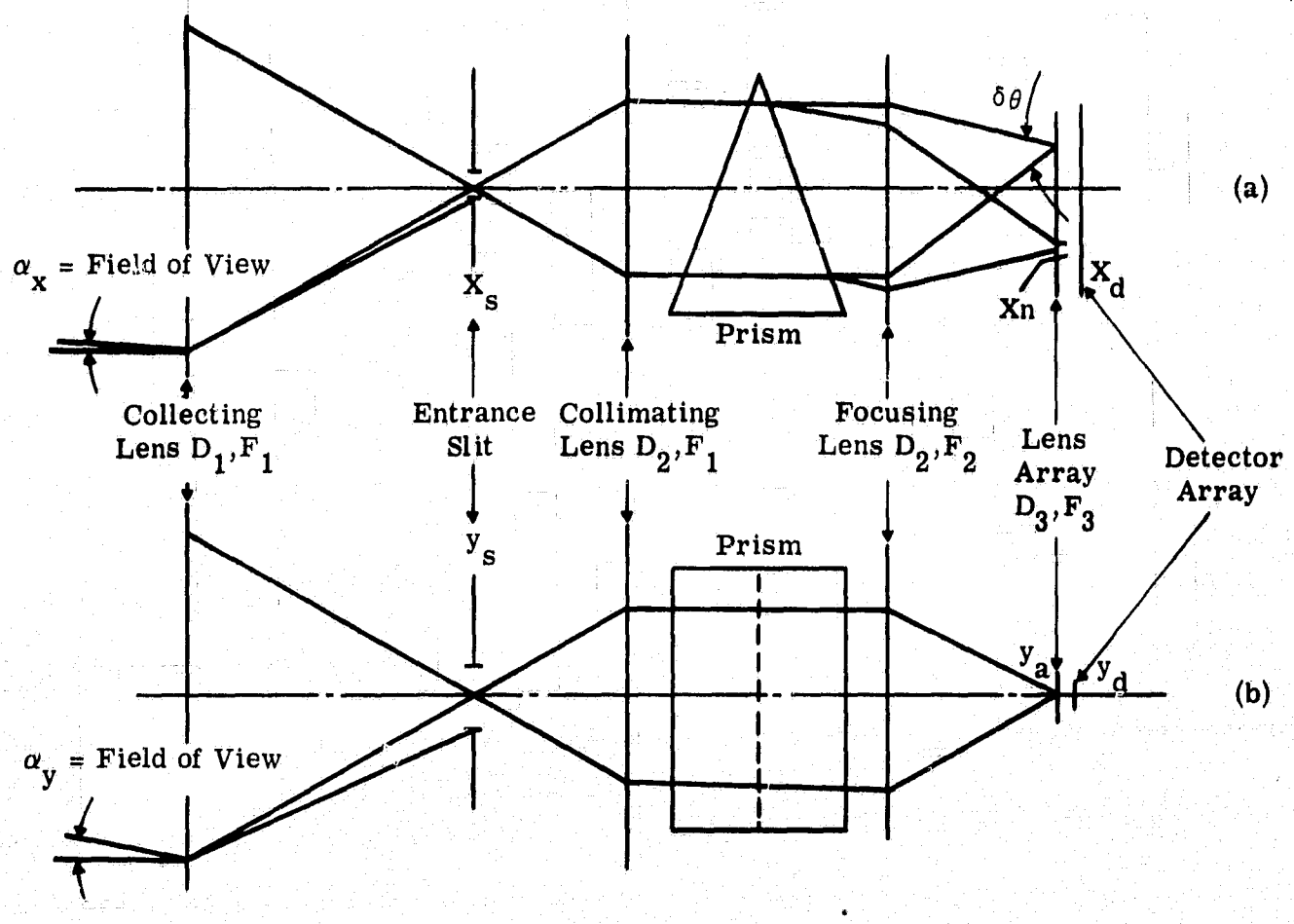


FIGURE 32. SCHEMATIC OPTICAL DIAGRAM OF THE SPECTROMETER. (a) Top view. (b) Side view.

The diameter $D_2$ of the collimating and focusing lenses is determined by the minimum angle $\delta\theta_{min}$ subtended by a spectral resolution element. In this case, $\delta\theta_{min}$ is the smallest angle subtended in the x plane by a lens in the lens array ($D_3$, $F_3$) with the focusing mirror ($D_2$, $F_2$). For maximum efficiency, this angle is equated with the angle subtended by the entrance slit with mirror ($D_2$, $F_1$) yielding

$$\frac{x_s}{D_2 F_1} = \delta\theta_{min} \tag{3}$$

Substituting (2) in (3) gives

$$D_2 = \frac{D_1 x}{\delta\theta_{min}} \tag{4}$$

To determine the size of the lenses in the lens array $D_3$, $F_3$, we write

$$\frac{y_s}{D_2 F_1} = \frac{y_a}{D_2 F_2}$$

Here $y_a$ is the height of a lens in the array, as shown in figure 32. Using the geometry of this figure, it follows that

$$y_a = D_1 F_2 \beta_y$$

$$y_a = a D_1 F_2 \beta_x$$

To determine the width $x_a$ of each lens in the array, observe that $x_a$ is directly proportional to $\delta\theta$ (the angle subtended by the spectral resolution element $\delta\lambda$). $\delta\theta$ varies with wavelength as $\delta\theta = \delta\theta_{min}$ where m contains the functional dependence of $\delta\theta$ on $\lambda$. We then have

$$\frac{x_a}{D_2 F_2} = \delta\theta = m\delta\theta_{min}$$

$$x_a = m_2 D_2 F_2 \delta\theta_{min} \tag{5}$$

Substituting (4) in (5) yields

$$x_a = m D_1 F_2 \beta_x \tag{6}$$

The diameter $D_3$ of the lenses in the array is the diagonal of the rectangle whose sides are $x_a$ and $y_a$ so that

$$D_3 = \sqrt{x_a^2 + y_a^2}$$

$$D_3 = D_1 F_2 \beta \sqrt{m^2 + a^2}$$

The focusing lens is imaged on the detector by a lens of the array. The detector area is given by

$$A_d = x_d y_d \tag{7}$$

Now

$$\frac{y_d}{D_3 F_3} = \frac{D_2}{D_2 F_2}$$

Thus

$$y_d = \frac{F_3}{F_2} D_3$$

Then substituting (6),

$$y_d = D_1 F_3 \beta_x \sqrt{m^2 + a^2} \tag{8}$$

$x_d$ is found by using a similar procedure:

$$x_d = D_1 F_3 \beta_x \sqrt{m^2 + a^2} \tag{9}$$

Substituting (8) and (9) in (7) gives

$$A_d = D_1^2 F_3^2 \beta_x^2 (m^2 + a^2) \tag{10}$$

The dwell time $\tau$ on a ground resolution element is multiplied by the factor b so that the electronic bandwidth $\Delta f$ is accordingly decreased and can be expressed as

$$\Delta f = \frac{1}{b2\tau} \tag{11}$$

Using $\tau = \frac{\omega n}{2\pi v/h} = \frac{\beta_x \beta_y \eta}{2\pi v/h} = \frac{a\beta_x^2 \eta}{2\pi v/h}$ in (11) yields the expression

$$\Delta f = \frac{\pi v/h}{ab\beta_x^2 \eta} \tag{12}$$

The preceding parametric relations are used to determine the SNR when the detector is limited by shot noise and current noise, respectively. From the appendix of reference 2, we find that the signal current and the shot noise current are given by the expressions

$$I_s = \frac{\pi}{4}\tau_0 N'_\lambda \delta\lambda\omega D_1^2 R_c$$

$$I_n = k\sqrt{2e\,\Delta f I_T}$$

For the large signal with which we are concerned, the total current $I_T \cong I_s$, so that

$$SNR = \frac{I_s}{I_n} = \frac{1}{k}\sqrt{\frac{I_s}{2e\,\Delta f}}$$

$$= \frac{1}{2k}\sqrt{\frac{\pi\tau_0 N'_\lambda \delta\lambda\omega D_1^2 R_c}{2e\,\Delta f}}$$

Substituting $\omega = a/\beta_x^2$ and $\Delta f = \frac{\pi(v/h)}{ab\beta_x^2 n}$

$$SNR = a\sqrt{b}\sqrt{\frac{\beta_x^2 n\tau_0 N'_\lambda \delta\lambda D_1^2 R_c}{8ke(v/h)}}$$

Thus, the SNR increases linearly with the multiplicative factor a and as the square root of the factor b.

The effect of changing the FOV on the SNR for the detector noise case is evaluated using the appropriate equation from reference 2:

$$SNR = \frac{\tau_0 N'_\lambda (\pi/4) D_1^2 D^* \omega}{\sqrt{A_d\,\Delta f}}$$

Substituting $\omega = a\alpha_x^2$ and equations 10 and 12 gives

$$SNR = \sqrt{\frac{a^3 b}{m^2 + a^2}}\,\frac{\tau_0 N'_\lambda \delta\lambda D_1 D^* \alpha_x^2}{\sqrt{4\pi(v/h)F_3}}$$

or, considering only the effects of changes in a and b, we can write

$$SNR \propto \sqrt{\frac{a^3 b}{m^2 + a^2}}$$

Table III summarizes the effects of changing the instantaneous FOV.

TABLE III. THE EFFECTS OF CLOSING A RECTANGULAR INSTANTANEOUS FIELD OF VIEW

| Parameter | Multiplicative Factor |
|---|---|
| $x_G$, $y_G$ } Size of ground-resolution element | b<br>a |
| $y_S$, Slit height | a |
| $D_3$ | $\sqrt{\frac{m^2 + a^2}{m^2 + 1}}$ |
| $x_d$(InAs), Detector width | $\sqrt{\frac{m^2 + a^2}{m^2 + 1}}$ |
| $y_d$(InAs), Detector length | $\sqrt{\frac{m^2 + a^2}{m^2 + 1}}$ |
| $\tau$ | b |
| $\Delta f$ | $(ab)^{-1}$ |
| SNR (shot-noise case) | $a\sqrt{b}$ |
| SNR (detector-noise case) | $\sqrt{\frac{a^3 b}{m^2 + a^2}}$ |

## REFERENCES


1. J. J. Cook, A Survey of Lunar Geology, Report No. 7815-12-T, Willow Run Laboratories of the Institute of Science and Technology, The University of Michigan, Ann Arbor (in publication).
2. J. Braithwaite, Dispersive Multispectral Scanning; A Feasibility Study, Report No. 7610-5-F, Willow Run Laboratories of the Institute of Science and Technology, The University of Michigan, Ann Arbor, September 1966.
3. I. J. Sattinger and F. C. Polcyn, Peaceful Uses of Earch Observation Spacecraft, Report No. 7219-1-F, Vol. III, Willow Run Laboratories of the Institute of Science and Technology, The University of Michigan, Ann Arbor, February 1966.
4. D. S. Lowe, J. Braithwaite, and V. L. Larrowe, An Investigative Study of a Spectrum Matching Imaging System, Report No. 8201-1-F, Willow Run Laboratories of the Institute of Science and Technology, The University of Michigan, Ann Arbor, October 1966.
5. R. J. P. Taylor (edit.), Earth Orbital Infrared - A Multidiscipline Scientific Experiment, NASA Earth Resources Infrared Team, unpublished report, 1966.
6. S. W. Athey, Magnetic Tape Recording, NASA SP-5038, Washington, D. C., January 1966, pp. 191-195.
7. E. E. Bisson and W. J. Anderson, Advanced Bearing Technology, NASA-SP-38, Washington, D. C., 1965.
8. A. I. Weinstein, A. S. Friedman, and V. E. Gross, "Cooling to Cryogenic Temperatures by Sublimation," Proc. IRIS, Vol. VII, No. 2, 1962, p. 187.
9. V. E. Gross and A. I. Weinstein, "A Cryogenic-Solid Cooling Jystem," Proc. IRIS, Vol. IX, No. 1, 1964, p. 23.
10. B. Brentnall, Experiment D4/D7, Celestial Radiometry and Space-Object Radiometry, NASA SP-121, Washington, D. C., 1966.
11. H. Pullan, "A Cooled Detector-Preamplifier System for Detection" (Confidential Paper), Proc. IRIS (U), Vol. X, No. 3, 1966, SECRET, p. 111.
12. D. E. Bode et al., "Characteristics of Mercury-Doped Germanium Detectors Under Reduced Background Conditions," Proc. IRIS, Vol. X, No. 3, 1966, p. 81.
13. G. L. Davies, Magnetic Tape Instrumentation, McGraw Hill, 1961, p. 72.
14. W. L. Brown and F. D. Farley, Geometric Distortions in Field of View of Rotating-Oblique Mirror Scanning System, Project MICHIGAN Report No. 6400-10-T, Institute of Science and Technology, The University of Michigan, Ann Arbor, August 1964.
15. F. J. Meyers, and M. N. Todd, Jr., "Perspective and Map Distortions in Line-Scan Strip Mappers," Proc. IRIS, Vol. VIII, No. 3, 1963, p. 129.